Formation of Specialized HSV-1 Egress Sites

Rebecca Merrill Mingo
Marion Station, Maryland

BS, Randolph-Macon College, 2004

A Dissertation presented to the Graduate Faculty
of the University of Virginia in Candidacy for the Degree of
Doctor of Philosophy

Department of Microbiology

University of Virginia
May, 2012
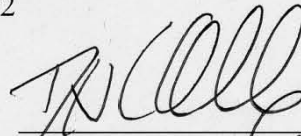
Abstract

In the final stages of the HSV-1 lifecycle, a viral nucleocapsid buds into a vesicle of TGN/endosome origin acquiring an envelope and an outer vesicular membrane. The virus-containing vesicle then traffics to the plasma membrane where it fuses, exposing an enveloped virion. Although the process of directed egress has been studied in polarized epithelial cell lines, little work has been done in non-polarized cell types, i.e. cells without extensive junctional complexes and compositionally distinct membrane regions. In the following report we describe a molecular and cellular study of HSV-1 egress as it occurs in non-polarized cells. Infected Vero cells were examined by electron, confocal, and TIRF microscopy. The results demonstrated that HSV-1 was released at specific pocket-like areas of the plasma membrane along the substrate-adherent surface and cell-cell adherent contacts. Both the membrane composition and cytoskeletal structure of these egress sites were found to be modified by infection. The membrane at release site "patches" was rich in virus-encoded glycoproteins, and accumulation of glycoproteins at exit sites began before viral transport. The use of a mutant unable to produce mature virions showed that glycoprotein patches formed normally even when virus trafficking was inhibited. Depolymerization of the cytoskeleton indicated that microtubules and actin were both important for trafficking of virions and glycoproteins to release sites. Furthermore, the actin cytoskeleton was found to be necessary for maintaining the integrity of egress sites once they formed. When actin was depolymerized, the glycoprotein concentrations dispersed across the membrane as did the surface-associated virus. Lastly, glycoprotein accumulation at release sites was found to be dependent on the

cytoplasmic tail of viral glycoprotein E. When cells were infected with gE deletion

mutants, patch sizes were significantly reduced, although the total amount of virus

released was increased. The results of this study are interpreted to indicate that egress of

HSV-1 is directed to virally induced, specialized egress sites that form along the cell

membrane. These sites share similarities with retroviral virological synapses and may

function in a similar manner during cell-to-cell spread.

Dedication

To all the friends and family who have supported me in this endeavor, I could not have done this without your love and encouragement. I particularly want to thank Jesse, who never seemed to mind when a date was interrupted by a timepoint.

Acknowledgements

First I'd like to thank my mentor, Jay Brown, for his guidance and support. I am grateful for his encouragement to try a project that was as much cell biology as virology. I am particularly appreciative for his willingness to tackle new areas of learning outside of structural virology in able to advise me in this project. I will be forever indebted to Dr Brown for his mentorship and for teaching me how to think like a scientist.

I would also like to extend my appreciation to my graduate committee: Dr David Castle, Dr Dan Engel, Dr Dean Kedes, Dr Ulrike Lorenz, and Dr Judy White. Their guidance has been invaluable in bringing this project to fruition. I was very lucky, indeed, to have such high caliber scientists advising my research! I particularly want to thank Dr Dean Kedes for serving as my committee chair and first reader. The administrative tasks associated with this position can be quite time consuming, and I am extremely grateful that he was willing to sacrifice that time.

I'd like to express my gratitude to the members of the Brown Lab as well. I'd especially like to thank Bill Newcomb for teaching me many basic research techniques and for assisting me with the electron microscope. You will all be missed!

Furthermore, I'd like to thank the members of Molecular Medicine and Systems Biology class of 2004. From study groups to birthday parties, you have all been there. Not every class is blessed with great people who support one another the way this one has!

Lastly, I'd like to thank my friends and my family. Everyone has been wonderfully supportive, even though few of them have any idea what it is I do. Thank you all!

Table of Contents

Figure List

Chapter V

Chapter VIII

Abbreviations

Bleb   Blebbistatin

CK2   Casein Kinase II

CyB   Cytochalasin B

DAG   Diacyl Glycerol

DNA   Deoxyribonucleic Acid

ESCRT   Endosomal Sorting Complex Required for Transport

gD   HSV-1 Glycoprotein D

gE   HS-1 Glycoprotein E

HIV   Human Immunodeficiency Virus

HPI   Hours Post Infection

HSV-1   Herpes Simplex Virus Type 1

IgG   Immunoglobulin

IP3R-I   Inositol Triphosphate Receptor-I

IS   Immunological Synapse

ITAM   Immunoreceptor Tyrosine-Based Activation Motif

MOI   Magnitude of Infection

MTOC   Microtubule Organizing Center

Noc   Nocodazole

PKD   Protein Kinase D

PFU   Plaque Forming Units

TER   Trans-Epithelial Resistance

TGN   Trans-Golgi Network

TIRFM   Total Internal Reflection Fluorescence Microscopy

V1   Ophthalmic Branch of the Trigeminal Nerve

V2   Maxillary Branch of the Trigeminal Nerve

V3   Mandibular Branch of the Trigeminal Nerve

VP5   HSV-1 Major Capsid Protein

VS   Virological Synapse

WGA   Wheat Germ Agglutinin

WT   Wild Type

I. Introduction

HSV-1 Disease

Herpes simplex virus type one (HSV-1) is a virus of the subfamily alphaherpesvirus. This virus is recognized as the cause of the common oral lesions referred to as cold sores. It infects epithelial cells of mucosal tissue and then spreads to the infiltrating neurons. Epithelial cell infections end in cell destruction, however, the virus spreads through facial sensory nerves and establishes latent infections within neurons of the trigeminal ganglion (Figure 1). These latant infections persist throughout life. While HSV-1 lesions are generally limited to the oral mucosa, this virus can also infect genital mucosal tissues, epithelial cells of the eye, or non-mucosal tissues that have a compromised skin barrier (e.g. atopic dermatitis, eczema) (30,173,216). In rare cases, HSV-1 can cause life-threatening encephalitis. Newborns can succumb to HSV encephalitis after being exposed to a large viral titre in the birth canal of an infected mother. Adults exhibit the symptoms of encephalitis when the infection moves up peripheral nerves into the central nervous system. In such cases the temporal lobes of the brain often become infected. This can lead to severe damage and death (13). Though rare, HSV encephalitis is a serious concern.

Virion Structure

The HSV-1 virion averages ~225 nm in diameter. It consists of a 152-kb genome of double-stranded DNA enclosed by an icosahedral capsid. Surrounding the capsid is a

Figure 1: Trigeminal Nerve Schematic. After formation of a primary lesion on mucosal surfaces of the lip, HSV-1 establishes latency within the trigeminal ganglion. This nerve has three branches: the ophthalmic branch (V1), the maxillary branch (V2), and the mandibular branch (V3). Upon reactivation, virus can move down the axons of any branch of the nerve but tends to favor the branch leading to the site of primary infection (3). Image is from Mosby's Medical Dictionary, 8th ed.

Trigeminal nerve

Ophthalmic branch (V$_1$)

Maxillary branch (V$_2$)

Superior alveolar nerve

Mandibular branch (V$_3$)

Lingual nerve

Inferior alveolar nerve
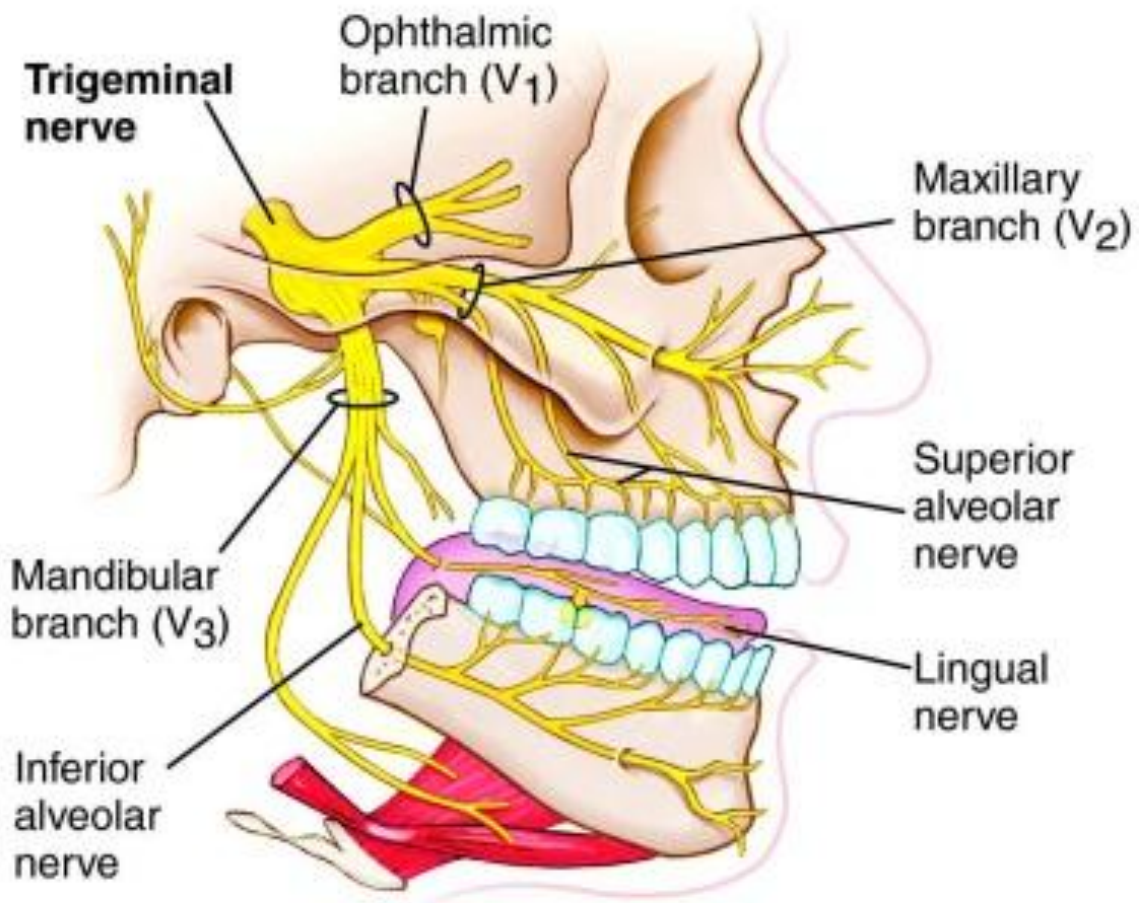
Figure 2: HSV-1 Virion. DNA is enclosed within an icosahedral capsid. Surrounding the capsid is a composite of multiple proteins that form the tegument. The last layer is a lipid envelope in which the viral glycoproteins are embedded. Image is by L. Stannard, Division of Medical Virology, University of Cape Town.
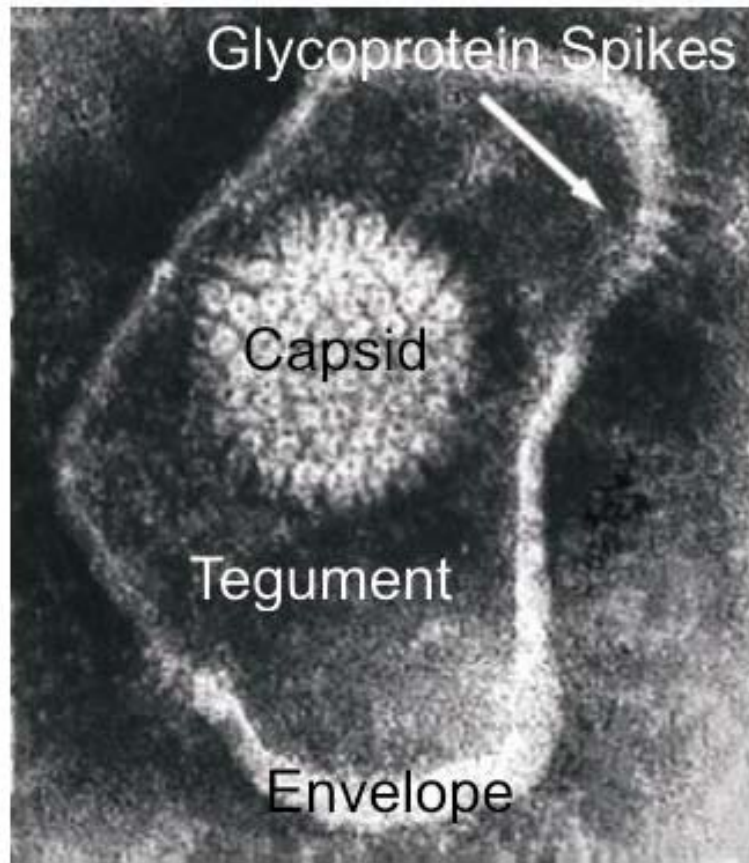
composite of approximately 20 proteins known as the tegument (Figure 2). Encasing the

tegument is a lipid envelope derived from host membranes. This envelope contains at

least 11 viral glycoproteins projecting spike-like from its surface. The tegument forms

the largest portion of the virion and can compose between 1/2 and 2/3 of the size. The

capsid forms the remaining 1/3-1/2 (69).

Viral Entry

The virion enters a cell through use of receptor binding. HSV-1 has been found to

utilize a variety of receptors with different degrees of efficiency depending on cell type.

In many cells glycoprotein D (gD) on the virion binds to nectin-1 or nectin-2 (HveC or

HveB) on the plasma membrane (61,207). These receptors localize to adherens junctions

of epithelial cells and the synaptic junctions of neurons (190). Other viral glycoproteins

facilitate entry by inducing cell attachment with the binding of heparan sulfate (93).

Once bound, glycoproteins gD, gB, and the gHgL complex are needed for fusion of the

viral envelope with the cell membrane (73). In many epithelial cell types the virus can be

endocytosed and fusion then occurs within endocytic vesicles (59,137). Within the

cytoplasm the de-enveloped capsid transverses along microtubules in the retrograde

direction to the nuclear envelope (45,154,180). Many viral proteins that modulate cell

function and create conditions conducive for infection are found in the tegument. The

virus loses most of its attached tegument as it transverses towards the nucleus and these

proteins become active (68,102,111). Once in contact with the nuclear membrane, the

virus threads its DNA through a pore into the nucleus where transcription and replication

ensue (Figure 3-1) (8,25,192).

Figure 3: Lifecycle of HSV-1. A virion binds to a receptor triggering fusion of the viral envelope with the cell membrane. The capsid moves along microtubules until it reaches the nuclear membrane. The capsid binds a nuclear pore and DNA is transported into the nucleus (step 1). DNA is transcribed and replicated. Viral proteins are transported into the nucleus. Proteins are assembled to form capsids, into which DNA is packaged (step 2). Capsids then exit in a process of primary envelopment and deenvelopment (step 3). Capsids bind tegument proteins and bud into cytoplasmic vesicles containing viral glycoproteins (steps 4-5). Virion-containing vesicles then move to the cell surface (step 6) and fuse releasing an enveloped virion into the intracellular space (step 7). Micrograph 1 from Ojala 2000 (143). Micrographs 2-5 from Mettenleiter 2002 (116). Micrographs 6-7 from Granzow 2001 (67).
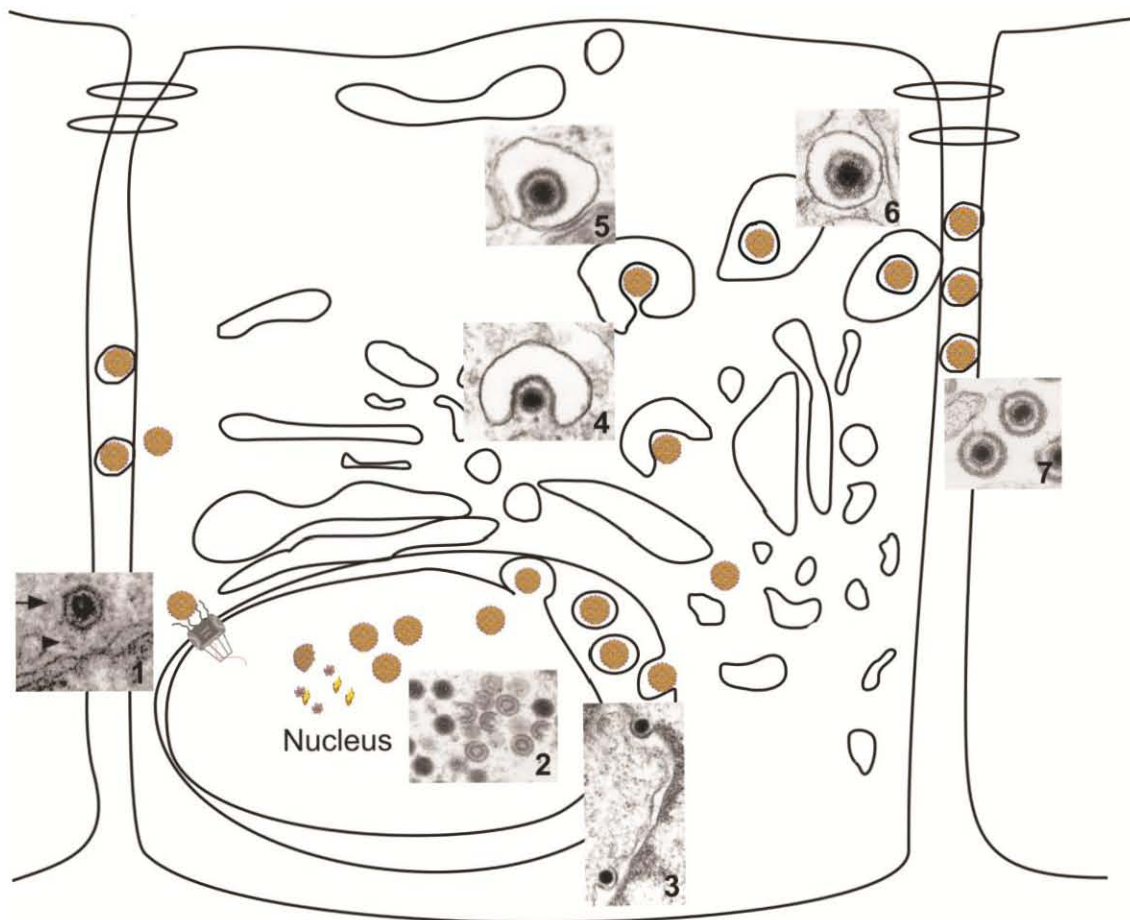
Nucleus

<u>Assembly and envelopment</u>

Capsid assembly occurs in the nucleus (Figure 3-2). Proteins needed for this process are translated in the cytoplasm and transported into the nucleus through the nuclear pore system (159,217). Once the genome has been encased and the capsid attains its icosahedral shape it buds through the inner nuclear membrane. In the process of budding, the capsid acquires a primary envelope. This primary envelope fuses with the outer nuclear membrane releasing a naked capsid into the cytoplasm (Figure 3-3) (67,175). Envelope glycoproteins are processed in the Golgi and appear to move through the typical membrane protein transport system. The Golgi becomes dispersed during infection in many cell types, making the organelle difficult to identify (17). During envelopment the capsid and viral glycoproteins meet on a vesicle that is believed to be derived from the trans-Golgi network (TGN).

This vesicle is identified as TGN due to the fact that several viral proteins independently localize to a compartment that stains for TGN marker TGN46 (9,12,26,33,101,114,187). It is assumed that all incorporated virion proteins must be present at the time of envelopment. Since many proteins are targeted to the TGN, this supports the hypothesis that this is the envelopment compartment. In addition, when viral glycoproteins are retained at the TGN with a 20ºC block during a synchronized infection, capsids are able to exit the nucleus and bind to the surface of the TGN. These bound capsids become infectious when the temperature inhibition is lifted (199). Furthermore, adding inhibitors of Protein Kinase D (PKD) and diacyl glycerol (DAG) (a protein and lipid known to be involved in cargo secretion from the TGN), stops

movement of virus away from TGN labeled compartments (158). Consequently, the

TGN is accepted as the HSV envelopment compartment.

During the process of envelopment several tegument proteins bind to the tails of

glycoproteins and interact with capsid proteins. Those tegument proteins then recruit

additional tegument proteins (116,118). Curvature and budding is induced by

recruitment of proteins of the ESCRT-III complex. In non-infected cells the ESCRT

complex proteins function in membrane budding into the lumen of multivesicular

endosomes- late endosomes that function to store or degrade membrane proteins

(156,196). In an infected cell capsids bud into the envelopment compartment with the

help of certain ESCRT-III proteins (16,27,147). This process is termed secondary

envelopment (Figure 3-4,5). Budding occurs such that the virus attains a double

membrane and morphologically appears as an enveloped capsid within a secretory

vesicle. The outer membrane then fuses with the cell membrane allowing the release of a

virion with one envelope (Figure 3-6,7) (117,175). It is this process of virion trafficking

to the cell membrane and egress on which this work focuses.

Cell Polarization

Polarized cells are defined as such because they have compositionally distinct

plasma membrane domains resulting from fractional sorting of proteins and barriers to

diffusion. Examples of polarized cells include highly differentiated epithelial cells and

neurons. Polarized epithelial cells have two distict domains: the apical domain, which is

the exposed or luminal surface of the cell, and the basolateral domain, which is located

along the sides and bottom of the cell. Around the apical surface, separating the two

domains is a tight junction. The tight junction encircles the cell like a metal hoop around

a wooden barrel. Proteins from one cell zipper with proteins on the other to form a seal

through which molecules of only a certain size and charge can diffuse. This junction

stops proteins and lipids of one surface from mixing with the proteins and lipids on the

other. In addition, the composition of and signaling motifs within proteins direct their

differential trafficking to either the apical or basolateral surface. It is therefore possible

to have two surfaces of different composition- the definition of polarization (88). In

neurons the membrane of the cell body and axon are separated by a region that contains

dense filamentous actin. The structure of this area limits movement of membrane

proteins into the axon (211). Sorting signal sequences and microtubule filament polarity

induce the specific trafficking of axonal proteins into axons (85,169,218). In this way the

neuron is polarized into the axon and somatodendritic regions.

Epidermal Structure

Mucosal tissues are composed of 2 layers: an epidermis consisting of stratified

epithelial cells and an underlying dermis made up of many components including

fibroblasts, adipocytes, and collagen fibers. Separating the two layers is the basement

membrane constructed of extracellular matrix secreted by cells in both layers (70).

Neurons thread through these tissues to receive sensory stimuli. HSV-1 forms lesions

within the upper epidermis. Infection can, in some cases, cross the basement membrane

into the dermis, but most lesions are limited to the epidermis (64,122). Within the

epidermis there are several layers of epithelial cells between the basement membrane and

surface: the basal layer (stratum germinativum), the spinous layer (stratum spinosum), the granular layer (stratum granulosum), and the cornified layer (stratum

corneum) (Figure 4). The vast majority of cells within these layers are keratinocytes. The other cellular components include melanocytes, Langerhans cells, and Merkel cells. The basal layer consists of less differentiated, columnar germinal cells that give rise to the cells in the upper layers. The spinous layer contains both stratified and squamous cells. It is referred to as spinous due to the presence of many desmosomes on these cells; when cells of the spinous layer are pulled apart the desmosomes appear as spines or prickles. The granular layer cells secrete granules into the extracellular space that contain protective lipids and enzymes. Lastly, the cornified layer expresses high levels of keratin to protect the integrity of the epidermal barrier (70). Cells of the basal layer do not have mature cell-cell junctions and are not polarized. As cells move upwards they develop more complex adherens junctions and express tight junctions. Cells near the top of the strata are highly differentiated and fully polarized (123,153,174). When an HSV-1 infection is reactivated from latency, virus spreads though the sensory neuron network to the dermatome enervated by these neurons. The first cells to become infected within the epidermis are basal cells. The infection then spreads to other cells in the strata (142). Egress of HSV-1 has been explored in polarized epithelial cells and polarized neurons, but little work has been done on egress in non-polarized epithelial cells, such as those found in the basal region of the epidermis.

Figure 4: Layers of the Epidermis. Image shows an H&E stain of an epidermal tissue section. Above the dermis and basement membrane there is, in ascending order, the basal layer (stratum basale), the spinous layer (stratum spinosum), the granular layer (stratum granulosum), and the cornified layer (stratum corneum). Cells of the basal layer are columnar in shape. Cells of the spinous layer are both stratified and squamous. Both the granular and cornified layers are squamous in nature. The presence and size of the cornified layer depends on the location of the epidermal tissue. Image is from the UCSF online Dermatology Glossary.

Stratum Corneum

Stratum Granulosum

Stratum Spinosum

Stratum Germinativum
a.k.a. Stratum Basale
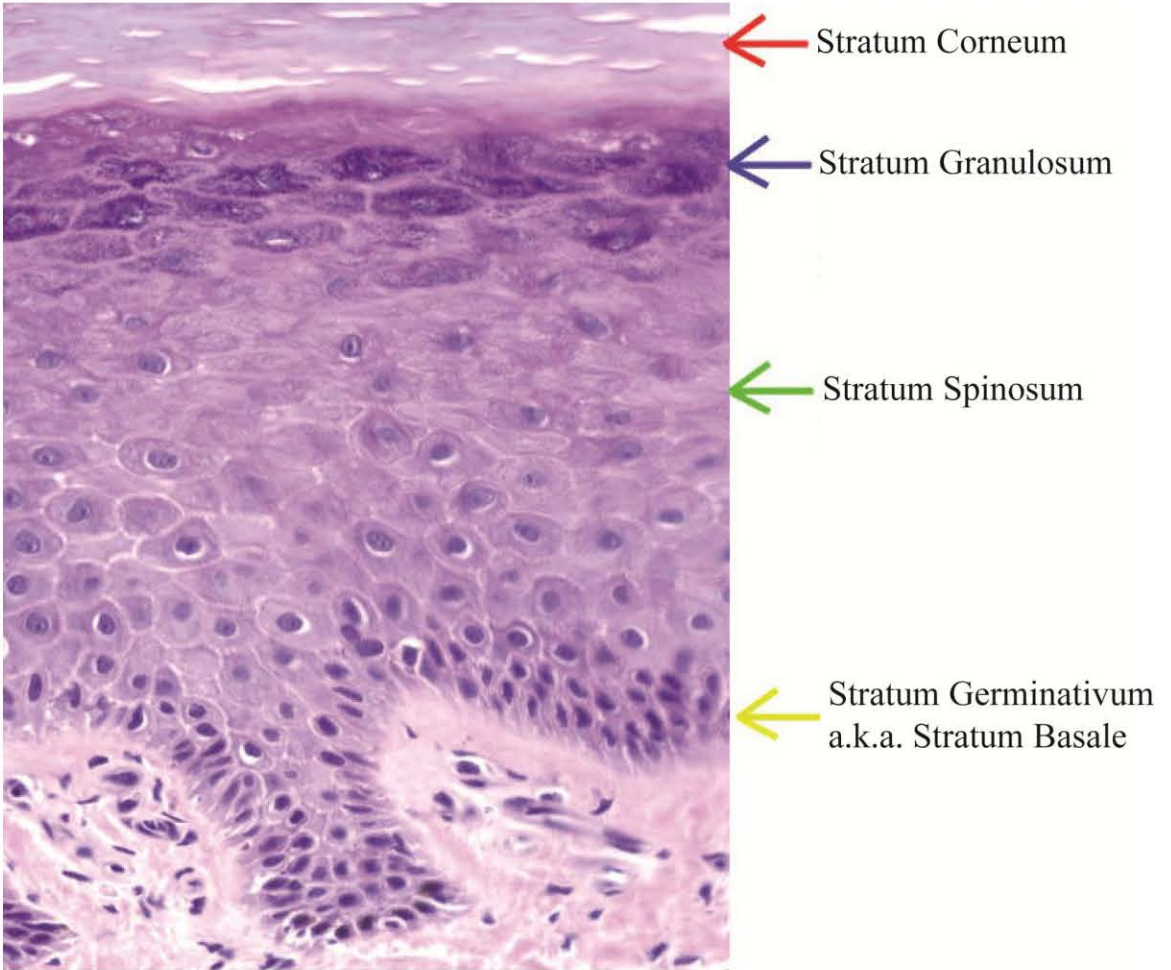
Figure 5: HSV-1 Egress in Polarized Epithelial Cells. Virions are delivered to the intercellular space along lateral cell junctions in polarized HEC-1A cells. Few virions are sorted to the apical or basal surface. Image is from Johnson 2001 (79).
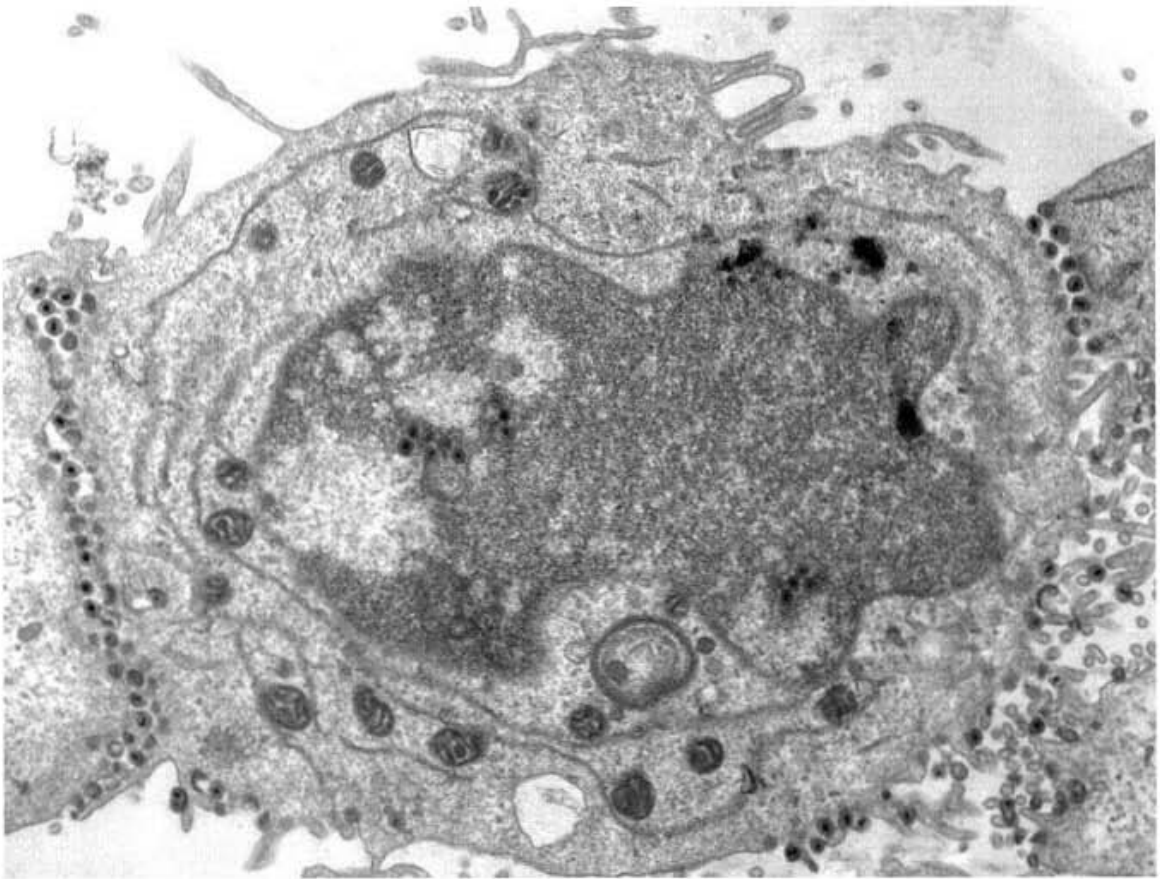
Viral Egress in Polarized Cells

Certain epithelial cell lines can be cultured to form a dense monolayer with high trans-epithelial resistance (TER)- a characteristic of polarization. In a few of these cell lines (HaCaT, HEC-1A, and MDBK), egress of HSV-1 occurs predominantly at lateral cell junctions. Very few virions are seen associating with apical surfaces in electron micrographs of these infected cells (Figure 5). A similar trafficking pattern is seen in less confluent monolayers. Virions go to cell-cell contact points and not free edges (79). It has been hypothesized that this is due to interactions between viral proteins and cellular proteins present at these junctional complexes. Polarized epithelial cells form adherens junctions beneath the tight junctions of adjacent cells. Adherens junctions are composed of a variety of proteins including E-cadherin and nectin, both of which are linked to the actin cytoskeleton through specific adaptor proteins (128). Egress at adherens junctions is advantageous to the virus in two ways. The virus is released into the intercellular space, which is protected from the effects of the humoral and phagocytic immune system. In addition, the newly released virus is in position for gD to bind nectin receptors associated with the junctions (59,78).

There is some evidence to suggest that junctional proteins are involved in viral egress as well as entry. Nectin associates with filamentous actin through a protein named afadin. Two reports have indicated that the nectin-afadin association may be important for cell-cell spread as shown by reduced plaque sizes in epithelial cells when this association is disrupted or afadin is absent (86,164). However, other groups have found that the absence of afadin or afadin binding has no effect on plaque size (48,90). It is,

therefore, yet to be determined if these junctional complexes are involved in viral release. One protein that is indispensable for directed egress and cell-cell spread in epithelial cells is viral glycoprotein E (gE) (39,41,79,151,208,213), which is discussed in detail below. The specificity for egress at cell junctions appears to be dependent on polarization status and junction formation. More highly transformed cells that have lost the expression of E-cadherin have been reported to release virions on all cellular surfaces (79).

HSV undergoes directed egress in neurons, as well. In this cell type, virions are trafficked down axons for release at synapses and varicosities (Figure 6). While some virus is released along dendritic junctions, the majority enter axons for release towards the epidermis. It is not advantageous to direct infection toward the central nervous system (195). HSV-1 has a particularly complicated process of egress in neurons. In this cell type, virions can undergo envelopment in either the cell body or the axon. Electron and immunofluorescence microscopy of infected neurons suggest that assembled capsids can traffic independently of glycoprotein-containing vesicles along axon microtubules (178,215). As unenveloped capsids are rarely seen at synapses, it is likely that envelopment occurs either along the way or at the axon tips (148). A recent report has suggested that culture conditions and neuron type can affect the ratio of enveloped to unenveloped virions observed moving within an axon (215). In addition, the virus can induce the creation of new synapses for viral release (19,31,165,194). The formation of these sites occurs down the length of the axon and is signaled through the action of viral gD. Soluble gD added to neurons can signal their formation, and when neurons are infected with a mutant lacking gD, construction of these sites is blocked (31). The

Figure 6: HSV-1 Release at Neuron Synapses. Electron microscopy images show HSV-1 virions within the growth cones of primary rat neurons. Black arrowheads point to virions. White lozenges in A point to neurovesicles. Bars are 500nm. Images are from Negatsch 2010 (131).
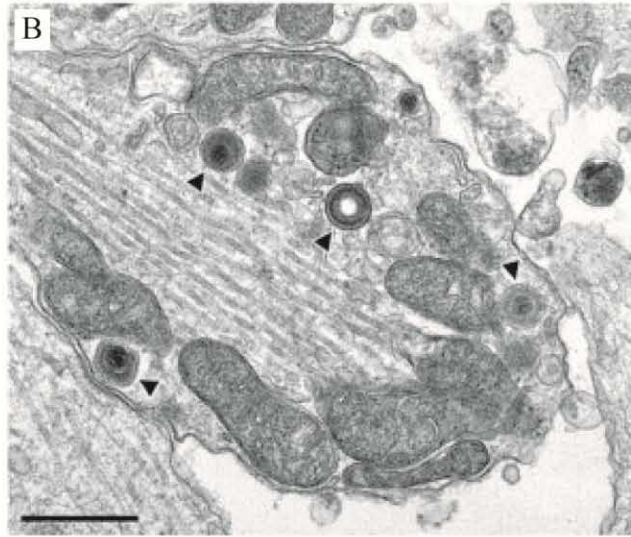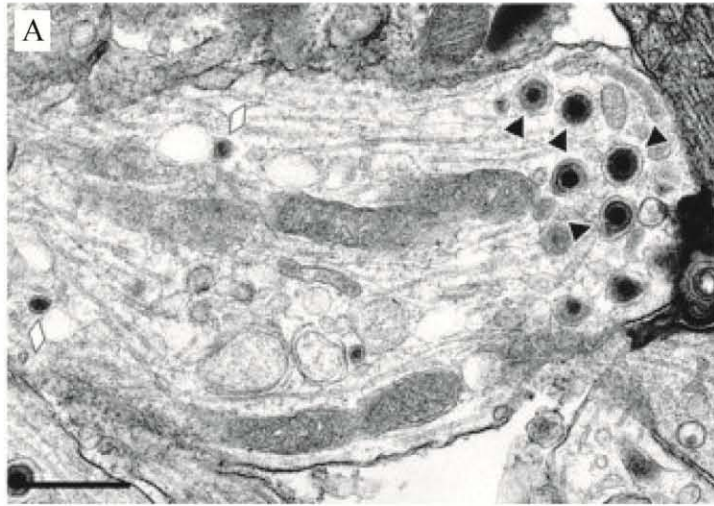
varicosities that form down the axon appear to have synaptic signaling capabilities.

Virions egress at these sites and are transferred to nearby cells (31). In general, synapses

are bounded by puncta adherens- small (0.1 μm or less) junctions containing nectins and

cadherins bound to the actin skeleton (similar to epithelial adherens junctions) (190).

This makes the sites particularly advantageous for release.

Entrance of capsids and glycoprotein vesicles into axons is dependent on viral

glycoproteins US9 and gE (discussed below). US9 appears to only function in neuronal

infections; its depletion has no effect in epithelial cells. This protein is a type II

membrane-anchored protein found in the tegument. Though it is a membrane protein, it

appears to travel with naked capsids during axonal transport. When US9 is deleted, both

glycoprotein containing vesicles and capsids are blocked in the cell body (94,177,193).

They appear unable to enter the axon while vesicles containing synaptic proteins can still

traffic down the axon normally. As virions back up in the neuron cell body, many are

shipped to dendrites that transfer the virus to nearby axons. Mutants lacking US9 are

thus more neuroinvasive.

HSV-1 Glycoprotein E Trafficking

Glycoprotein E (gE) is a 550-amino-acid type I viral membrane protein that has

been found to dimerize with glycoprotein I (gI), a 390-amino-acid type I transmembrane

protein (76). Early during infection gE/gI is found colocalizing with the TGN marker

TGN46 (Figure 7) and is incorporated into newly formed virions in the envelopment

process. As infection proceeds in polarized epithelial cells, the gE/gI complex moves to

Figure 7: gE/gI Cellular Localization as Determined by Immunofluorescence

Microscopy. gE/gI localizes with TGN46 in the TGN early in infection and then moves

with TGN46 to cell junctions labeled with β-catenin late in infection. Image is from

McMillan 2001 (114).
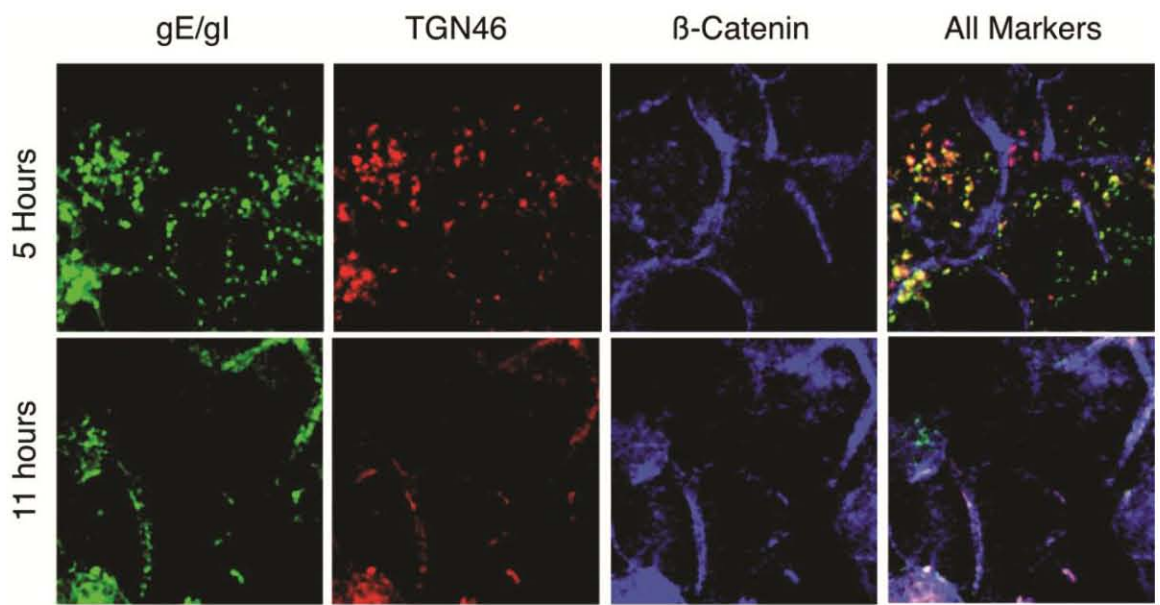
cell surface egress locations, i.e. the cellular junctions (41,53) along with certain TGN proteins such as TGN46 and carboxypeptidase D (Figure 7). This movement can occur with or without the envelopment and trafficking of mature virus (214). Other viral proteins are more widely dispersed over the apical and basal surfaces (41).

Localization of gE/gI to the envelopment compartment is mediated by the cytoplasmic tail of gE (114). When exogenous gE is expressed in uninfected cells it localizes to the TGN without the aid of other viral proteins (41). This is not the case with gE mutants missing the cytoplasmic tail; gEΔCT protein is dispersed among the cytoplasmic membranes with the majority on the plasma membrane (1). During infection with a gEΔCT mutant virus, less gE in the envelopment compartment leads to lower incorporation into the virion (213).

Movement of gE to the cell surface during infection is due to the action of gI. When gI is deleted in infection, gE remains in dispersed cytoplasmic vesicles that colocalize with TGN46 (114). gE containing vesicles appear unable to fuse with or remain at the cell surface. In addition, the cytoplasmic tail of gE contributes to the directed movement to the cell surface. In polarized epithelial cells infected with a gEΔCT mutant, less gE/gI concentrates at the cell junctions. A large amount is dispersed onto other membranes (213). Though gE/gI is highly conserved among the alphaherpesviruses and is incorporated into the virion, the proteins are not essential for replication in culture conditions (213).

<u>Virulence of gE Mutants</u>

When gE or gI is deleted, HSV replicates normally and produces wild type levels

of infectious virions (7,39,40,113,205); virus particles form and are enveloped normally.

However, virulence is severely reduced *in vivo*. The inhibition is believed to occur at the

stage of cell-to-cell spread. When mouse ears were infected with gE or gI deletion

mutants, the infection did not propagate beyond the inoculation site and quickly resolved

(7). Similar results were seen when the corneas of mice and rats were injected with gE or

gI null mutants. Compared to WT infections, much smaller lesions formed in the corneas

and the infection did not spread. Furthermore, wild type virus was transferred to the

brain through the optic nerve inducing encephalitis, but no such dissemination or disease

was seen with the mutants (39,40). The above effects were seen early, before the

development of a humoral immune response. Sequences within the extracellular domain

of gE were found to be necessary for efficient cell-neuron-cell spread in an animal model.

Disruptive linker mutations inserted into areas of this domain (Figure 8) blocked the

formation of zosterform lesions when virus was inoculated into the flanks of mice but did

not appear to affect the function of the protein in other ways. The mutants also did not

spread from the inoculation site into the CNS and cause encephalitis (167).

<u>gE in Epithelial Cell Egress</u>

Evidence for disrupted cell-to-cell spread in ΔgE/gI infections has been observed

in tissue culture systems as well. In several cell lines, plaque sizes are reduced when gE

or gI is deleted (7,205,213). Similar results are seen with a gEΔCT mutant (213). Since

equal amounts of infectious virus are produced in these cell lines, decreased plaque size is interpreted to result from a block in transfer. When polarized epithelial cell lines are infected with wild type KOS HSV virus, released virions are observed associating with cell membrane at the cell-cell junctions (Figure 9). In one study 19X more progeny virions were counted at cell junctions than on the apical surface of infected HEC-1A cells as shown by electron microscopy (79). There were 12.5X more at junctions in MDBK cells. When these cells were infected with ΔgE or gEΔCT virus there was a 17-22X decrease in the number of virions at junctions and a 3-6X increase in virus at the apical surface (Figure 9). In addition, there was a 4X rise in the number of enveloped capsids counted in the cytoplasm concomitant with a 4X drop in the number of virus particles at the cell surface (79). The lack of gE led to a decrease in the number of enveloped capsids released at the surface and a misdirection of virions from cell junctions to apical surfaces in these cell types. In infected HEp-2 and Vero cells, which do not form extensive cell-cell junctions, there was more virus at the apical and basal surfaces compared to the junctions, and this did not change when cells were infected with the gE deletion mutants (79).

The lack of an effect on directed egress when gE is deleted is particularly interesting because it has been reported that plaque sizes are reduced in HEp-2 and Vero cells when they are infected with ΔgE or gEΔCT mutants (7,113,205), though another report disagrees (39). This observed decrease in plaque size when there is no change in release pattern may indicate that the block in cell-cell spread is not completely explained

Figure 8: gE Sequence and Functional Regions. Functional Regions are listed at bottom.

Text color corresponds to highlighted region in/below sequence.

MDRGAVVGFLLGVCVVSCLAGTPKTSWRRVSVGEDVSLLPAPGPTGRGPTQKLLWAVEPLDGCGPLHPSWVSLMPPKQVPET

VVDAACMRAPVPLAMAYAPPAPSATGGLRTDFVWQERAAVVNRSLVIHGVRETDSGLYTLSVGDIKDPARQVASVVLVVQPA

PVPTPPPTPADYDEDDNDEGEDESLAGTPASGTPRLPPPPAPPRSWPSAPEVSHVRGVTVRMETPEAILFSPGETFSTNVSIHAI

AHDDQTYSMDVVWLRFDVPTSCAEMRIYESCLYHPQLPECLSPADAPCAASTWTSRLAVRSYAGCSRTNPPPRCSAEAHME

PVPGLAWQAASVNLEFRDASPQHSGLYLCVVYVNDHIHAWGHITISTAAQYRNAVVEQPLPQRGADLAEPTHPHVGAPPHA

PPTHGALRLGAVMGAALLLSALGLSVWACMTCWRRRAWRAVKSRASGKGPTYIRVADSELYADWSSDSEGERDQVPWLAPP

ERPDSPSTNGSGFEILSPTAPSVYPRSDGHQSRRQLTTFGSGRPDRRYSQASDSSVFW

Signal Peptide
Extracellular Domain
Transmembrane Domain
Cytoplasmic Domain
Proposed gI Binding Domain
Cell-Cell Spread
IgG Binding Region
Tyrosine Sorting Motifs
Highly Phosphorylated Serines
TGN Localization
Envelopment
Trafficking to/Retention@ Junctions

Figure 9: gE Directed Sorting of HSV-1 Virions. In a wild type infection virus is released along cell junctions in HEC-1A cells (top panel). Few virions can be observed along the apical cell surface. However, when HEC-1A cells are infected with a gE deletion mutant, the virus is no longer sorted to the junctions and large amounts of virus can been seen on the apical membrane (bottom panel). Images are adapted from Johnson 2001(79).

HEC-1A-W.t.

1µm

HEC-1A-gE⁻

1µm
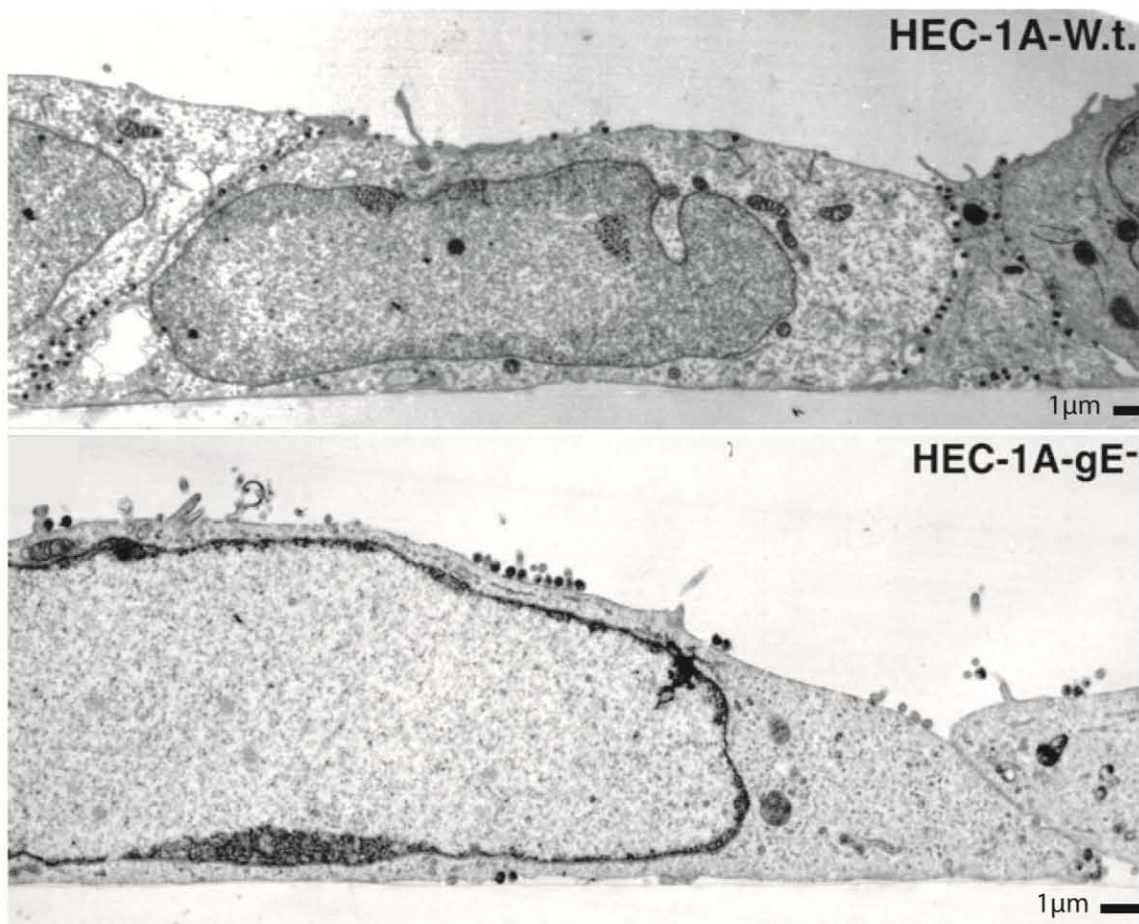
by non-directed egress. Further evidence in support of this possibility was found when polarized epithelial cells were infected with Ad vectors to express exogenous gD, gE/gI, or gEΔCT/gI and then infected with wild type virus. Cells overexpressing gD or gEΔCT/gI produced wild type levels of infectious virus that trafficked to cell junctions but were unable to spread to the adjacent cells. A buildup of 3-4 rows of virions could be seen within the intercellular space, but these particles were unable to enter the next cell. The overexpression of gD on the cell surface presumably sequestered the nectin-1 receptors on the adjacent cell, blocking entry; the number of plaques that formed when virus was added to the cell media was reduced 10X and plaque size was significantly decreased. Therefore, virions egressed normally but were inhibited in entry from both the supernatant and from neighboring cells in cells pre-expressing gD. However, cells overexpressing the gEΔCT/gI protein complex on cell surfaces were as infectable as control cells; the same number of plaques formed, though plaque size was reduced to 35% the size seen in non-expressing cells. Expressing both gD and gEΔCT/gI together did not further reduce plaque size. Infecting gEΔCT/gI expressing cells with a ΔgE mutant also did not lead to an additional decrease in plaque area. Overexpression of WT gE/gI had no effect on either infectivity or cell-cell spread (24). In sum, overexpression of the gE extracellular domain was able to induce a gEΔ phenotype of reduced cell-cell spread without affecting directed egress.

In later studies it was observed that, as with neuronal spread in the mouse flank scratch model, the extracellular domain of gE is necessary for cell-cell spread in cultured epithelial cells (Figure 8). Several mutants were made with small insertions in the

extracellular domain. These folded normally, were incorporated into the virion, and moved to the cell surface but were deficient in cell-cell spread as determined by plaque size reductions (151). Therefore, current evidence suggests that directed movement of virions to egress sites and the process of cell-cell spread in polarized epithelial cells are dependent on sequences in both the extracellular domain and cytoplasmic tail of gE.

<u>gE in Neuronal Egress</u>

gE/gI directs the trafficking of outgoing virus in neurons as well as epithelial cells. This is demonstrated by the reduced spread in animal model neural networks described above. In addition, when primary rat sensory neurons are cultured and infected with a low MOI of virus, spread of infection to nearby neurons is reduced by half when infections are with ΔgE or ΔgI virus (40). Reduced spread is believed to be due to a block in trafficking of viral proteins into the axons.

In the corneal infection model, HSV injected into the vitreous humor infects the retinal ganglia that then traffic newly made virions down their axons to infect post-synaptic neurons. Their axons are long and bundle to form the optic nerve, allowing transport within these axons to be easily visualized. In a wild type infection the optic nerve stains for a variety of viral proteins. However, when retinal ganglia are infected with a ΔgE mutant, capsid proteins, tegument proteins, and glycoproteins cannot be observed in the optic nerve (Figure 10). The neuron cell bodies stain brightly for these proteins, but transport into the axons is blocked. Interestingly, it was found that mutating sequences in the extracellular domain of gE blocked this transport (Figure 8) (18,204).

The extracellular domain is located in the lumen of vesicles with some exposed extracellularly on the neuron body and axon surface. How it functions in directing trafficking is unknown.

In a similar study SK-N-SH neuroblastoma cells were infected with ΔgE, ΔgI, or WT HSV-1 virus. Cells infected with either of the two mutants had 4X fewer capsids visible in the axons (as shown by immunofluorescence) and 1.3X fewer glycoprotein-containing vesicles in the proximal axon portion with 5X fewer glycoprotein vesicles in the distal portion. gEΔCT infected cells had an intermediate phenotype. Reduction in capsid trafficking was seen even though there appeared to be no colocalization between capsids and gE (18,177). This suggests that gE may globally affect transport routes. Interestingly, the block in axon entry observed with ΔgE mutants is very similar to that seen with ΔUS9 mutants. Both proteins appear to regulate the same process. However, ΔgE infections are also inhibited in retrograde dendrite-to-axon spread and this type of trafficking is increased in ΔUS9 infected neurons, indicating that there are key differences (177).

gE in Epithelial Cell-Neuron Spread

In the process of disease dissemination in an HSV-1 infection there is epithelial cell-to-epithelial cell viral transport (to form a lesion) and neuron-to-neuron transport (to establish latency in neural networks). In addition there is epithelial cell-to-neuron and neuron-to-epithelial cell spread. The former occurs during establishment of a primary

Figure 10: gE and Axonal Transport. Fluorescence micrographs of the optic nerves of mouse eyes infected with WT or gEΔ HSV-1. Optic nerves were harvested and stained for glycoprotein, capsid, and tegument antigens. Neurons are labeled in green and HSV antigens in red. Large arrows point to the bundled axons of the optic nerve. Small arrows point to the axon hillock. Ganglia cell bodies would be to the right of the small arrows if shown. Note that viral antigens do not enter the optic nerve in a gE null infection. No HSV proteins were observed in the axons of gE null infected neurons even with a higher MOI and extended infection period. The gE mutant rescue virus restored transport into the axons. Image is from Wang 2005 (204).

	WT Day 5 4×10^2 PFU	WT Day 5 4×10^4 PFU	NS-gEnull Day 8 4×10^5 PFU	Rescued NS-gEnull Day 5 4×10^4 PFU
Polyclonal Anti-HSV				
VP5 (Capsid)				
VP22 (Tegument)				
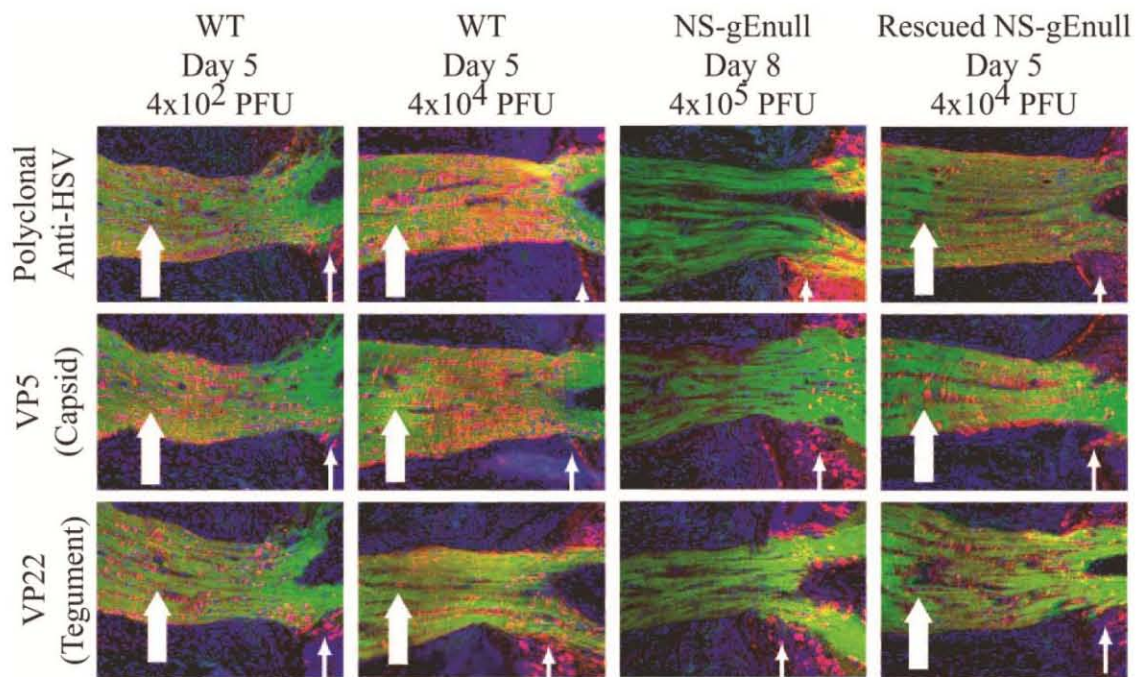
infection and the latter occurs during reactivation of an existing latent infection. Little is known about this form of conveyance other than that gE is necessary for it to occur. In neuron to epithelial cell spread, the inability of ΔgE mutant viral proteins to enter the axon makes trafficking to the epidermis difficult (18,177,204). Additionally, there is also a block in epithelial cell to neuron spread. This has been demonstrated in Campenot culture chambers in which neurons extend their axons through a barrier into an adjacent chamber where epithelial cells are located. It was found that infecting these epithelial cells with ΔgE virus (MOI 5) led to a robust infection that was almost completely blocked from transfer to the neurons through the cell-axons contact sites. ΔgE virus was not inhibited in entry into axons: direct inoculation of axons led to a wild type level infection in the neurons. However, epithelial cell-to-neuron transfer was blocked (113,205). Interestingly, the amount of inhibition in spread to axons seen in these cell types (HaCaT, Vero, HEp-2, HEC-1A, and 293T) corresponded to plaque size reductions when monolayers were infected with ΔgE virus. There was also a correlation with cell polarization status. When HaCaT cells were cultured for a week to form a well-defined monolayer with high TER, fewer neurons were infected than when HaCaT cells were grown for only 24 hours (113). Therefore, current evidence indicates that gE is critical for efficient epithelial cell to neuron spread of infection.

Possible Role for gE in Syncytia Formation

Another form of cell-to-cell spread is syncytia formation. This occurs when viral glycoproteins induce the fusion of two or more cells resulting in multinucleate cells (74). Low levels of syncytia can be observed in biopsies of lesions from patients (11,43,210).

However, virus strains isolated from lesions do not form syncytia in cell culture.

Nevertheless, it is common for syncytial mutants to arise during passage of viral isolates.

The mutations that induce this behavior are often located in glycoprotein B (7,15,23,51).

Likely, viral glycoproteins build up at cell-cell contact points and modify the membrane

to allow fusion. Antibodies specific for several viral glycoproteins can block syncytia

formation (65,138). In addition, several glycoprotein null mutants cannot form syncytia

(29). There is some indication that gE may assist in this process. As with other

glycoproteins, reports suggest that antibodies to gE can block the formation of syncytia in

human fibroblasts. Furthermore, deletion of gE stops fusion in a syncytial background

(7,22,29). The exact role gE plays in cell-cell fusion has yet to be fully explained.

Role of gE in Immune Evasion

Like many viral proteins, gE has more than one function during infection. In

addition to directing viral trafficking and assisting cell-cell spread, gE contributes to

immune evasion. gE with its binding partner gI form a fully functional Fc gamma

receptor (FcR) (46,71). FcRs are typically found on the surfaces of phagocytic cells of

the immune system including macrophages, monocytes, and granulocytes (171). Upon

binding to antigen-linked antibody, clustering of receptors in these immune cells is

induced by phosphorylation of the FcR cytoplasmic tail (57). This phosphorylation

occurs on ITAM motifs that contain specific tyrosine sequences. Once receptors are

clustered, endocytosis is induced and the antigen/antibody complex is internalized for

degradation (188,189). Similar tyrosine sequences can be found on the cytoplasmic tail

of gE (Figure 8). gE associates with gI and binds antibody through its extracellular

domain: soluble gE can bind soluble gI and bind to Fc regions of IgGs (20). Though the Fc binding region of gE is close to the sequences necessary for cell-to-cell spread, they are not overlapping (Figure 8) (167,204,208). gE/gI Fc binding is species specific; it will react with human and rabbit IgGs but not mouse or rat. Histidine 435 between CH_2 and CH_3 of the antibody is important for binding to gE/gI (20), similar to Staph protein A.

Though the gE/gI FcR can bind to nonimmune serum IgGs, it preferentially binds α-HSV IgGs (57). This occurs through a process called antibody bipolar bridging (200). α-HSV antibodies bind to glycoprotein antigens on the cell surface and undergo a conformation or spatial change that increases gE/gI's affinity for the antibody's Fc region. The antibody is then bound to HSV glycoproteins on both the epitope-binding end and the Fc end. Under certain conditions, capping of viral glycoproteins can be observed, and this capping action is dependent on gE. When gE is absent, capping is significantly decreased (55,160). This action may be signaled through gE's cytoplasmic tail, as phosphorylation has been shown to increase with antibody binding (36). Multiple reports have suggested that gE/gI Fc binding is protective for both free virions and infected cells. When pooled human IgGs (containing α-HSV antibodies) were added to infected fibroblast monolayers, titres from ΔgE infected monolayers fell 100-200X compared to wild type (39). Virus with an FcR⁻ mutation decreased infectivity 100-125X when exposed to human α-HSV antibodies and complement while wild type virus infectivity decreased only 2-3X. There was no difference in neutralization when the experiment was repeated with mouse antibodies, indicating that it is Fc binding that is

conveying this protection. The same group infused wild type and FcR$^-$ infected mice with human α-HSV antibodies. Wild type virus-infected mice had much lower disease scores than FcR$^-$ virus-infected mice (129). Therefore, gE affects antibody neutralization in an active infection.

gE in Envelopment

During the process of envelopment, multiple proteins interact to anchor the envelope onto the tegument and capsid. Deleting any one glycoprotein does not significantly affect virion envelopment. However, deleting in combination helps expose redundant functions. gE deletion and gD deletion mutants replicate and undergo envelopment normally. However, deleting both proteins results in a block in maturation. Unenveloped virions accumulate in the cytoplasm along with aggregated tegument (52,54). The tegument proteins with which the cytoplasmic tail of gE interacts are believed to include VP22 and UL11 (54,136,185).   When gE and gD are not available to promote membrane-tegument interactions, envelopment does not occur.

gE and Protein Localization

In addition to assisting the process of envelopment, gE can affect the localization of viral proteins with which it does not directly interact. Viral protein ICP0 is an example. It is found in the nucleus early in infection and disperses in the cytoplasm late. ICP4 is found specifically in the nucleus. In a ΔgE or ΔgI infection, these proteins are found in cytoplasmic aggregates throughout infection. It appears that shuttling to the nucleus is a dynamic process and removing gE/gI blocks it (82). gE also affects the

distribution of IP3R-I (inositol triphosphate receptor-I), an intracellular Ca^{2+} channel. In uninfected cells the IF staining for IP3R is light and diffuse. However, during infection with HSV-1 the distribution changes and IP3R is found in perinuclear aggregates. Infection with a ΔgE mutant blocks this redistribution; IP3R remains dispersed. Furthermore, expressing exogenous gE/gI in HEp-2 cells induces IP3R to aggregate as in infected cells. These concentrations occasionally colocalize with gE, but colocalization is not extensive (83).

Sorting/Signaling Motifs in the Cytoplasmic Tail of gE

The cytoplasmic tail of gE has several possible sorting and signaling motifs (Figure 8). It has two canonical tyrosine YXXØ motifs (X is any amino acid and Ø is any hydrophobic residue). Such motifs can be phosphorylated by tyrosine kinases and recruit proteins for the induction of downstream signaling events (87,95,98,170). In addition, sequences such as these are known to interact with the μ subunit of AP clathrin adaptors to induce endocytosis from the cell membrane or sorting into vesicles at the trans-Golgi for trafficking to the basolateral membrane (44,105,186). When the cytoplasmic tail of gE is deleted the protein relocates from the TGN to the cell membrane (1). In addition, splicing the tail of gE onto gD caused it to relocalize from the cell membrane to the TGN (114). This suggests that an endocytic motif within the tail is active. Observations of different gE truncation mutants have suggested that the first tyrosine motif (463-466) is responsible for endocytosis and TGN localization (1,53). Though there have been reports of tyrosine phosphorylations in gE homologs (36), studies have suggested that gE isolated from the lysates of HSV-1 infected cells is only

phosphorylated on serines, not threonines or tyrosines (213). In fact 80% of the

phosphorylations are on serines 476,477, and 479 (120,213). These serines are within an

acidic region that appears to be a casein kinase recognition sequence (Figure 8). Casein

kinase recognition motifs can be phosphorylated by a ubiquitous serine/threonine kinase

named casein kinase II (CK2), which is involved in a wide range of cellular processes. It

has been found that transfected gE can be phosphorylated by cellular kinases and that

CK2 can phosphorylate gE in *in vitro* protein experiments (120,136). The role of these

phosphorylations is unknown; virus with gE constructs lacking those 3 serines spread

quite well and gE appears only slightly mislocalized (1,213). Future studies will

determine what role gE's tyrosine motifs, CK2 recognition sequence, and other

phosphorylated serines play in infection.

II. Statement of Purpose

A virus has one goal: to spread and produce progeny virions. Millions of years of coevolution between viruses and hosts have resulted in highly efficient infections. This efficiency can be seen in the process of egress. There is little benefit to random viral release in most *in vivo* systems. Therefore, viruses have developed a myriad of ways for directed release onto or near uninfected cells. For example, there have been reports of viruses that are released in between contacting cells, viruses that can be transferred from the surface of a parent cell to an uninfected cell as part of a biofilm-like structure, viruses that are propelled between cells on actin tails, and viruses that can travel down nanotubes to uninfected cells (50,145,176,181). Herpes Simplex Virus is a ubiquitous pathogen in the human population that can at times induce life-threatening encephalitis. It infects highly polarized and less polarized epithelial cells of the dermis as well as the sensory neurons that innervate these areas. In polarized epithelial cells the virus is released at cell junctions in close proximity to the adjacent cell region that is enriched in HSV receptors. In neurons the virions are released in synapses where they can enter the contacting neuron dendrite efficiently. These cell types are difficult to culture and the junctions are challenging to clearly visualize. Egress in less polarized cells has not been extensively studied. During reactivation from latency, virus first spreads to the less differentiated non-polarized cells within the basal layer of the epidermis before moving to the polarized epithelial cells within the strata. Not only are non-polarized cells physiologically relevant, but they are easier to culture and infect and thus, serve as a convenient model for study. The purpose of the research described herein was to characterize the formation

and morphology of egress locations in non-polarized cells to help clarify this process in this and other cell types. As viral mutants that affect the process of egress have shown, inhibiting this step can be highly effective at blocking dissemination of infection. A clear understanding of HSV release is the first step in developing a drug to inhibit it.

III. Experimental Procedures

Cells and Viruses

Vero African Green Monkey kidney cells, HeLa epithelial cells, and HEC-1A

endometrial cells were grown in DMEM (Gibco) with 10% FBS (Atlanta Biologicals).

Cells were incubated at 37°C in 7% CO_2 and passaged every 4-6 days with a media

change at day 2. Viruses used were the K26GFP (VP26-GFP) mutant developed by

Prashant Desai (32), KOS-HSV-1, and the KUL25NS mutant (ΔUL25) developed by

Fred Homa (115). Both the K26GFP mutant and the WT KOS HSV were passaged on

Vero cells. gE mutants whose development is described below were passaged in a

similar manner on Vero cells. The ΔUL25 mutant stocks were made on the 8-1

complementing cell line (115).

Antibodies

gB (DL16) and gD (DL11) monoclonal antibodies were a kind gift from Gary Cohen and

Roselyn Eisenberg. Each was used at a 1:1000 dilution in 1% BSA. gE polyclonal

antibody was generously provided by Harvey Friedman. It was used at a 1:6000 dilution.

8F5 monoclonal antibody (197) was used to label major capsid protein VP5 at a 1:1500

dilution. Commercially available antibodies were monoclonal anti-α-tubulin (Sigma

T6074) 1:1000 and monoclonal anti-vinculin (Sigma V-9131) 1:600. Actin was labeled

with Texas Red-X phalloidin (Invitrogen T7471) at 1:500 in PBS. Rhodamine-labeled

wheat germ agglutinin (WGA) was obtained from Vector Laboratories (RL-1022),

Burlingame CA, and diluted to 2.5ug/ml in PBS. Alexa Fluor 594 goat anti-mouse IgG

(Invitrogen A11005) and Alexa Fluor 488 goat anti-mouse IgG (Invitrogen A11001) were the secondary antibodies used throughout. They were used at a 1:1000 dilution.

Infection Protocol

Cells were plated on glass coverslips in 6-well plates at 3×10^5 cells/well. 24 hours later cells were infected on ice (MOI of 10 unless otherwise stated) in 1% FBS DMEM media for 1 hour. Cells were then warmed for 1 hour at 37°C following which they were acid washed (40 mM citric acid, 10 mM KCl, 135 mM NaCl, pH 3) for 1 minute to inactivate extracellular virus (14). Acid was removed with 3 rinses in warm 1% FBS DMEM media and cells were returned to 37°C. Cells were fixed at noted times with 4% PFA for 10 minutes. Those that required antibody staining were permeabilized with 0.2% Triton X-100 5 mins/RT and incubated in blocking buffer (10% goat serum and 1% BSA in PBS) for 1 hour/RT.

Electron Microscopy

At 12hpi, coverslip grown Vero cells infected as described above were fixed in 2.5% glutaraldehyde for 12 hours. Samples were then post-fixed for 30 minutes in 1% (w/v) osmium tetroxide, dehydrated in increasing concentrations of ethanol, and infiltrated with epoxy resin (EPON-812, Electron Microscopy Sciences, Inc). Embedding was achieved by inverting epoxy filled BEEM capsules onto the coverslips. To remove BEEM capsules with the embedded samples from coverslips, samples were transferred between liquid nitrogen and boiling water, causing the glass coverslip to separate from the resin. Ultrathin sections (70-80 nm) prepared on a Leica Ultracut UCT ultramicrotome using a

Diatome diamond knife were collected on 200 mesh copper grids and contrast stained

with lead citrate and uranyl acetate as described previously (134).   Images were recorded

on film using a Philips 400T transmission electron microscope operated at 80,000 eV.

Immunofluorescence Microscopy

TIRF images were obtained on an inverted IX70 Olympus microscope with a 1.45 NA

(oil) Plan-Apochromat 60× TIRFM objective lens, fitted with a Ludl modular automation

controller (Ludl Electronic Products) operated by MetaMorph software (Invitrogen).

Images were acquired with a charge-coupled device camera (Retiga Exi; Qimaging).

Confocal images were taken on a Zeiss LSM 510 scanning confocal microscope with use

of a Plan Apochromat 100x/1.4 na oil immersion lens. Samples were excited with an

argon laser and a 543 nm HeNe laser with PMT image detection.

Nocodazole/Cytochalasin B/Blebbistatin Treatment

4, 8, or 11.5 hours post infection either 1.7 µg/ml cytochalasin B (Sigma C6762), 10

µg/ml nocodazole (Sigma M1404), 50µM blebbistatin (Sigma B0560), or equal volumes

of DMSO (Fisher BP231) dissolved in 1% FBS DMEM were overlaid onto infected Vero

cells. All three drugs were solubilized in DMSO. At 12hpi cells were fixed in 4%

paraformaldehyde 10mins/RT and processed for immunofluorescence microscopy. In a

second experimental design, cells that were treated with cytochalasin B at 11.5hpi were

rinsed at 12hpi with 2 rinses in PBS and 2 rinses in warm 1% DMEM media. Incubation

then continued at 37°C until 12.75 hpi. At this time cells were fixed with 4%

paraformaldehyde and processed for immunofluorescence microscopy.

Image Analysis

TIRF images of 20-30 cells per sample set were analyzed with ImageJ software. The
pixel area was calculated for both the total cell area and the patch areas as determined by
WGA staining. Virion density was determined by transferring the outlines of these areas
determined on combined channel images onto the green channel pictures. Background
was subtracted in these pictures by using the rolling ball algorithm (182) and setting the
radius to 50 pixels. Integrated density was then calculated and divided by the area in
question. P-values were calculated using t-Test for 2-samples assuming equal variances.
$P(T<=t)$ two-tail results were used for verification of statistical significance.

Determination of Viral Output

To determine the effect of the noted treatments/conditions on the amount of infectious
cell-associated and released virus, both supernatants and cell samples were collected.
Infected cells were frozen 2X and placed in a bath sonicator for 5 seconds. Titre was
then determined by limiting dilution assay with a 4% agar overlay. On day 3, plaques
were detected by a 5-hour incubation in 0.5 mg/ml Thiazolyl Blue Tetrazolium Bromide
stain (Sigma M2128).

Construction of Recombinant HSV gE Mutants

A bacterial artificial chromosome (BAC) containing the HSV-1 KOS strain genome was
used to generate recombinant viruses. The detailed protocol has been described
previously (6). A gE-null mutant (gEΔ) was made by replacing the gE start codon ATG
with stop codon TAA. Similarly, a gE cytoplasmic tail deletion mutant (gEΔCT) was

generated by adding two copies of stop codon (TAATAA) between residues W446|R447, right after the transmembrane domain. gEΔCTrescue virus was generated by removing the stop codons. Correct clones were verified by HindIII digestion, PCR analysis and DNA sequencing of the corresponding region. The resulting BAC plasmids were purified and then transfected into Vero cells with lipofectamine 2000. After the appearance of cytopathic effects (3- 4 days), transfected cells were harvested and used to infect new Vero cell monolayers in order to produce a viral stock.

Analysis of gE Mutant Expression and Virion Incorporation

Vero cells were infected with wild type HSV or gE mutants at an MOI of 5. To analyze gE expression, the media were collected at 16-20 hours post infection, cleared at 2,500 rpm for 10 min, and then centrifuged at 26,000 rpm for 1 h at 4°C in a Beckman SW41 rotor through a 30% (wt/vol) sucrose cushion (1.7 ml). The pellets were dissolved in 100 μl 1xSDS-PAGE sample buffer, and equal quantities of virus were loaded into an SDS-PAGE gel for Western blot analyses. The infected cell lysates were also analyzed for the expression levels of gE and its mutants. Blots were stained with α-gE polyclonal antibody (see above) at a 1:6000 dilution.

IV. Adapted from:

Replication of Herpes Simplex Virus: Egress of Progeny Virus at Specialized Cell Membrane Sites

Rebecca M. Mingo[1], Jun Han[2], William W. Newcomb[1], Jay C. Brown[1*]

[1]Department of Microbiology, Immunology, and Cancer Biology, University of Virginia, Charlottesville, VA, USA

[2]Department of Microbiology and Immunology, Penn State University College of Medicine, Hershey, PA, USA

In the following work Jun Han created the gE mutants and William Newcomb obtained the electron microscopy images. Rebecca Mingo performed all other experiments.

Acknowledgements

INTRODUCTION

To ensure efficient transmission and replication, many viruses have developed mechanisms for directed spread (reviewed in (126)). As infection moves from cell to cell, it is more advantageous for a virus to be released at locations adjacent to sites of entry than travel to entry sites after egress. Although many viruses share common pathways in the process of directed spread, each virus is unique in its approach (56,78,100,144,145,198,221).

The virion of HSV-1 is composed of 3 layers: an inner capsid, a composite of proteins that form the tegument, and a host derived envelope with incorporated viral glycoproteins (see chapter I). DNA is packaged into the capsid in the nucleus, but the virus undergoes envelopment in the cytoplasm (75,118). In the process of envelopment the capsid encounters viral glycoproteins on a vesicle that is believed to be derived from the TGN (114,158,187,199). The capsid buds into the vesicle acquiring an envelope and an outer vesicular membrane. This virus-containing vesicle then moves to the plasma membrane where it fuses releasing a mature enveloped virion. Most released virions remain cell-associated until very late in infection (135).

In a natural infection, HSV infects epithelial cells of mucosal surfaces and then moves on to establish latent infections in the sensory neuronal network that innervates these areas. Mucosal tissues consist of highly polarized epithelial cells in the apical layers of the epidermis as well as less differentiated cells in the basal regions. It has been suggested that infection spreads cell-to-cell in different directions depending on a cell's

location in a tissue layer and the cell's differentiation status (124,142,221). Virus is released at cell junctions in highly polarized epithelial cell lines (79). Within a tissue this would allow rapid spread through the monolayer and the formation of a lesion or cold sore. In neurons, newly formed virions are released at synaptic terminals and at virally induced varicosities (31,37). This allows swift movement through neural networks, back to epithelial surfaces where replication is reinitiated in an area that is advantageous for host-to-host spread. Directed egress in less polarized cells of the epidermis has not been extensively examined, although previous electron microscopy studies have suggested that virus is randomly released in this case (79). In both polarized epithelial cells and neurons, directed spread of the virus is dependent upon viral glycoprotein E (gE) (7,39,40,79,112,113,204,205,213).

gE is a transmembrane protein that forms a dimer with gI (76,77). Early during infection gE colocalizes with TGN46 in the trans-Golgi network, while at late times gE moves to cell junctions in polarized epithelial cells (41,114). Although gE is not essential for HSV-1 growth in culture, virus mutants lacking gE are severely limited in spread *in vivo*. The inhibition appears to occur after envelopment, as mutants produce the same amount of infectious virus as WT HSV-1 (7,39,40,113,205). In highly differentiated, polarized epithelial cells, virus lacking gE becomes randomly released rather than specifically directed to cell junctions, and virus spreads cell-to-cell much less efficiently (79,213). In addition, progeny virus is unable to transfer from infected epithelial cells to neurons, even though ΔgE mutants are not inhibited in neuron entry (113,205). In

neurons infected with a ΔgE mutant, virus cannot efficiently enter into and traffic down axons (112,177,204). Infection is, therefore, much more limited.

In the study described here, we examined the process of HSV egress as it occurs in a non-polarized epithelial cell line. In contrast to our expectation of random release based on earlier work (79), we observed that progeny virus was released at specific sites on the plasma membrane. These sites were concentrated along the substrate-adherent surface of the cell as well as cell-cell contact areas despite the lack of mature junctional complexes at these locations. EM, confocal, and TIRF microscopy were employed to characterize the formation and expansion of egress sites along the substrate-adherent surface of the infected cells. The location of viral release sites allowed a clear visualization of the spatial relationship between the cell surface and the released virions using TIRF microscopy. This model will be useful for studying many different aspects of HSV-1 fusion and release.

RESULTS

Virus egress occurs at specific sites on adherent surfaces of Vero cells. In the present study, electron microscopy was used to observe egress of HSV-1 virus in Vero cells. Glass-grown Vero cells were infected at an MOI of 10, and at 12 hours post infection cells were fixed on coverslips and processed for thin sectioning. At this time point, progeny virions that were not transferred to nearby cells remained associated with the parental cell surface (Figure 11), so the release pattern could be visualized. Micrographs showed that at 12 hpi, the majority of virions were observed at specific areas on the cell surface, rather than in a randomly dispersed release pattern (Figure 12). These regions were located at cell-cell contact sites and at areas along the adherent cell surface. At both the substrate-adherent surface and cell-cell contact site egress locations, additional membrane was present allowing a curvature in the membrane at the site and the creation of a pocket-like structure (Figure 12(A-C)). This was not the case in the uninfected cell samples; the adherent cell membrane of mock infected Vero cells was tightly apposed to the coverslip surface (Figure 12(E-F)). Although many virions were observed exterior to the plasma membrane, none were observed along the interior of the membrane (Figure 12(A-D). The few virions seen on the apical surface were in areas adjacent to cell-cell contacts (Figure 12(D)). Similar results were obtained whether the cells were in a confluent monolayer or if they were less densely plated. This observation suggests that movement of virions to the substrate adherent surface was not induced by a lack of available cell-cell adherent surfaces.

Figure 11: HSV-1 Titre at Spaced Timepoints During Infection. Supernatant and cell

lysates were collected from 2-12 hpi. Titre is represented as PFUs/ml. Note that

infectious virus is first detectable between 6 and 8 hpi, and little virus is released from the

cell surface into the supernatant during this time course.

Titre Timecourse
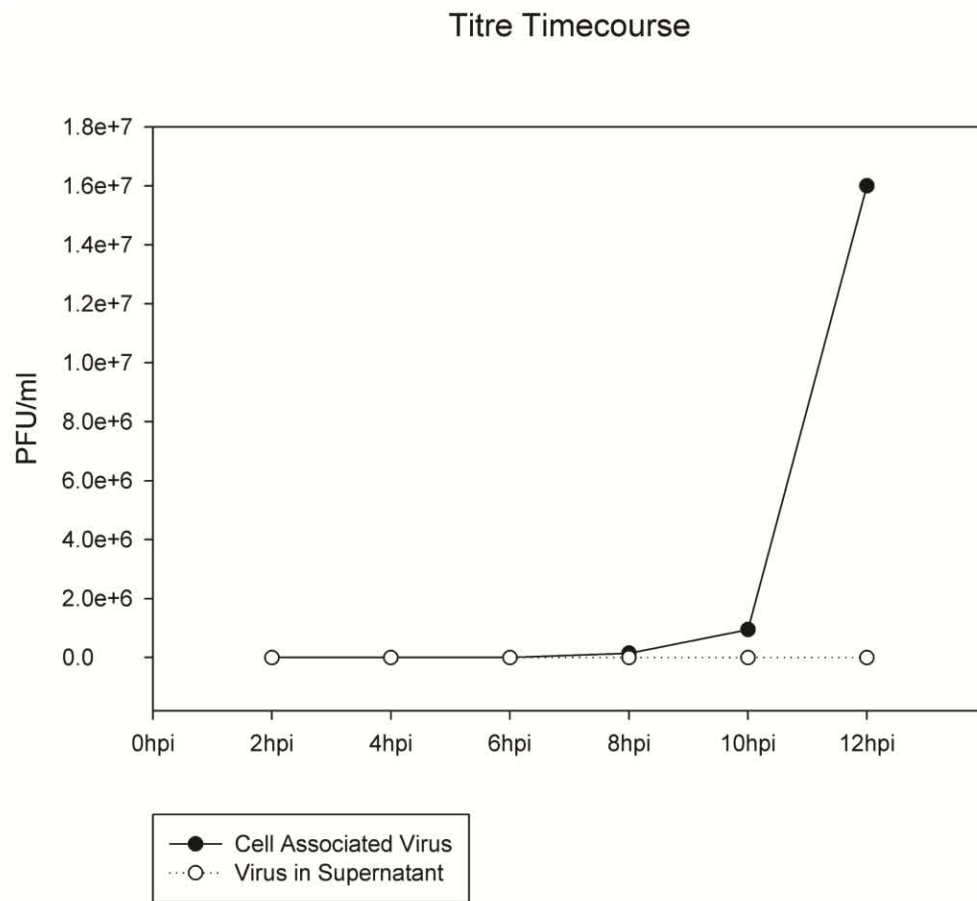
Figure 12: Location of progeny virions in HSV-1 infected Vero cells. A-D) Thin section electron micrographs of infected Vero cells fixed and processed on coverslip at 12hpi. Note the majority of virions are released in pockets along the adherent cell surface (arrowheads) and cell-cell contact points (arrows) with some virus above cell-cell contacts (bracket). B is an enlargement of the left arrowhead in A. C is an enlargement of the right arrowhead in A. E-F) Micrographs of mock infected Vero cells. Note that, unlike infected cells, cell membrane is closely apposed to the coverslip edge.

(G) Consecutive Z-stack confocal images of a representative Vero cell infected with VP26-GFP mutant virus. Sections begin at the coverslip and go up by 0.25 μm increments. Asterisks mark the two sections above the coverslip where the majority of virions can be seen attached to the bottom cell surface. Other sections have far fewer virions. The nucleus (containing VP26-GFP labeled capsid assembly areas) is outlined. Arrows indicate virus released along a cell-cell contact. Images were obtained with a Philips 400T transmission electron microscope (A-F) and a Zeiss LSM 510 confocal microscope with an inverted 100X lens (G).

A

B

C

D

E

F

G   Slice 1   Slice 2   Slice 3   Slice 4

Slice 5   Slice 6   Slice 7   Slice 8
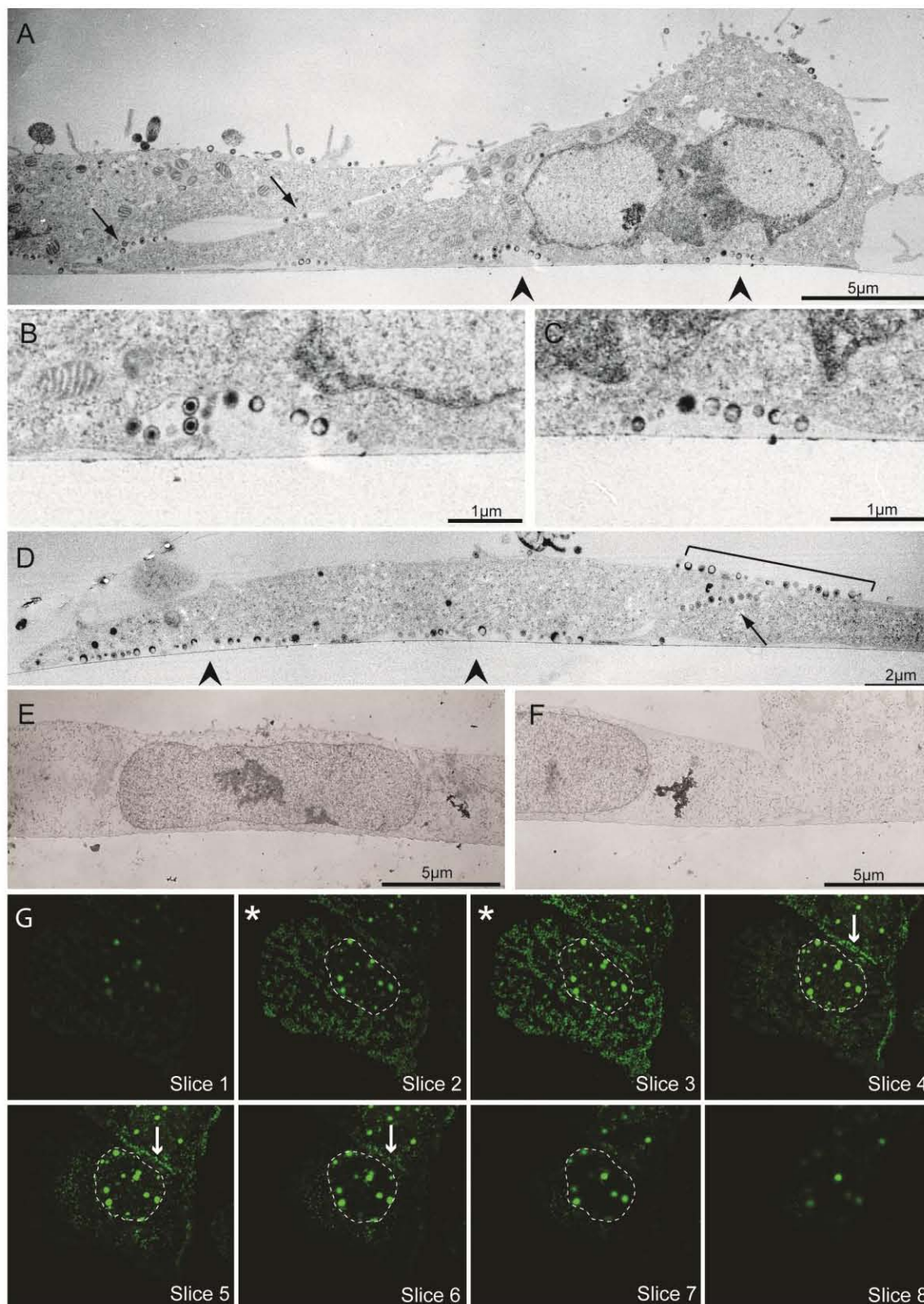
Confocal microscopy was utilized to analyze the release of virions in larger

numbers of infected Vero cells. Cells grown on glass coverslips were infected at an MOI

of 10 with a capsid-tagged VP26-GFP mutant (K26GFP) and fixed at 12 hpi. Confocal

Z-stack images showed that GFP-labeled virions were concentrated along the adherent

surfaces of cells. A representative series is shown in Figure 12(G). Most virions were

detected at the two planes closest to the coverslip (those marked by an asterisk). The

majority of those that were visible above those planes were located at cell-cell contact

points (Fig 12(G), slice 4-5 arrows). The large GFP-containing areas are capsid assembly

compartments located in the nucleus (inside the dotted lines). At late time-points in

infection, cells exhibited a more pronounced cytopathic effect with loss of cytoskeletal

structure and cell rounding. From 16 hpi onward polarity in virus trafficking was no

longer apparent (data not shown), and most cell surfaces were covered in virions. In the

following work I further characterize the egress sites that form along the coverslip-

adherent cell surface.

Viral egress sites are enriched in glycoproteins. We found that, due to a high

cytoplasmic signal of viral proteins, egress sites along the adherent cell surface were best

visualized using total internal reflection fluorescence microscopy (TIRF). This method

allowed the area of excitation to be restricted to a small plane above the coverslip. A

standard TIRF field is 70-300 nm above the coverslip. The angle of the laser can be

adjusted to obtain the desired excitation field within this range (168). In the following

studies, the laser was set at the maximum angle to allow excitation of the largest area

possible. Therefore, the area of emission in these studies was approximately 300 nm above the coverslip.

Using TIRF microscopy, we found that GFP-labeled virions clustered at specific sites along the adherent cell surface in a similar manner to that observed with EM (Figure 13). In addition, infection induced the modification of the membrane at these egress locations. Wheat germ agglutinin (WGA) binds to N-acetylglucosamine and N-acetylneuraminic acid (sialic acid) residues on glycoproteins (150). When infected Vero cells were fixed and stained with rhodamine-labeled WGA it was observed that the viral release sites stained much more strongly than the surrounding cell membrane (Figure 13(A)). This indicates that the regions of the membrane where cell-associated virions were observed had a much greater concentration of glycoproteins. Such focal concentrations were absent in uninfected cells where the WGA stain was light and diffuse (Figure 13(D)). There were often several viral egress "patches" per infected cell, yet cells with a single large patch were also seen. Patches could be expansive and were often observed along the peripheral cell edge. Many glycoprotein-staining patches resembled a donut in shape (arrowheads). This phenomenon was due to the pocket-like structure of these sites. The "holes" in the donuts were the result of the membrane rising above the 300nm excitation limit in the center of the patches.

Viral glycoproteins were found to be concentrated in the WGA-staining patches. Infected Vero cells were fixed at 12hpi and stained with α-gB or α-gD monoclonal antibodies (Figure 13(B-C)). Both glycoproteins were found in greater amounts in the

Figure 13: Glycoprotein enrichment at adherent surface egress sites. TIRF micrographs of

(A) VP26-GFP HSV-1 infected Vero cell at 12hpi stained with rhodamine-conjugated

WGA to mark glycosylated proteins. As in EM pictures, GFP-labeled virions were found

to cluster at specific sites along the cell surface. Note that glycosylated proteins

accumulate at these sites. (B) VP26-GFP HSV infected Vero cell at 12hpi treated with α-

gB (DL16) antibody. (C) VP26-GFP HSV infected Vero cell treated with α-gD antibody

(DL11). Alexa-594 conjugated secondary antibodies were used in B and C. Staining

indicates that viral glycoproteins are components of the egress site membrane.

Arrowheads mark two egress sites where the pocket-like structure of the sites is apparent.

The holes in the "donuts" are areas where the membrane has extended beyond the 300nm

excitation range. Virus is rarely visible in the holes, indicating that virions are closely

bound to the cell membrane. (D) Mock infected Vero cell stained with WGA shown at

that same exposure as infected cell in A. Cell edge is outlined. Outline of cell was

determined by increasing the brightness of the image until cell edge was visible.

Virus | WGA | Merge

Virus | α-gB | Merge

Virus | α-gD | 10μm | Merge

WGA
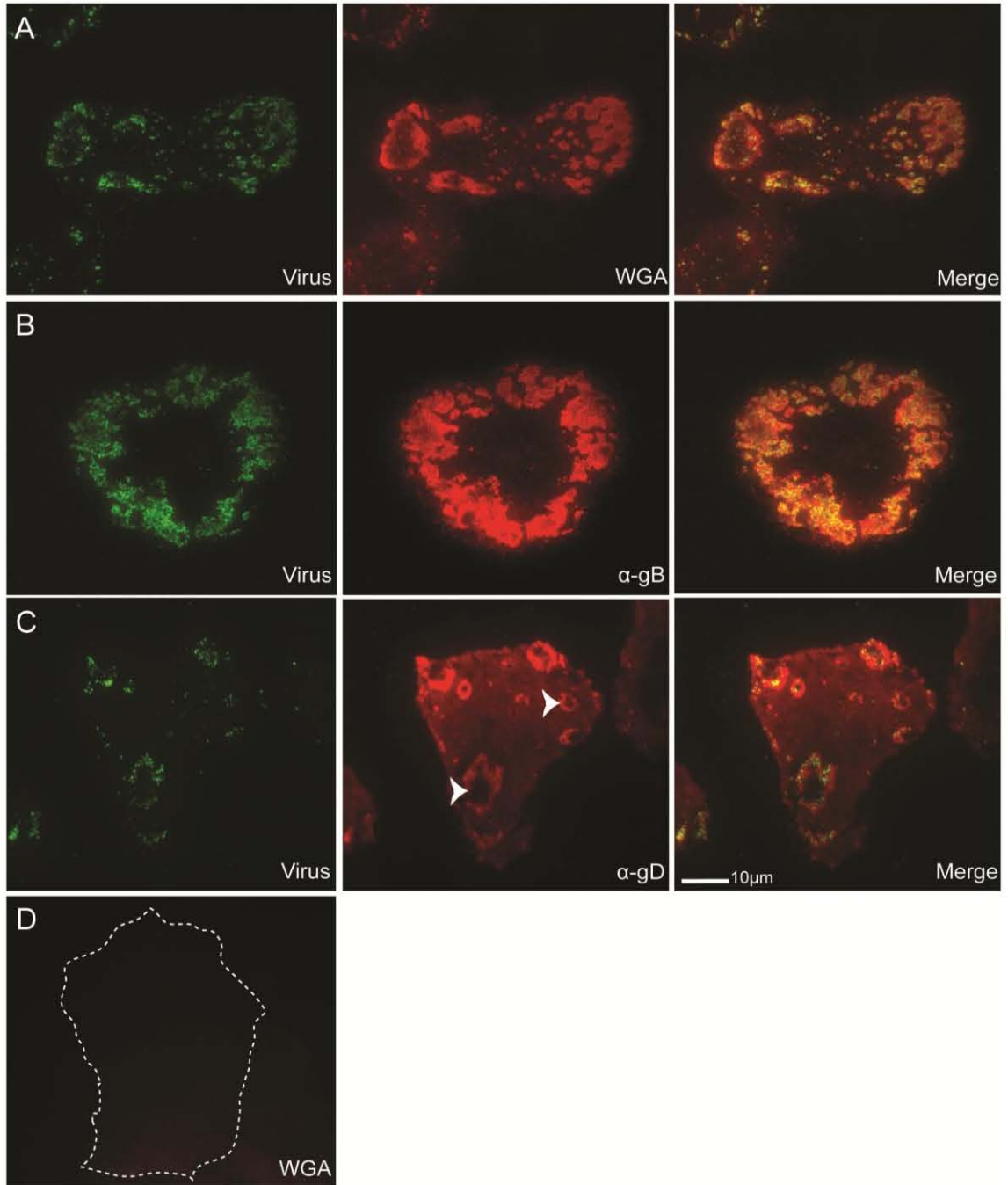
Figure 14: Formation of adherent surface egress sites in non-polarized and polarized cell types. (A) VP26-GFP HSV infected HeLa cells stained with WGA. Note that patches of glycoproteins are visible by TIRF microscopy along the adherent surface of this non-polarized cell. (B) VP26-GFP HSV infected HEC-1A cells stained with WGA. No glycoprotein patches are visible along the basal surface as shown by TIRF microscopy. Bottom panels in both A and B depict the wide-field view of the same cell shown by TIRFM. Green signal within the outlined nuclei labels the VP26-GFP positive capsid assembly compartments. The nuclear GFP signal in B is of equal or greater intensity than the signal shown in A, indicating that the lack of visible patches in B is not due to a lower infection level. Though little glycoprotein staining was observed along the basal surface in HEC-1A cells, glycoproteins accumulated at cell junctions (arrow), the reported site of egress in this cell type. These results suggest that non-polarized but not polarized cells form egress sites at the adherent cell surface.

HeLa Cells (Non-polarized)

HEC-1A (Polarized)
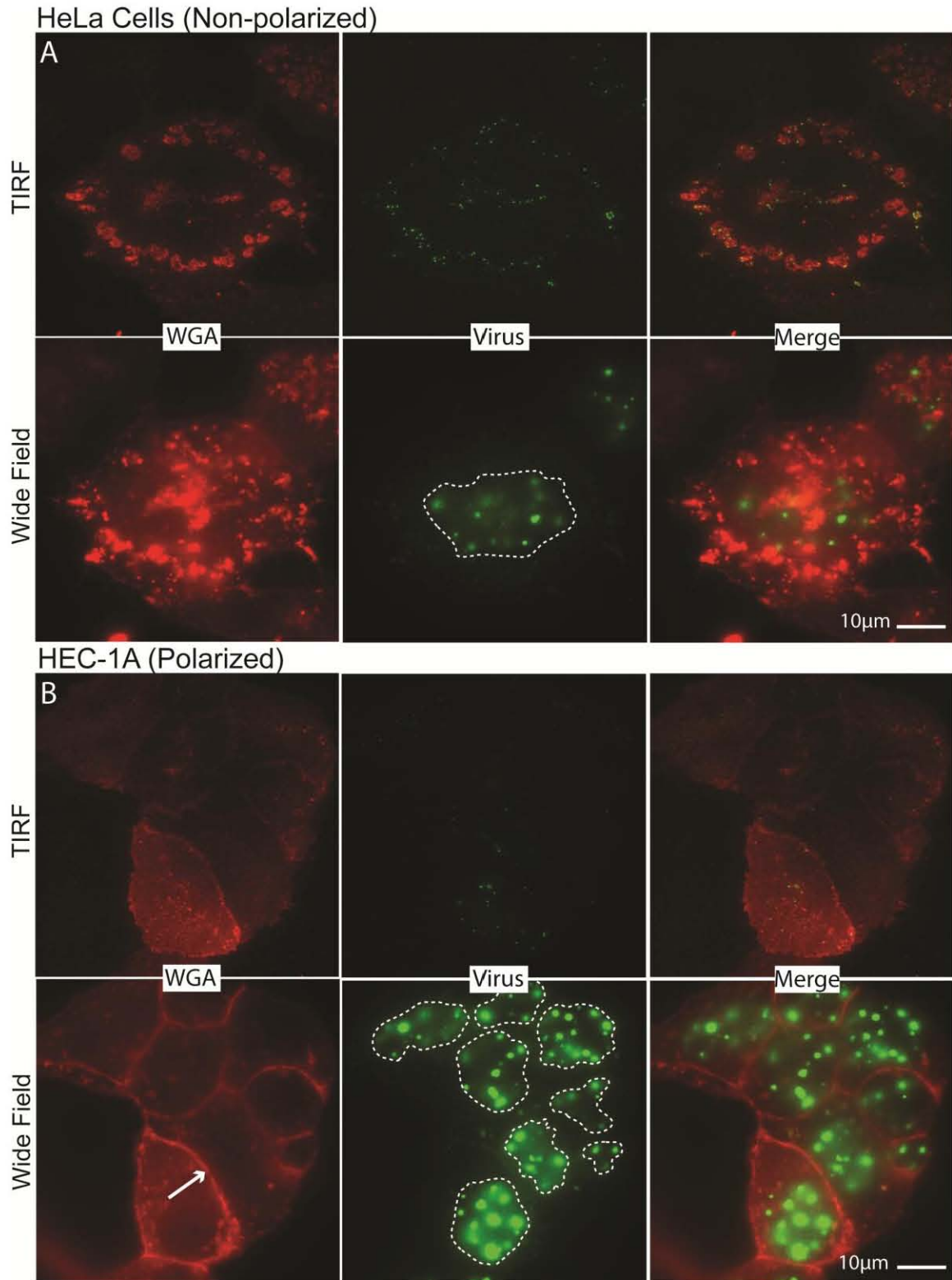
membrane regions where cell associated progeny virus was concentrated compared to the surrounding membrane. Viral proteins appear to be a large component of egress sites.

Concentrations of virions and glycoproteins along the adherent surface were not specific to Vero cells but seemed to be associated with a non-polarized state. Similar adherent-surface glycoprotein patches were observed in infected HeLa cells (a non-polarized cell type), but glycoproteins appeared to accumulate only at cell-cell junctions in polarized HEC-1A cells (Figure 14).

Glycoprotein patches form independently from trafficking virions. Vero cells infected at an MOI of 10 showed neither glycoprotein staining nor a virion signal at 4 hpi (Figure 15(A), top panels). At 6 hours post infection, small glycoprotein patches were detectable, although virions were rarely seen associating with these areas (Figure 15(A), middle panels). By 8 hpi, glycoprotein patches were more widespread and low levels of virus were consistently detected associating with the patches (Figure 15(A), bottom panels). This observation indicated that the release sites were determined early in infection. Glycoproteins arrived first, modifying the composition of the egress site membrane. Virions then associated with these membranes at later time points.

To further explore the differential trafficking between virions and glycoproteins, Vero cells were infected with a ΔUL25 mutant (KUL25NS). The gene product of UL25 is needed for packaging of DNA into the capsid. When it is absent, DNA is not packaged and capsids do not exit the nucleus. However, protein expression continues normally (115). If glycoprotein movement to the cell surface were induced by virus trafficking and

Figure 15: Formation of glycoprotein patch sites uncoupled from virus egress. (A) Vero cells infected with VP26-GFP HSV were fixed at 4, 6, and 8 hpi. Patch glycoproteins were labeled with rhodamine-WGA. All images were taken at that same exposure. Cell edge is outlined in 4hpi image. Outline of cell was determined by increasing the brightness of the image until cell edge was visible. Note that neither glycoprotein patches nor virus are visible by TIRF microscopy at 4hpi. By 6hpi glycoprotein patches are beginning to form (arrow), but virus still is not evident. At 8hpi there is pronounced glycoprotein staining on the cell surface and virions are beginning to accumulate in these areas. Images indicate that patches form before viral egress. (B) Vero cells infected with wild type KOS HSV-1 (top) or UL25Δ mutant HSV (bottom) were fixed at 12hpi. In a UL25Δ infection capsids are retained in the nucleus. Egress site glycoproteins were labeled with WGA. Virus was labeled with α-VP5 major capsid protein antibody and Alexa-488 labeled secondary antibody. Infections suggest glycoprotein patches form independently of viral release.
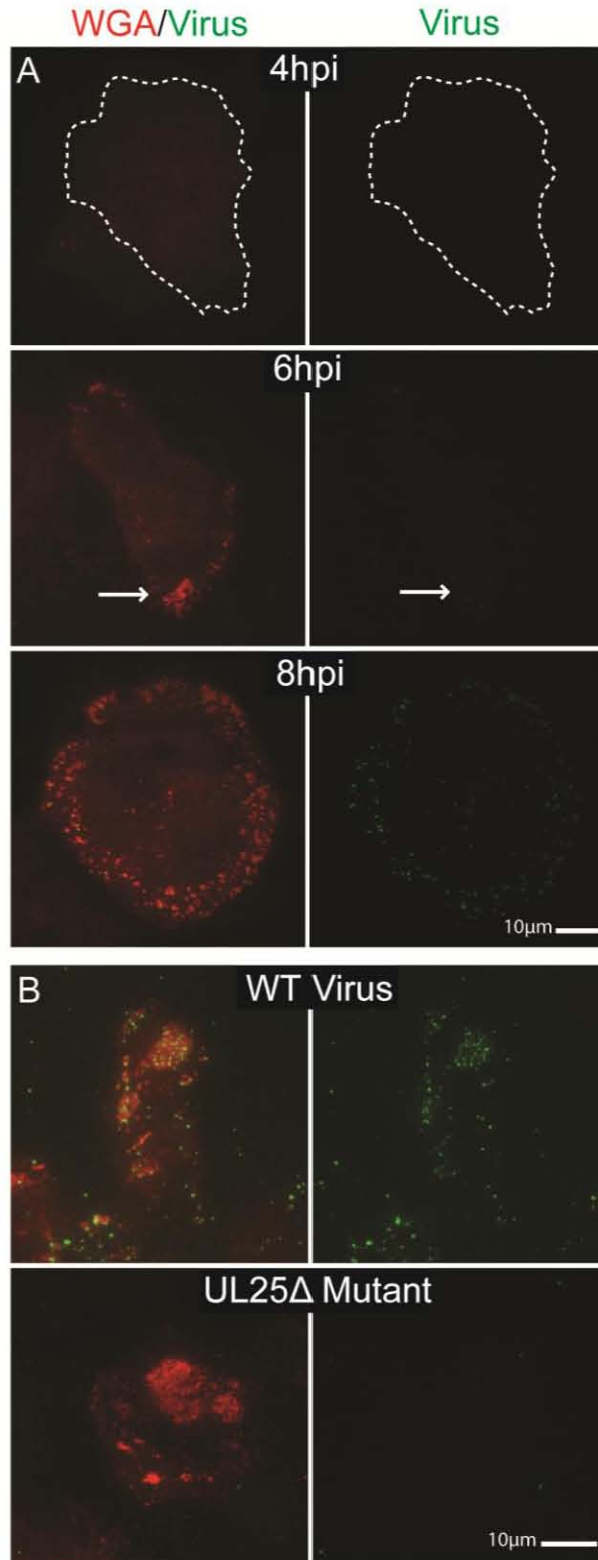
envelopment, then we would expect to see a decrease in the size of glycoprotein patches in cells infected with the ΔUL25 virus compared to WT.

Vero cells were infected with either WT KOS-HSV-1 or the ΔUL25 mutant for 12 hours. Cells were then fixed and stained with WGA. Capsids were labeled with α-VP5 (binds major capsid protein (197)) monoclonal antibody and Alexa-488 labeled secondary antibody. In the KOS infected cells, virus and glycoproteins were found to colocalize at release site patches as expected (Figure 15(B) Top). In ΔUL25 mutant infected cells, however, glycoproteins formed normal patches in spite of the fact that capsids were not present at these sites (Figure 15(B) Bottom). In addition, the glycoprotein patches were approximately equal in size to those formed in the infection with the wild type UL25 gene product (data not shown). This result provides further evidence that in infected Vero cells glycoproteins traffic to and accumulate at viral egress sites independently of virions.

Release sites are depleted of cytoskeletal elements. In a minority of infected cells we observed small glycoprotein aggregates in linear formations pointing toward larger glycoprotein patches. Figure 16(A) shows three cells where viral glycoprotein gD stained "dots" (arrows) form a line to a gD-labeled patch. We hypothesized that these dots could be associated protein surfing along the cell surface or a vesicle moving along a cytoskeletal track directly beneath the plasma membrane. To address the latter possibility and determine what cytoskeletal elements could be contributing to viral/glycoprotein trafficking, infected Vero cells were fixed at 12 hpi and stained with α-alpha-tubulin to label microtubules, phalloidin to label actin, and α-vinculin to label focal

Figure 16: Location of cytoskeletal elements in relation to viral egress sites on the adherent surface of HSV-1 infected Vero cells as shown by TIRF microscopy. (A) Sections from three infected cells stained with α-gD antibody illustrating a linear configuration of gD-stained "dots" adjacent to gD-stained patches. Bracket highlights three lines in panel 1. Arrows point to linearly arranged dots in the following two panels. Linear arrangement suggests vesicles may travel along cytoskeletal elements to egress sites. (B-D) VP26-GFP HSV infected Vero cells stained with α-tubulin antibody (B), phalloidin (C), or α-vinculin antibody (D). Starred area is adjacent uninfected cell in C. Note that areas of patch formation are depleted of cytoskeletal elements. (E-G) Mock infected cells stained with α-tubulin antibody (E), phalloidin (F), or α-vinculin antibody (G). Large areas of cytoskeletal depletion are rarely seen in uninfected cells. Alexa 594-conjugated goat anti-mouse secondary antibody was used in A-B and D-G. Size marker in G is relevant to images B-G.

gD   gD   gD   10µm

Virus   Tubulin   Merge

Virus   Actin   Merge

Virus   Vinculin   Merge

Tubulin   Actin   Vinculin   10µm
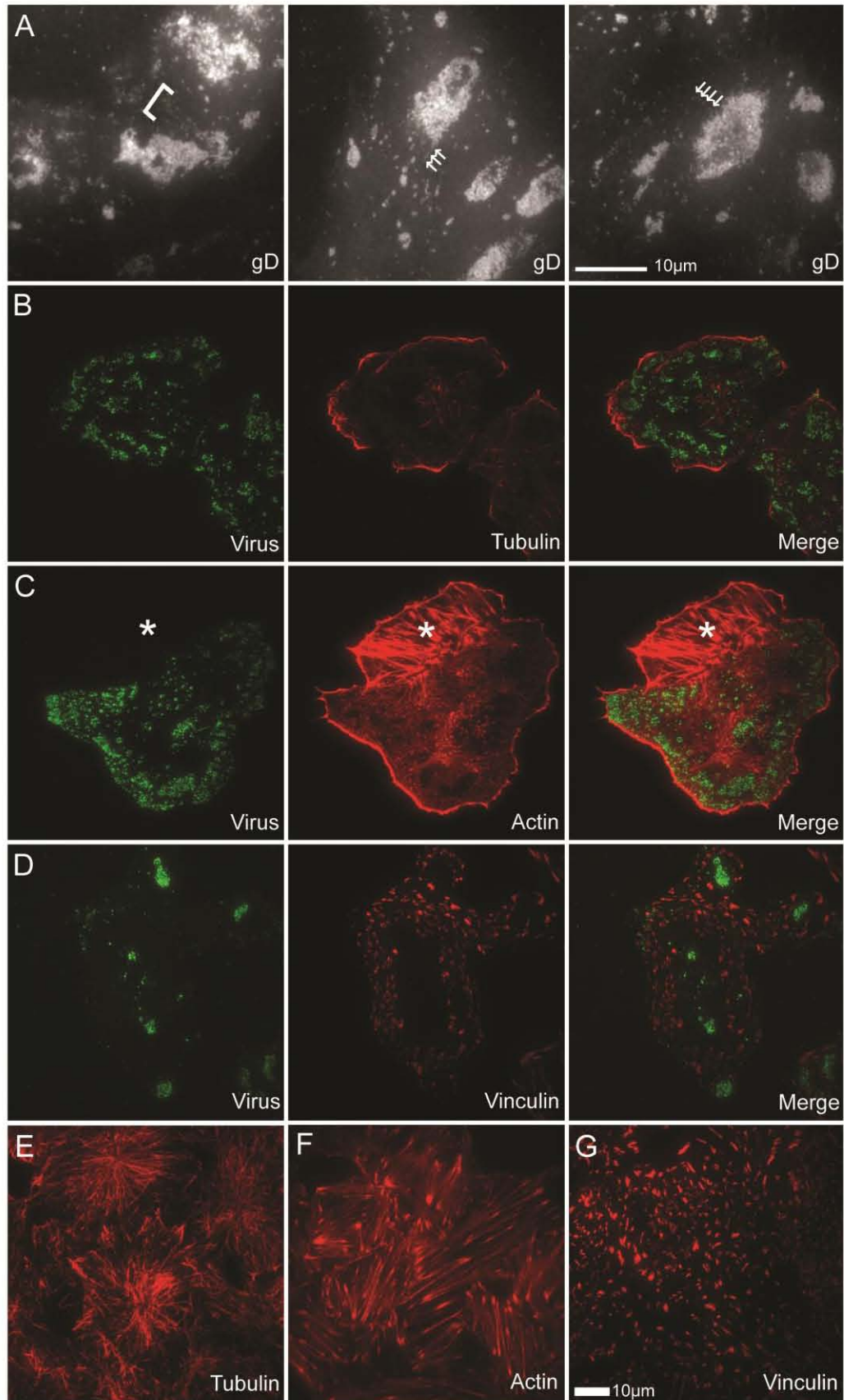
Figure 17: Actin is depleted in areas of virus release. High resolution image of VP26-GFP HSV infected Vero cell at 12hpi. Cell has been stained with Texas red-phalloidin. Top image is virus and actin. Bottom image is actin alone. Three representative actin-depleted areas are outlined.

Actin and Virus
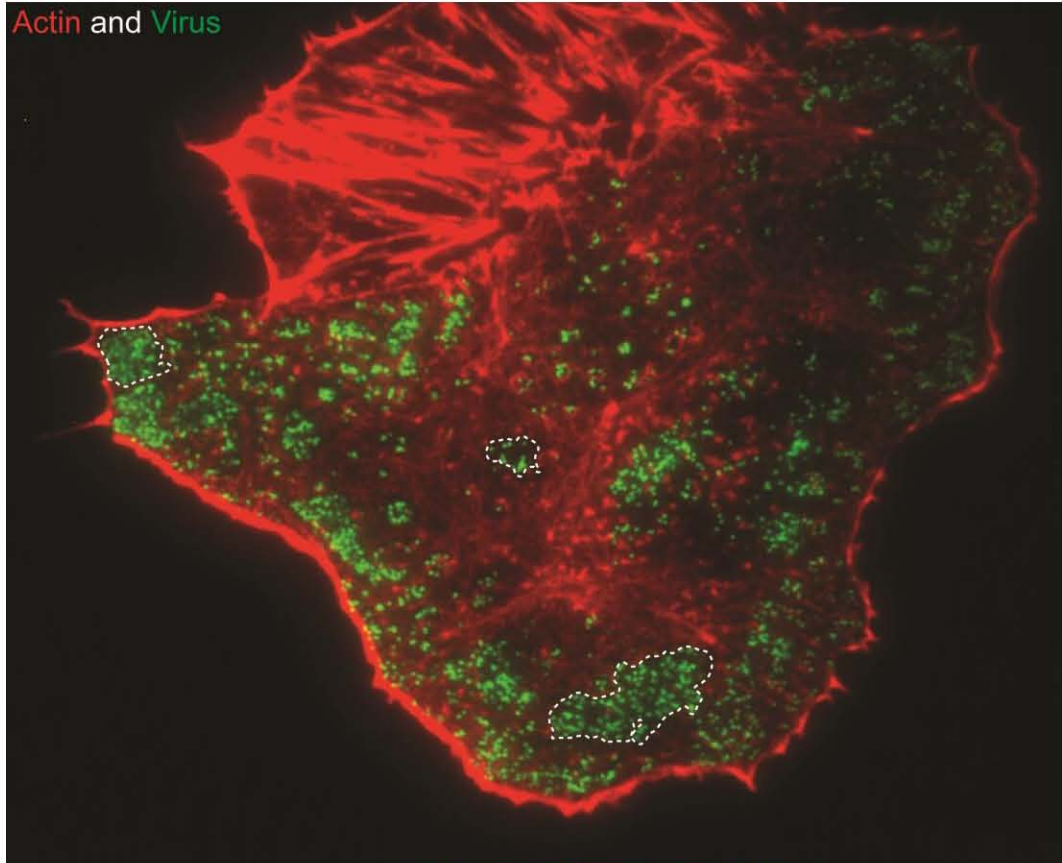
Actin

Figure 18: Actin "holes" are likely not due to limitations in TIRF range. HSV-1 infected Vero cells were fixed at 12hpi and stained with Texas-Red Phalloidin to label actin and anti-gD antibody to mark the glycoprotein enriched patches. Two representative images are shown with 2-3 cells in each frame. Images on the left show only the actin stain. Images on the right show both actin and gD labeling. Note that actin has been depleted in areas where patches have formed. Little actin is visible even though the cell membrane is fully within the range of the TIRF laser as determined by gD-labeling.
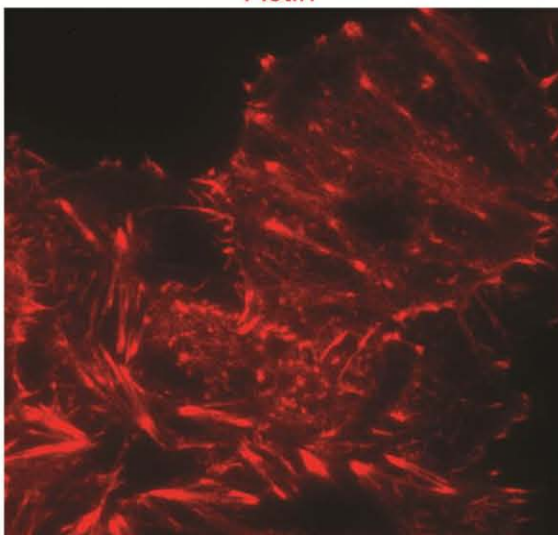
Actin   Actin/gD
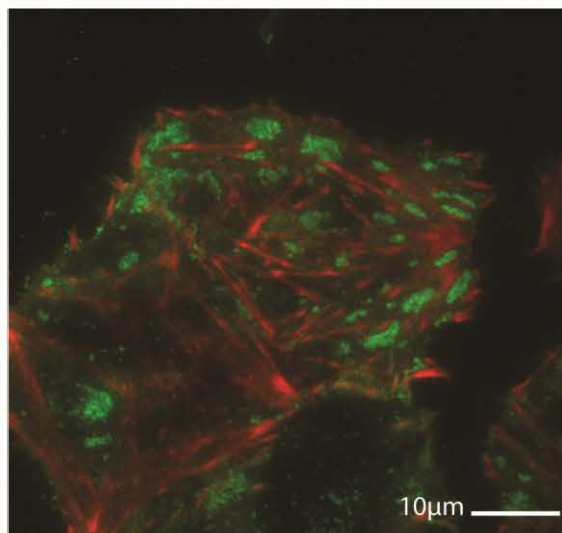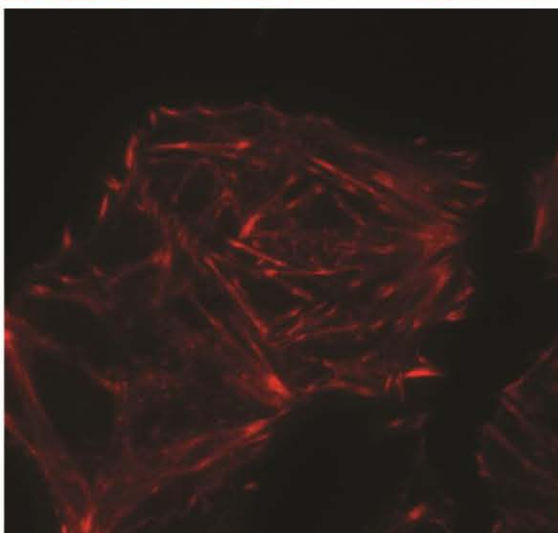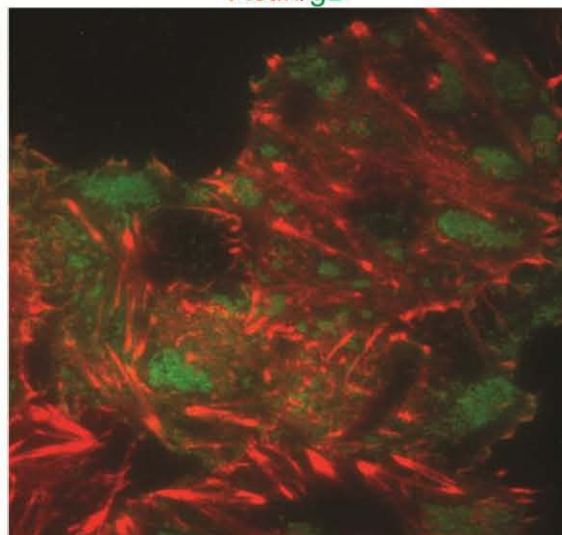
10μm

adhesions. It is known that the cellular cytoskeleton is altered during HSV-1 infection.

The microtubule organizing center (MTOC) is disrupted and microtubules become sparse

and disorganized (89,99,206). Although peripheral microtubules could be seen in our

samples, results showed that microtubules did not colocalize with virions at peripheral

egress sites (Figure 16(B)). Actin stress fibers are also largely depolymerized during

HSV-1 infection ((72,139,202,212) and Figure 16(C)). When infected cells were stained

for actin, few stress fibers were visible but the actin cortex (the unbundled, highly

branched actin lining the cell membrane) could still be seen in most cases. Contrary to

our expectations, the actin cortex was found to be completely depleted at the viral egress

sites (Figure 16(C)). The outline of the depleted areas often followed the outline of the

glycoprotein concentrations (see Figure 17 for enlarged view of 16(C)). Actin depletion

was observed even when the gD-labeled membrane of an egress site remained within the

range of the TIRF laser (Figure 18); it is unlikely that the actin "holes" are an artifact of

the visualization technique. A similar result was observed with focal adhesions (Figure

16(D)). Although the patches often formed shapes that mimicked large focal adhesions,

focal adhesions were not present at the viral egress sites; they were depleted in areas

where the patches formed. As the patches enlarged during infection, focal adhesions

retracted further (data not shown). Areas of microtubule, actin, and focal adhesion

depletion were rarely detected in mock infected cells (Figure 16(E-G)). They appeared

only after HSV infection.

Both actin and microtubules contribute to glycoprotein patch formation and virion

trafficking to release sites. Although viral egress sites were depleted of cytoskeletal

elements, it was likely that microtubules, actin, or both were involved in virus trafficking. The expected size and density of virus-containing vesicles along with the non-random release of virions suggested that a structural element was assisting their movement and delivery to their destination. The possible role of microtubules and actin in viral egress was investigated by depolymerizing their structure at increasing intervals after infection. VP26-GFP HSV-1 infected cells were treated at 4hpi (before patches were visible and infectious virus detectable), 8 hpi (patches were expanding, few virions could be seen), and 11.5 hpi (patches were large and contained many virus particles) (Figure 19(A)). Treatment included either 10 µg/ml nocodazole to depolymerize microtubules, 1.7 µg/ml cytochalasin B to depolymerize actin, or 3.3 µl/ml DMSO as a control. After treatment, cells were fixed and stained with rhodamine-WGA to define the patch outlines. Resulting TIRF images (Figure 19(B-D)) were then analyzed as described in the Materials and Methods.

It was found that depolymerization of the microtubules during infection caused a significant reduction in the percentage of cell membrane covered by glycoprotein patches. Greater effects were observed at the earlier time-point addition (Figure 19(C and E). The number of patches remained about the same but they were reduced in size (data not shown). In addition, depolymerization at early time points caused a reduction in the total number of virions on the visible cell membrane at the adherent surface (Figure 19(C and F). No effect was observed when nocodazole was added later in infection after patches had formed and many virions were present. Titre samples were collected to determine if nocodazole treatment had an effect on the production of infectious virus.

Figure 19: Role of microtubules and actin in virus/glycoprotein trafficking and patch

formation. (A) Experimental Design showing addition of nocodazole, cytochalasin B, or

DMSO to VP26-GFP HSV-1 infected Vero cells at 4, 8, or 11.5hpi. Fixation and analysis

occurred at 12hpi. (B) TIRF micrograph of DMSO treated sample stained with

rhodamine-WGA to mark glycoprotein patches. (C) TIRF micrographs of infected cells

treated for noted intervals during infection with 10 µg/ml nocodazole. Cells were stained

with WGA. Note that patches are smaller with fewer virions compared to control. (D)

TIRF micrographs of infected cells treated for noted periods with 1.7 µg/mlcytochalasin

B. Patches were labeled with WGA. Note that treatment has disrupted glycoprotein

patch structure. (E) Graph depicts the percent of cell membrane that is covered in

glycoprotein rich patches. Numbers were obtained by dividing the sum of the patch areas

by the total area of the cellular adherent membrane visible in TIRF micrographs. (F)

Graph depicts the amount of virus on the cellular adherent membrane visible by TIRF

microscopy. 25 cells per sample set were analyzed. Error bars are for the standard error

of the mean. p-value of treated samples compared to DMSO control are labeled as

follows: * <0.05, ** <0.005, *** <0.0005.

A — Timeline: Infectious Virus First Detectable — 6 hpi; Small Patches, Few Virions — 8 hpi; Large Patches, Dense Virions — 11.5 hpi. Treatment timelines: 4hpi, 8hpi, 11.5hpi.

WGA — Virus — Merge

B — DMSO 4-12hpi

C — Noc 4-12hpi; Noc 8-12hpi; Noc 11.5-12hpi

WGA   **Virus**   **Merge**

D

CyB 4-12hpi

CyB 8-12hpi

CyB 11.5-12hpi

E — Patch Area / Total Surface

F — Virus / Total Surface
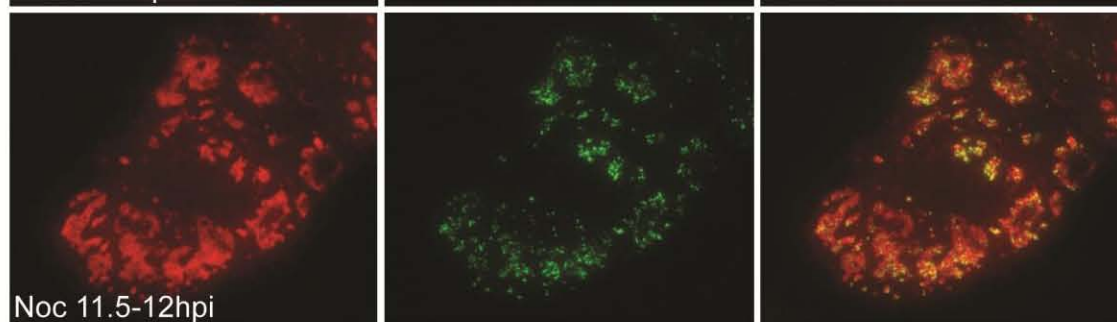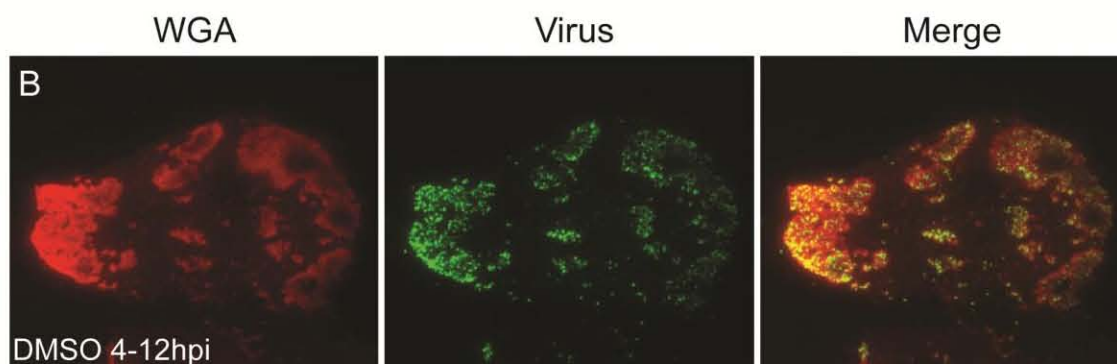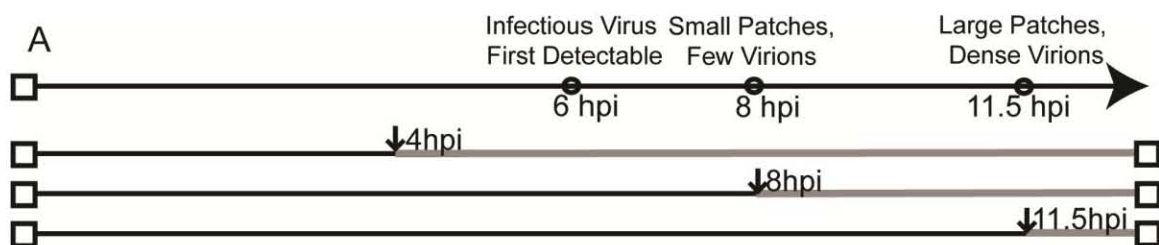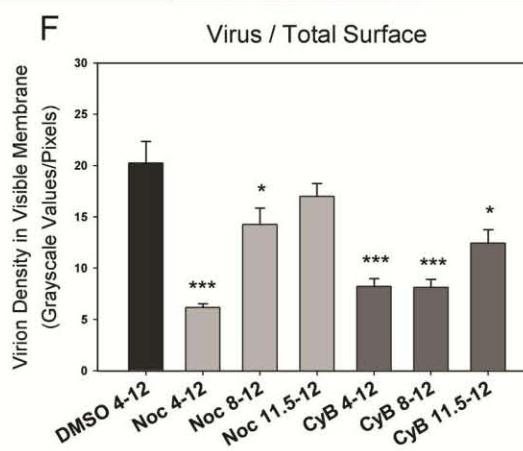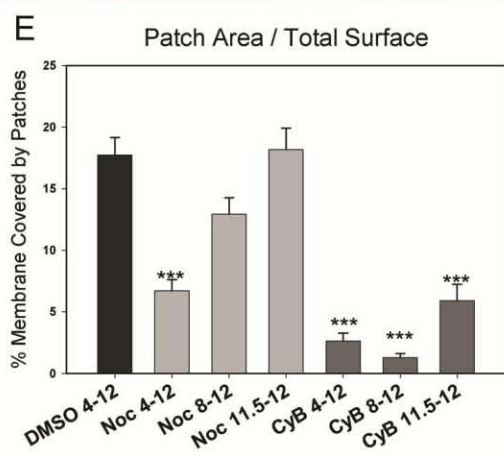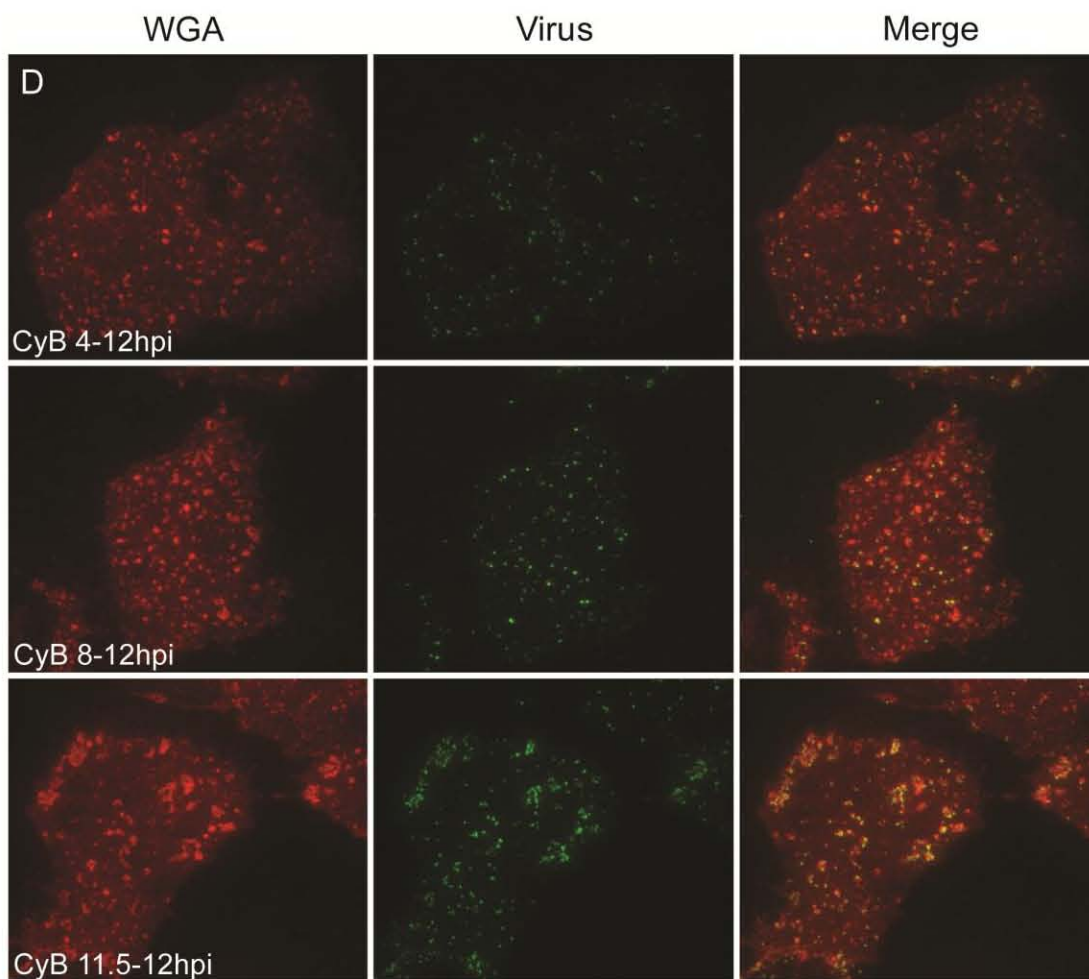
Figure 20: Effect of cytoskeletal depolymerization on progeny virus titre. Vero cells were infected at an MOI of 10. At 12 hpi cells were separately collected and processed as described in the Materials and Methods. Titre was then determined by limiting dilution assay. Results shown are that of 3-4 separate experiments carried out under the same conditions. Each repetition is a different color. Some were titred in duplicate and show the variation. Samples in red were collected in the same experiment with the samples used to determine patch size and virus changes by TIRF microscopy. In the top figure depicting the effect of nocodazole treatment, the blue dots not visible are hidden from view behind the yellow dots.

Effect of Nocodazole on Production of Virus
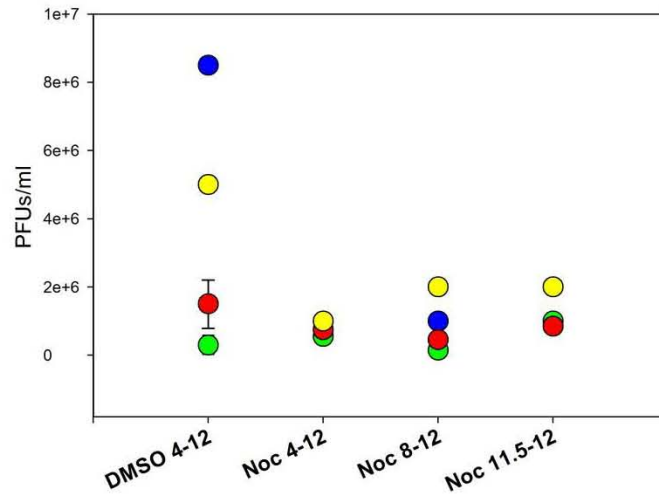
Effect of Cytochalasin B on Amount of Virus
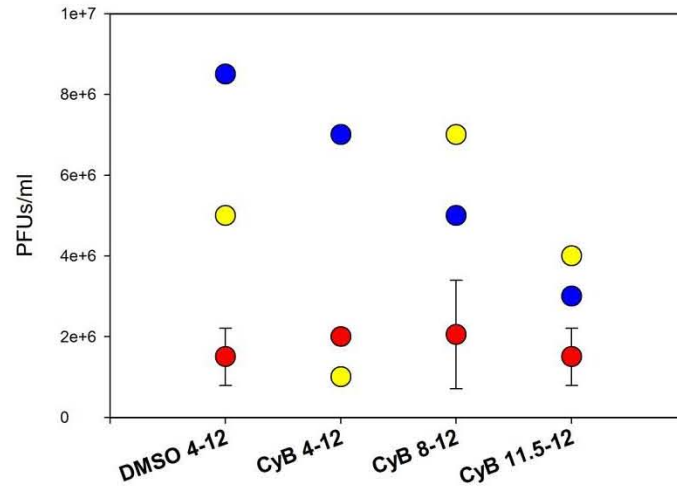
There was no statistically significant effect on titre over several experimental repetitions (Figure 20). Nocodazole did not block viral production though the titre changes suggested by the viral fluorescence decrease may not be detectable with this method. In sum, results indicate that absence of microtubules impedes trafficking of glycoproteins to the cell surface. The decrease in virus at the cell membrane is also likely due to inhibited transport to the surface, however, depolymerization of microtubules could be hindering envelopment of virus as well.

Surprisingly, it was observed that disrupting the actin cytoskeleton decreased the number and size of patches at all time-points tested (Figure 19(D-E)). This effect was most extreme when the cytoskeleton was depolymerized early in infection, but it was also seen when actin was depolymerized after patches had already formed. As the actin was disrupted, the patches that had formed were dispersed into components, very small glycoprotein aggregations in the cell membrane with the occasional associated virion. Therefore, actin appeared to be maintaining the structure of the egress sites. In its absence, the egress patches broke apart.

Treatment with cytochalasin B early in infection decreased the amount of virus on the cell membrane (Figure 19(F)). This suggested that actin is involved in trafficking of virus/glycoproteins to egress locations as well. There were no statistically significant differences in titres for all treatments (Figure 20), although as with the nocodazole treated samples, the resulting titres varied between experiment repetitions. Dispersing the patches with cytochalasin after formation did not induce the release of the surface virions into the supernatant (data not shown). The decrease in the amount of virus detectable on

the membrane when cells were treated from 11.5hpi-12hpi was likely due to diffusion of virus particles from the substrate-adherent surface to the upper membrane where they could not be detected using TIRF microscopy. We conclude that actin contributed to virus trafficking to the egress sites and to the maintenance of the viral components at these sites.

Myosin II is important for viral egress. We hypothesized that the glycoprotein dots aligned in linear formations near patches could be due to "surfing" of virus and glycoproteins to patch sites after fusion elsewhere on the cell surface. In the process of viral surfing, virions interact with the actin cytoskeleton through a receptor protein. The actin filament itself then moves relative to the surrounding filaments through the action of non-muscle myosin IIA. Once a virion is bound to its receptor, it is pulled (a movement that resembles surfing) to an area on the cell body where efficient endocytosis or fusion can occur (154,203). HSV-1 has been shown to surf on the surface of filopodia during entry (42,141), and a recent report has suggested that myosin IIA can directly serve as an entry receptor for glycoprotein B due to virally induced expression of myosinIIA on the cell surface (5). To test the possible role of myosin IIA directed surfing in the action of clustering at release sites, the myosin II inhibitor blebbistatin was used to treat infected cells at 4, 8, and 11.5hpi. Cells were then fixed at 12hpi and analyzed as described in the Materials and Methods. If actin surfing was involved in movement of virus/glycoproteins to patch sites, then its inhibition would result in dispersed viral proteins.

The results suggested that myosin II was not necessary for patch formation (Figure 21). In blebbistatin-treated cells, glycoproteins still concentrated in patches and virus still associated with them when the action of myosin II was blocked. However, the size of the patches and the number of virus particles on the cell surface were reduced when cells were treated early in infection (Figure 21). Blebbistatin did not appear to affect envelopment, as the amount of infectious cell-associated virus remained the same (data not shown). The results were interpreted to suggest that myosin II plays a role at a step preceding vesicle-surface fusion.

The structure of egress sites can reform after disruption. During the process of secretion in secretory cell types, actin is locally depolymerized in the cortex allowing passage of a vesicle. Existing studies have found that the depolymerized areas are often not much larger than the secreted vesicle and the cytoskeleton generally reforms after exocytosis has occurred (63,157). One explanation we considered for the existence of actin "holes" at viral egress sites was that actin depolymerized to allow exocytosis of the virus and a viral protein blocked its repolymerization. Stress fibers are disrupted in infected cells through the action of viral kinase US3 (103,202). This protein induces depolymerization by influencing cellular signaling pathways through the action of PAK2 (127). We hypothesized that an unidentified viral protein could be inhibiting actin filament polymerization globally, resulting in the formation of holes in the actin cortex.

To test the above idea, Vero cells with observable patches were treated with 1.7 µg/ml cytochalasin B for 30 minutes. Actin was depolymerized as expected as shown in

Figure 21: Effect of myosin II inhibitor blebbistatin on patch formation and virus/glycoprotein trafficking. (Top) TIRF micrographs of VP26-GFP infected Vero cells treated with DMSO or 50uM blebbistatin at 4, 8, or 11.5 hpi. Cells were fixed at 12hpi and stained with rodamine-WGA to label patches. (Bottom) Quantitation of the percentage of cellular membrane covered by glycoprotein patches and the amount of released virus associating with the cell membrane when samples were treated with blebbistatin or DMSO at noted times. Note that both the size of patches and the amount of virus on the cell surface decreased with treatment. Error bar is standard error of the mean.25 cells were analyzed per sample set. p-values of treated samples compared to DMSO sample are labeled as follows: * <0.05, ** <0.005, *** <0.0005.

Patch Area / Total Surface

Virus/ Total Surface
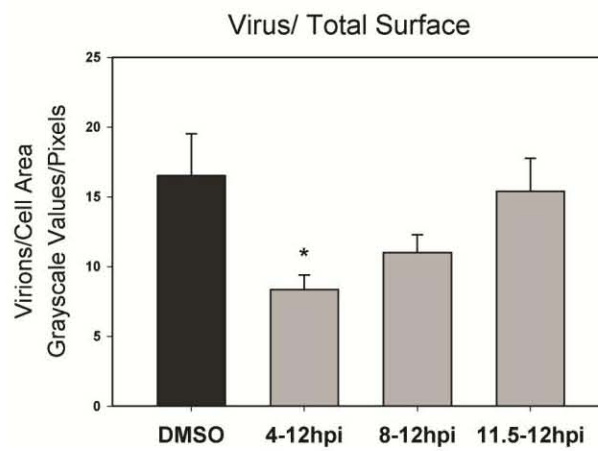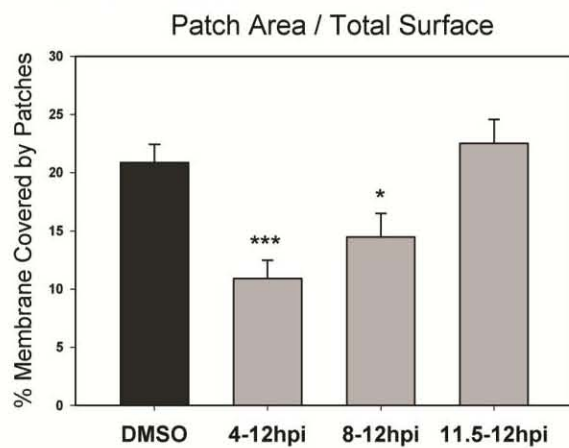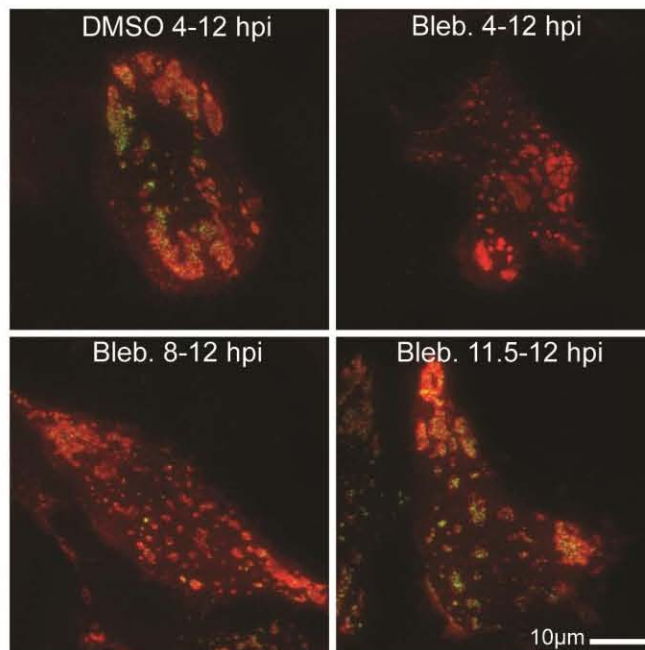
Figure 22. The drug was then rinsed out, infection was continued for another 45 minutes, and cells were fixed and stained with WGA or phalloidin. The results showed that the actin cortex repolymerized normally, and patches consisting of dense glycoproteins and GFP labeled virus were visible after the 45 minute recovery period (Figure 22). It is unclear whether the dispersed virus/glycoproteins reformed into patches or the visible patches were simply new virus that has been released since the restoration of the actin cortex. In either case, we concluded that actin was able to polymerize normally and infected cells were able to create new egress sites late in infection. There appeared to be no global inhibition of actin polymerization. The decrease in actin at these sites was most likely locally induced.

Glycoprotein E is necessary for efficient trafficking of glycoproteins but not virus to release sites. Directed egress in polarized cells such as keratinocytes and neurons is dependent upon viral glycoprotein E (gE). This glycoprotein is not essential for viral replication; the existing gE null mutants produce normal levels of progeny virus. However, there is a block in cell-to-cell spread (40,79,113,177,204). In both epithelial cells and neurons the virus is unable to traffic to its specified egress location and spread of infection is inhibited. To test the role of gE in the formation of the egress sites that form along the coverslip-adherent surface of Vero cells, we created ΔgE, gEΔCT, and gEΔCTrescue mutants. Using a bacterial artificial chromosome system the start codon of the gE gene (US8) was replaced with a stop codon. To create the gE cytoplasmic tail deletion mutant, two stop codons were added at residue 446 directly after the

Figure 22: Egress site reformation after actin depolymerization-induced disruption.

VP26-GFP infected Vero cells were treated with 1.7 µg/ml cytochalasin B for 30

minutes. Toxin was then rinsed out and the infection continued for another 45 minutes.

Sample cells were fixed at each step and stained with Texas red-phalloidin or rhodamine-

WGA. Note that egress sites were able to reorganize after disruption. (TIRF microscopy)

WGA/Virus   Actin/Virus

11.5hpi   11.5hpi

30min CyB Treatment   30min CyB Treatment

45min Recovery   45min Recovery

12.75hpi No Treatment   12.75hpi No Treatment

10µm
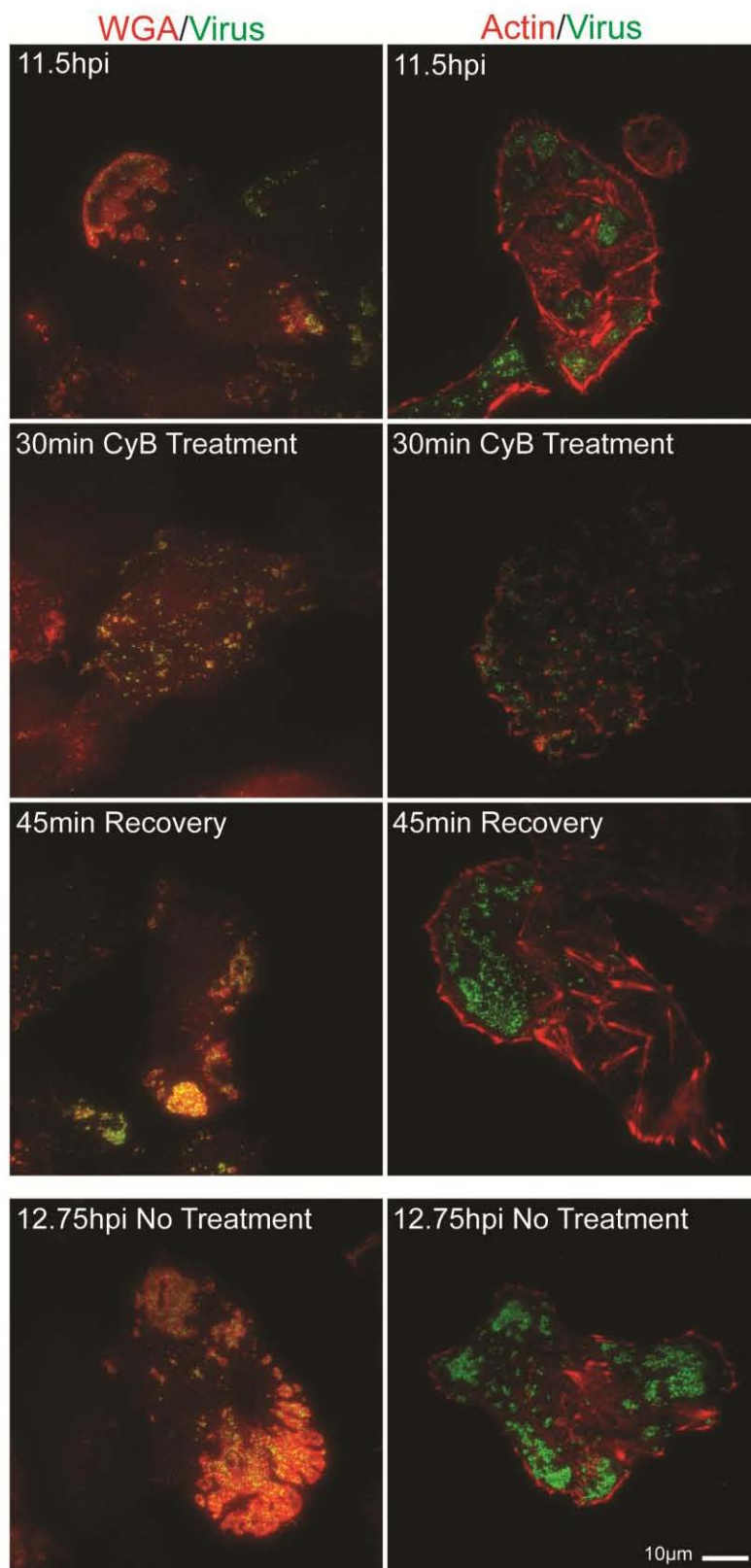
transmembrane region. Expression of gE was rescued by removing these stop codons.

Construction of the mutants was verified by harvesting the supernatant and cell lysates of infected Vero cells and using a western blot to stain for the appropriate protein (Figure 23). The results showed that staining for gE was seen in the WT and rescue infection but was absent in the lysates and supernatant media of the gE deletion mutants. The gE cytoplasmic tail deletion protein was less stable than its full length counterpart. In cell lysate samples, the gE band is shifted compared to virions due to the presence of large amounts of immature gE.

To test the role of gE in creation of release sites and the egress of virions at these sites, Vero cells grown on glass coverslips were infected with ΔgE, gEΔCT, and gEΔCTrescue mutants. A low MOI was used to ensure infections arose from a single virion. To compare virus production, supernatants and cell lysates were collected at 10 hpi, a time at which each original infected cell was producing virus but second generation infected cells were not yet doing so (Figure 11). In this way the effect of the gE deletions on the formation of infectious virus could be determined separately from effects on cell to cell spread. At 12hpi infected Vero cells were fixed with 4% PFA and treated with α-VP5 antibody and Alexa-488 conjugated secondary antibody. Samples were then stained with rhodamine-WGA to label glycoprotein patches and viewed using TIRF microscopy. 20 cells per infection sample were measured as described in the Materials and Methods for patch coverage and density of virions on the cell surface.

The results showed that the lack of gE or the gE cytoplasmic tail caused a significant reduction in the percentage of cell surface covered in glycoprotein patches compared to the rescue virus (Figure 24). However, while there was an inhibition in glycoprotein trafficking, the number of virions on the cell surface of the ΔgE mutants increased for unknown reasons. There was no statistical difference in titres, however, indicating that the production of progeny infectious virus was not affected (Figure 24). The results were interpreted to indicate that the cytoplasmic tail of gE is important for the formation of glycoprotein patches at egress locations but not for trafficking of virions to the egress sites. As gE is known to be crucial for cell-to-cell spread, one could hypothesize that the observed glycoprotein concentrations may contribute to the transfer of virions to adjacent cells in this cell type.

Figure 23: Western blot analysis of expression of gE by deletion and rescue mutants.

Cell lysates and supernatants of wild type HSV and gE mutant infected Vero cells were

collected at 18hpi. Samples were run on an SDS-polyacrylamide gel, transferred, and

blotted with α-gE antibody. α-VP5 was used as a loading control. Note that gE is

expressed normally in the WT and rescue samples (gEΔCT.R) but not the deletion mutant

infected samples. Arrowhead points to non-specific band. Truncated gE is starred.
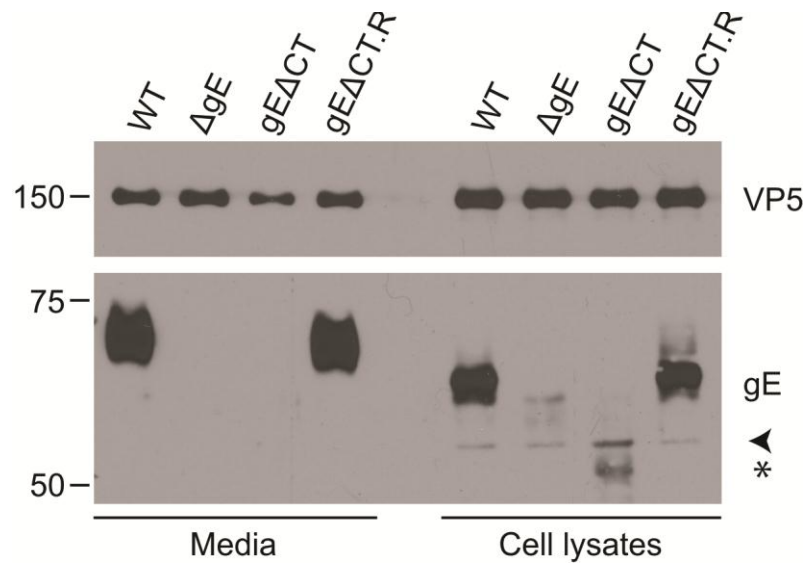
Figure 24: Effect of gE and gE cytoplasmic tail deletions on patch formation and progeny

virion trafficking. (Top) TIRF images of Vero cells infected with the ΔgE mutant, the

gEΔCT mutant, or the gEΔCT rescue virus at an MOI of 0.3 for 12 hours. Cells were

fixed and treated with rhodamine-WGA and α-VP5 antibody with Alexa-488 conjugated

secondary antibody. Note that patches are smaller in the gE deletion mutant infected cells

but virion number in those patches is increased. (Bottom) Quantitative determination of

the percent of adherent cell membrane covered by glycoprotein patches and the amount

of virions on the total adherent membrane. Quantifications support the visual data.

Infected cells were scraped at 10hpi and titre was determined by limiting dilution plaque

assay. Note that gE deletions had little effect on the production of progeny virus titre in

spite of the observation that the number of virions on the adherent surface was increased.

p-values of deletion mutants compared to rescue virus are labeled as follows: * <0.05, **

<0.005, *** <0.0005. Bars represent standard error of the mean.

Rescue | WGA | α-VP5 | Merge

ΔgE | WGA | α-VP5 | Merge

gEΔCT | WGA | α-VP5 | 10μm | Merge

Patch Area / Membrane Area

Virions / Total Surface

Titre
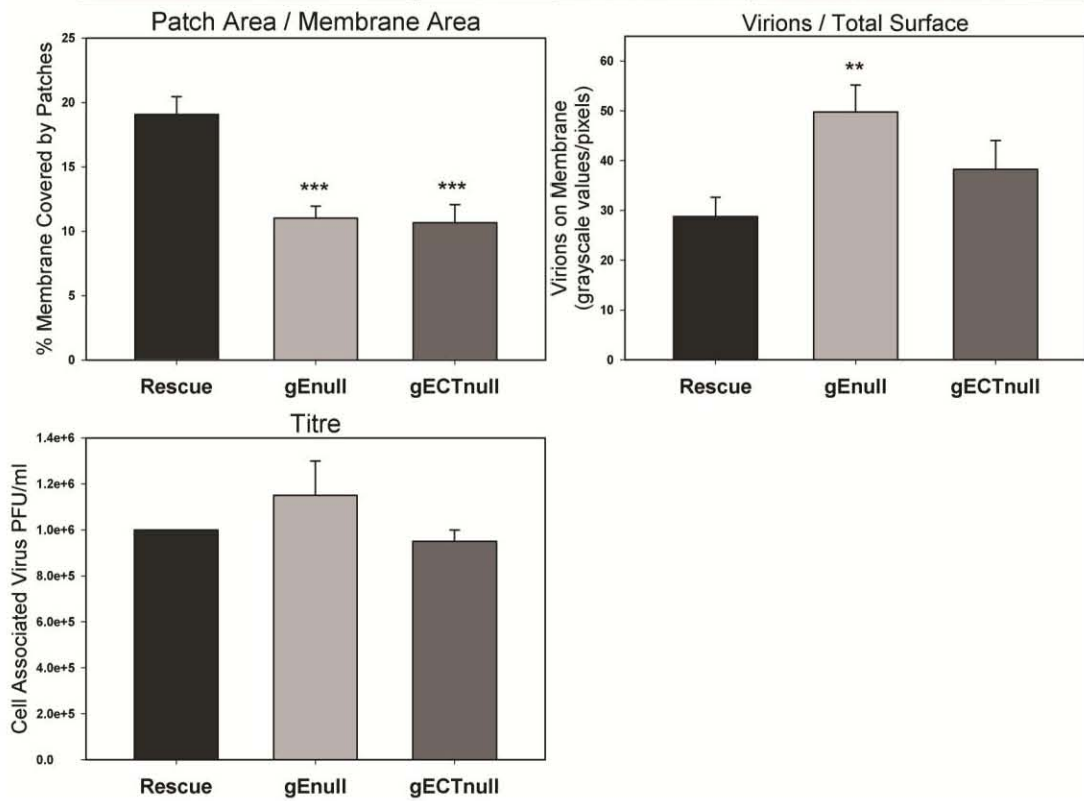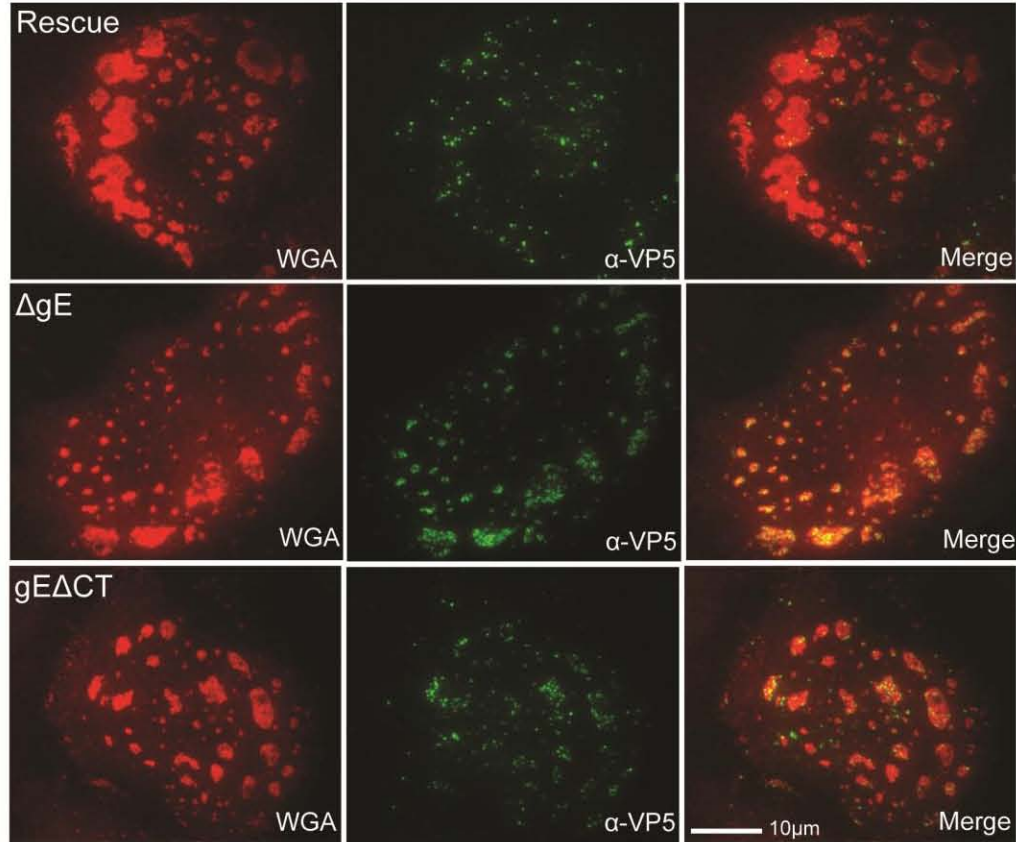
DISCUSSION

Within tissues where herpetic lesions form there are both highly differentiated and less differentiated epithelial cells depending on stratification within the epidermis. While there has been some study of directed egress in polarized epithelial cells, egress in non-polarized cell types has not been explored as extensively. Here we report the results of a study in which the release of HSV virions in non-polarized, transformed cells was investigated. The findings are summarized as follows: 1) HSV-1 egress in non-polarized cells is a directed process that occurs at adherent surfaces. 2) Both the membrane composition and cytoskeletal structure of egress sites is modified during infection. Both membrane and cytoskeletal modifications begin before virus is released and they occur even when virion trafficking is blocked. 3) Trafficking of both virus and membrane components are dependent on microtubules and, to a lesser extent, actin. 4) Actin determines the structure of egress locations; when actin is depolymerized the sites disperse. 5) Viral glycoprotein E aides in the formation of egress sites. The above findings are discussed in greater detail below.

Virus is directed to adherent surfaces rather than junctional proteins in Vero cells.
In infected Vero and HeLa cells the vast majority of newly secreted virus was observed associating with the cell membrane at specific sites along cell-cell and cell-coverslip contact areas. This indicates that the sorting of virus in non-polarized cells is a directed rather than random process. Previous reports have shown a random, dispersed association of virions with the surface of HEp-2 non-polarized cells at 17hpi (79). We observed that by 17hpi, infected Vero cells displayed cytopathic effects and virus

appeared to cover most cell surfaces. Directed egress occurred earlier in this cell type, between 8 and 16hpi. It may be that HEp-2 cells exhibit directed sorting at earlier times as well. Although it has been hypothesized that the release of virions at cell-contacting lateral surfaces in polarized epithelial cells is determined by the presence of junctional complexes (41), our results suggest that directed egress can be a more simplistic process. Vero cells do not express E-cadherin and exogenously expressed nectin-1 does not traffic to egress sites (our unpublished observations). The state of simply being adherent to a substrate or cell may, therefore, be sufficient to direct egress in some cell types, including Vero cells.

Infection induces the creation of specialized egress sites that may function as virological synpases. In the course of infection, the adherent surfaces of Vero cells were modified to create discernable viral egress sites. Firstly, pocket-like membrane invaginations formed at these locations that were visible by both EM and TIRF microscopy. Invaginations were rarely observed in uninfected Vero cells; the plasma membrane of these cells was generally tightly apposed to the cover slip. Secondly, the cell membrane at egress sites was extremely rich in glycoproteins. Glycoprotein concentrations were not observed in uninfected cells. Lastly, cytoskeletal structures were modified at release sites. It was observed that nascent viral egress locations were depleted of microtubules, actin, and focal adhesions. Infected cells formed actin "holes" that often followed the outline of the glycoprotein patches. Similar areas of cytoskeletal clearance were rarely observed in uninfected cells. Interestingly, glycoproteins began to accumulate in small patches 1.5-2 hours before capsids became visible at these sites,

signifying that the egress site locations were determined early in infection, before virion trafficking began. Furthermore, glycoprotein patch formation was not affected even when capsid maturation was blocked with a ΔUL25 mutation. The induction of membrane modifications, therefore, appeared to be independent of virus trafficking.

Overall, release of HSV-1 at these egress sites shares similarities with the formation of virological synapses by retroviruses. Virological synapses form at areas of adhesion between infected and non-infected cells, exocytosis is polarized toward these areas, and viral and cellular proteins are recruited to these sites (80). We found that HSV-1 infection induced the creation of specialized sites on adherent surfaces of Vero cells, and the lack of viral glycoprotein concentrations on non-adherent surfaces suggests that secretion was polarized toward these structures. It is likely that the egress locations that form at the glass coverslip are structurally comparable to those that form along cell-cell contact sites. The egress sites explored in this paper are located along glass coverslips where the infected cells are attached. Although distinct from *in vivo* conditions, they share many similarities with cell-cell adherent sites. Coverslip-adherent sites build up concentrations of virions and membrane glycoproteins as do the cell-cell contact sites. In addition, both have a buildup of TGN markers (unpublished observations). Glycoproteins traffic to exit sites independently of capsids, as has been shown in polarized epithelial cells and neurons (178,214). Lastly, the lack of gE affects the formation of egress sites, and previous reports have concluded that Vero cells infected with a ΔgE mutant are inhibited in cell-cell and cell-neuron spread (7,113) - interpreted as a possible disruption of cell-cell contacts. We propose that the creation of the egress

sites described in this paper assists cell-to-cell spread of the virus in a process resembling the creation of virological synapses. The model we have described for studying their formation should be useful for further exploration in this area.

The cellular cytoskeleton assists viral trafficking. Although viral release sites were depleted of cytoskeletal elements, both microtubules and, to a lesser extent, actin were important for movement of viral components to these locations. Microtubules are known to function in the long distance movement of secretory vesicles, while actin has been reported to act as both a barrier and aide to secretion. Both elements appeared to function in a similar manner in HSV-1 infected Vero cells. In addition, inhibiting myosin II with blebbistatin decreased the size of glycoprotein/virus patches, suggesting that the contractibility of the actin cytoskeleton was important for expansion of release sites. The fact that patch formation could still occur to some extent when myosin II was inhibited indicates that actin surfing is not the driving force behind patch formation. If it were, then inhibiting actin surfing would result in dispersed virus and glycoproteins. However, there are many other ways myosin II could be assisting this process. Previous studies have shown a role for this protein in cell motility, spreading, cytokinesis, endocytosis, and exocytosis (49,63,203). Active actin remodeling guided by myosin II may be necessary for efficient formation or expansion of egress sites. It is also possible that fusion of virus-containing vesicles with the cell membrane is assisted by myosin II driven motility.

In addition to our results indicating a role for myosin II in HSV infection, there is a report indicating that myosin IIA is reorganized in infected cells and can directly

interact with viral protein VP22 (201). Also, virus release is decreased when myosins are inhibited with general myosin ATPase inhibitor butanedione monoxime (161). Another myosin, myosin Va, has also been reported to be involved in the transfer of enveloped virions to the cell surface (161). It is our hope that further work will clarify the mechanism by which myosins promote trafficking and secretion of HSV-1 virions.

Extracellular virions associate with a protein that is maintained at egress sites by the actin cytoskeleton. In addition to assisting virus/glycoprotein trafficking, actin was found to play a structural role in the maintenance of HSV egress sites. When the actin cortex was depolymerized, glycoprotein patches and associated virions dispersed across the cell surface. It has been previously proposed that virions remain associated with the cell surface through general nonspecific interactions or through binding to heparan sulfate. Large numbers of cellular glycoproteins incorporate heparan sulfate groups (28). The maintenance of virions at the observed egress sites suggests a specific interaction with a protein in these glycoprotein rich areas. The expected protein is potentially in a complex with many other proteins or has a large cytoplasmic tail and is unable to move past the "actin fence" (91,125). It is also possible that the putative protein is bound directly or indirectly to the actin cytoskeleton. The depletion of actin observed at egress sites makes the former a likely possibility. A protein named tetherin has been reported to function in tethering multiple viruses to the cell surface. However, tetherin not only leashes virions to the surface but induces endocytosis and degradation of the virions. It is an interferon-inducible form of innate immunity (47). In addition to many other viral families that have developed ways to overcome this obstacle, Kaposi's sarcoma-

associated herpesvirus is able to downregulate tetherin from the cell surface (146). It is likely that HSV-1 has developed a similar mechanism. Also, Vero cells do not produce interferon, making the expression of tetherin less likely (34). Future work should be able to further characterize the proposed specific association between virus and cell surface protein.

Glycoprotein E directs trafficking of glycoproteins to egress sites. Lastly, it was found that the cytoplasmic tail of viral glycoprotein E played a role in release site formation. gE has been reported to direct trafficking of progeny virions to cell junctions in epithelial cells and synapses in neurons (31,37,79). Surprisingly, the lack of gE did not decrease the amount of virus associating with bottom surface egress locations. In fact, the number was increased. ΔgE did, however, decrease the amount of glycoproteins at exit sites, resulting in much smaller egress patches.

We considered the possibility that the observed patch decrease was due to loss of gE stabilization of surface glycoprotein aggregations. Though a slight dispersal is perhaps visible in ΔgE and gEΔCT infected cells, it is not definitively more dispersed than in the rescue virus images (Figure 24). If the lack of gE is inducing disruption of patch glycoproteins and an increase in glycoprotein staining outside of patches is not visible on the cell surface, then those dispersed glycoproteins must be removed from the surface, i.e. endocytosed. We think it is unlikely that slightly disrupted (complete disruption would lead to no patches) glycoprotein aggregations would be endocytosed at the egress sites, and minimally disrupted aggregations would be unlikely to diffuse past the actin fence to areas where endocytosis would be more likely to occur. In the event

that glycoproteins are held at the egress sites by linkage to low levels of actin within the patch areas rather than bounded by a fence, one could argue that gE could be involved in this linkage. However, previous studies have not been able to observe a link between gE and the cytoskeleton; when the cytoskeleton is isolated from detergent disrupted cells, gE remains in the soluble portion (41). We interpret these observations to suggest that in non-polarized cells, gE either directs the trafficking of glycoproteins to release sites or is the main constituent of the egress site patches. A small decrease in patch size would be expected when a viral glycoprotein is deleted. However, if the decrease in patch size observed is due to the absence of the gE protein within patches, then size of the decrease observed would suggest that there is more gE in the patches than all other cellular and viral glycoproteins combined.

Previous work supports the evidence described here that viral glycoprotein-containing vesicles can traffic independently to egress locations (177,178,193,214). gE and TGN46 have been found to move to lateral cell junctions late in infection in polarized epithelial cells even when capsids were retained in nucleus with a temperature sensitive mutation (41). In some HSV-1 infected neurons, capsids are shipped down the axon in unenveloped form (119,178,215), and glycoproteins are transported on separate vesicles. It is believed that envelopment occurs near the egress site. Glycoproteins, therefore, can be individually targeted to egress locations. When gE is absent, trafficking of both capsids and glycoprotein-containing vesicles into axons is greatly reduced (112,204). It is surprising that capsid trafficking is affected since capsids without glycoproteins are assumed to have no membrane and no membrane-protein association

(177). However, this study of axonal transport indicates that gE can direct movement of viral proteins by direct or indirect means. If gE is targeting vesicles for transport in non-polarized Vero cells, then this action is limited to glycoprotein only-containing vesicles.

In view of our observations, it is reasonable to ask: what role do glycoprotein enriched patches play in an epithelial cell infection? In one relevant report it was found that transfer of virus from infected epithelial cells to neurons is almost completely blocked in a gE null infection. However, gE null virus added to axons directly has no trouble entering and traveling to the cell body to initiate infection (113). Similar results are seen with HSV-2 (205). As it only takes a small number of virions to create a productive infection, it is difficult to imagine that random secretion rather than directed egress would be sufficient to create such a block. However, if in addition to the presence of a virion, transmission requires a specific site conducive to transfer, then these results would be easier to interpret. Since free virus is able to enter both epithelial cells and neurons without difficulty, it is not necessary for viral proteins on an infected cell to induce the creation of a specialized entry site on an adjacent non-infected cell (although it would be advantageous from the stand point of immune evasion and efficiency). However, since the majority of progeny virions remain tethered to the cell surface until late in infection, it is quite possible that proteins recruited to egress sites are necessary for viral release. The methods described above for the observation of coverslip-adherent surface egress sites will be particularly useful for exploring these possibilities. TIRF microscopy allows clear visualization of the spatial relationship between released virions

and the parental cell surface. It is likely that the egress sites characterized in this paper share many similarities with egress sites in other cell types.

V. Conclusions and Interpretations

<u>Infection Model</u>

Many viruses have developed mechanisms to direct cell-to-cell spread. One virus can follow multiple pathways depending on the cell type in which it is replicating and the cell type to which it is being transferred (75,80,108,181). In this thesis, I have explored mechanisms used for efficient cell-to-cell transmission by herpes simplex virus type 1 in a non-polarized cell infection. Non-polarized cells are less differentiated than polarized cells and lack fully formed junctions. Cells that fit the non-polarized classification can be found near the basal surface of mucosal tissues (123,152,153,209). Reports have indicated that there is a difference in spread between these less polarized epithelial cells and the cells that have undergone greater differentiation near the tissue's apical surface (124,142).

In an *in vivo* mouse system that models viral reactivation from latency, infection spreads from the trigeminal ganglion to the cornea through sensory neuron axons. Upon reaching the stratified epithelial cells in the cornea, the infection spreads first to non-polarized basal cells. From the basal cells the infection is transferred up toward the apical surface of the tissue, rather than laterally. Once infection reaches the more differentiated, polarized squamous epithelial cells, the infection spreads cell to cell laterally (142). This results in a cone-shaped lesion with a small number of infected cells at the bottom and a large number of infected cells at the top (Figure 25), a structure that is presumably advantageous for host-to-host spread. This corneal infection model indicates

Figure 25: HSV-1 Corneal Lesion. Virus injected into the mouse trigeminal ganglion spreads through the neuronal network to the corneal epithelium of the eye. From the innervating axons, infection is first transferred to basal cells at the bottom surface of the tissue strata. From there it spreads upward to the squamous epithelium, while lateral spread is limited. In squamous epithelial cells the virus spreads cell to cell laterally. As a result of apical viral spread in basal cells and lateral spread in squamous cells, the lesion that forms is cone-shaped. This section has been stained with toluidine blue to show structural detail. In addition, the section has been immunostained with HRP-conjugated anti-HSV polyclonal antibodies and treated with Ni-DAB. Arrows point to the the edges of the lesion as defined by anti-HSV staining (dark blue/green). Star indicates where epithelium has separated from the underlying stroma during processing. Image is from Ohara et al. 2000 (142).
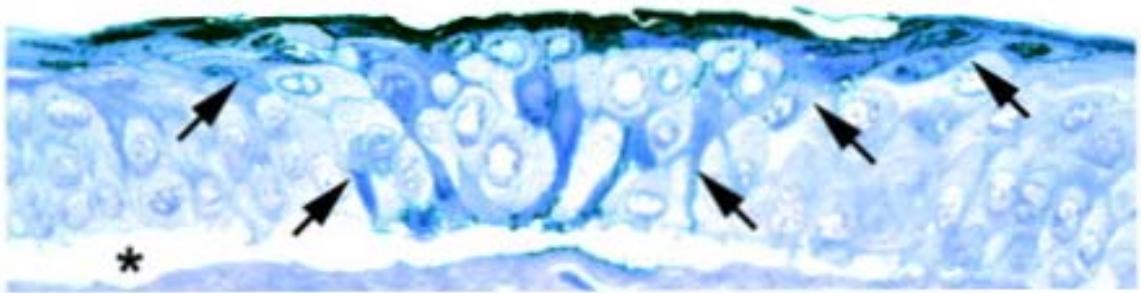
that cell-cell spread in cells near the basement membrane occurs in a different manner from viral spread in cells near the apical surface. It is important to study the HSV-1 lifecycle in a variety of cell types to determine how differing cellular characteristics can affect the process of viral replication and spread. Little work has been done on the process of targeted viral release in non-polarized cells. No work has been published thus far on the composition of the viral egress sites in any cell type. In this thesis, the process of HSV-1 egress was further clarified.

The model I used for studying the process of viral egress was the Vero cell line plated on glass coverslips. Vero cells are epithelial cells from a monkey kidney that have lost their polarization through transformation (10,219). As is the case with many transformed cell lines, this transformation induced a less differentiated phenotype. The basal cells in stratified epithelia give rise to the differentiated cells in higher strata, and thus have a less differentiated non-polarized cell phenotype (152,209,220). Vero cells, therefore, share characteristics with a class of cells that are found to be infected in an *in vivo* infection. Glass coverslips are not directly representative of *in vivo* conditions. I did not coat the coverslips with proteins found in the basement membrane of the epidermis, nor is this glass surface representative of a cell-cell contact site. However, our findings showed that HSV is released at both cell-cell and cell-glass adherent surfaces in non-polarized cells. Therefore, factors other than protein specific surface-surface interactions can determine polarized transport of virus. The egress patches that develop at the cell-coverslip interface appear to share similarities with those that develop at cell-cell contact surfaces; both show a concentration of virions and viral glycoproteins. The

understanding of viral egress gained by studying these release locations at the coverslip interface broadens the comprehension of viral egress as a whole.

Development of Specialized Egress Sites or 'Virological Synapses'

To increase the efficiency of cell-cell spread, several viruses induce the creation of what has become known as a "virological synapse" (VS) (56,133). It was originally named a virological "synapse" due to the similarities observed between immunological synapses (IS) and the egress sites created by human immunodeficiency virus (HIV). When an HIV infected cell (macrophage, dendritic cell, or T cell) engages with a T cell it forms a structure along the cell-cell contact site that appears morphologically similar to an immune synapse and recruits many of the adhesive proteins found in an IS. The formation of this site is driven by HIV env protein interacting with its receptor, CD4, on the cognate cell, rather than the binding of MHC to TcR (80). There are some key differences between these sites as well. Viral proteins concentrate at VS locations and certain cellular proteins that aren't typically found in an IS are recruited (66,100,140,191). The virus appears to co-opt the pathway used for IS formation, but it does not appear to use existing, unmodified ISs for cell-cell spread. VSs can form between an infected cell and multiple uninfected cells at the same time (163). Multiple viruses have been found to use a VS, as defined by an area of adhesion between an infected cell and uninfected cell that is induced or modified by infection for the purpose of efficient cell-to-cell spread (56,133).

In the work discussed in the previous chapter, we found that HSV-1 is released along an adherent surface of the cell that is modified by infection to create a site that is likely advantageous for viral release. Relevant modifications include the rearrangement of the actin cytoskeleton and the recruitment of large concentrations of viral and possibly cellular glycoproteins that are maintained at the site by filamentous actin. The fact that egress sites form along adherent surfaces is not surprising. *In vivo*, adherent surfaces are most often in contact with another cell. The formation of egress sites at adherent surfaces rather than at specific junctional complexes allows viral transfer to different cells with compositionally distinct junctions within the epidermis. However, as the lack of lateral spread to adjacent basal cells in the mouse cornea shows, there is more to the story. The existence of any adherent surface drives directed egress in cultured Vero cells but is not sufficient to do this in all cell types and situations. Our finding that the HSV-1 virus is released at specific areas that undergo modification indicates that, as with many other viruses, it is released at unique sites that can be defined as virological synapses.

Cytoskeletal Trafficking

Trafficking of HSV-1 virus to egress sites has been studied more extensively in neurons than in epithelial cell types. In neurons, microtubules are critical for long distance transport down the axon length. Both capsids and glycoprotein-containing vesicles can be seen associating with microtubules during trafficking, and kinesin motors are believed to assist this transport (37,96,103,148,154,155,172). Little work has been done in epithelial cells, although one previous study found that microtubule

depolymerization with nocodazole or microtubule stabilization with taxol decreases titre by one log (89).

We found that disrupting microtubules during infection in Vero cells resulted in smaller egress site glycoprotein patches and decreased amounts of virus present at these locations. This finding was not overly surprising since outgoing capsids and glycoproteins have been found to associate with microtubule filaments in neurons. In addition, it is likely that virions are too large and dense to traffic without the help of a cytoskeletal track (179). The observed decrease in glycoproteins at the surface of nocodazole-treated epithelial cells is likely due to an inhibition in trafficking from their resident vesicular compartment to the surface. The decrease in virus number at glycoprotein patches could be due to either an inhibition in transport to the cell membrane or to a disruption in envelopment. The amount of virus at the adherent cell surface decreased approximately 4-fold. Titre decreases of this magnitude are difficult to accurately measure, so either scenario could be taking place.

As with nocadazole treated samples, small effects of cytochalasin B on titre were difficult to measure; a trend was not apparent in any sample set. Analysis of viral levels on the cell surface showed a decrease that was interpreted as being partly due to diffusion of virions away from the adherent surface and partly due to a small inhibition in viral release. It has been previously reported that the actin cortex can assist the process of vesicle secretion in uninfected secretory cell types (38,97,104). In addition, it has been found that actin motor myosin Va is important for HSV secretion (161). This myosin processes along actin filaments and powers secretory vesicle movement to the cell

surface (35). We found that inhibiting myosin II also decreased the expansion of egress

sites and the trafficking of virions to these sites. This myosin has been found to play

many roles in a cell, one of which includes assisting exocytosis (4,110,130). Peter

O'Hare's group has described a rearrangement of myosin II in infected Vero cells from a

generally diffuse distribution to a central concentration with spoke-like lines radiating

from a perinuclear area (201). They also observe this protein at cell-cell contact sites at

late timepoints of infection. Therefore, our results are in accordance with previous

reports and indicate that both the microtubule and actin cytoskeleton are important for

trafficking of glycoproteins and virus to egress sites.

Putative Cell Attachment Protein

In our experiments to determine the role of the cytoskeleton in viral trafficking,

we found that depolymerizing filamentous actin after glycoprotein patches had formed

led to a dispersal of these assemblies. This finding suggests that actin is involved in

maintaining the structure of egress sites. Actin could do this by directly binding to

glycoproteins in patches or by the creation of an actin fence. Actin fences are so named

because actin filaments are, in many cases, narrowly spaced from the plasma membrane

and are often bound to the membrane through adaptor proteins. This tight association

limits the diffusion of membrane proteins (91,125). Proteins with large cytoplasmic tails

or proteins that are associating with a number of other proteins are the most limited in

movement. In the experiments discussed in the previous chapter, we showed that actin

was depleted in areas where patches had formed. This makes the actin fence possibility

likely, although, low levels of actin that do not stain with phalloidin could still be present within egress locations.

We observed that virus that had fused with the cell surface was found in association with glycoprotein patches. It was very rare to see a virion outside of these areas. This lack of diffusion across the cell surface indicates that the virus is likely associating with a specific protein at patch sites. As mentioned above, the putative protein is expected to be limited in diffusion or directly linked to the actin cortex. At this time, the nature and identity of the tether protein(s) is unknown.

There have been reports of a viral tether protein called tetherin restricting the release of viruses from the cell surface. This protein functions as a form of innate immunity. After interferon induction, tetherin captures budding virions, tethers them to the cell surface, and then induces endocytosis. These virus-containing endocytic vesicles then mature to late endosomes/lysosomes, and the virions are degraded (47,121,149). Many viruses are able to down-regulate tetherin from the cell surface and sequester it in late endosomes (81,84,106,166). Tetherin was discovered when mutations in certain viral proteins allowed the tether to become active (132). It is likely that HSV-1 has such a mechanism; another herpesvirus- Kaposi sarcoma associated virus- can induce the degradation of tetherin (146).

There is a small possibility that HSV could modulate tetherin's function and block endocytosis so that it assists cell-cell transfer rather than inhibits it. However, there have been no previous reports of a virus modulating tetherin's function in such a fashion and

Vero cells do not express interferon, making the expression of tetherin doubtful (34). It's

likely that another viral or cellular protein functions in the HSV-1 tethering process. It's

also possible that the tether action is much less specific. It may be that certain viral

proteins are able to weakly interact in trans. This would lead to a Velcro-like bond

between the virion and glycoprotein patches. In such a scenario, the action of binding to

a receptor on the opposite cell would, presumably, disrupt this bond. The fact that the

virus maintains this connection with the cell surface for significant periods of time during

infection suggests that it is advantageous for efficient cell-cell spread.

<u>Glycoprotein Trafficking</u>

HSV-1 egress sites on the adherent surface of glass plated Vero cells are

characterized by dense concentrations of glycoproteins, which form whether or not

virions are being enveloped and released. We have considered two possible explanations

for the concentration of glycoproteins at these sites. The first is that glycoproteins are

trafficked from the envelopment compartment to the cell surface in vesicles that may or

may not contain an enveloped virus particle (Figure 26). This bulk-phase transport

pathway would begin before virions are being enveloped and would continue whether or

not virus is present within the vesicle, resulting in patches of equal size. The second is

that glycoproteins accumulate at the cell surface by following a separate protein

trafficking pathway from the vesicles the virus uses (Figure 26). Virus is then targeted to

glycoprotein-containing sites, adding few additional glycoproteins with fusion. The two

pathways are not necessarily mutually exclusive. Both could be occurring to some

degree.

Figure 26: Schematic representing the two possible pathways that glycoproteins can follow to the cell surface. The two pathways are not mutually exclusive. Glycoprotein enriched membranes are depicted in red. Other membranes are in blue. In the first pathway, virions bud into glycoprotein enriched vesicles that move from the envelopment compartment to cell membrane carrying the glycoproteins with them. This movement of vesicles from the envelopment compartment to membrane would occur whether or not a virion budded into the lumen. In the second pathway, virions bud into a vesicular membrane through small areas that are enriched in glycoproteins. Glycoprotein poor vesicles then traffic from the envelopment compartment to cell surface. Patch glycoproteins arrive at egress sites by following a separate vesicular sorting pathway.
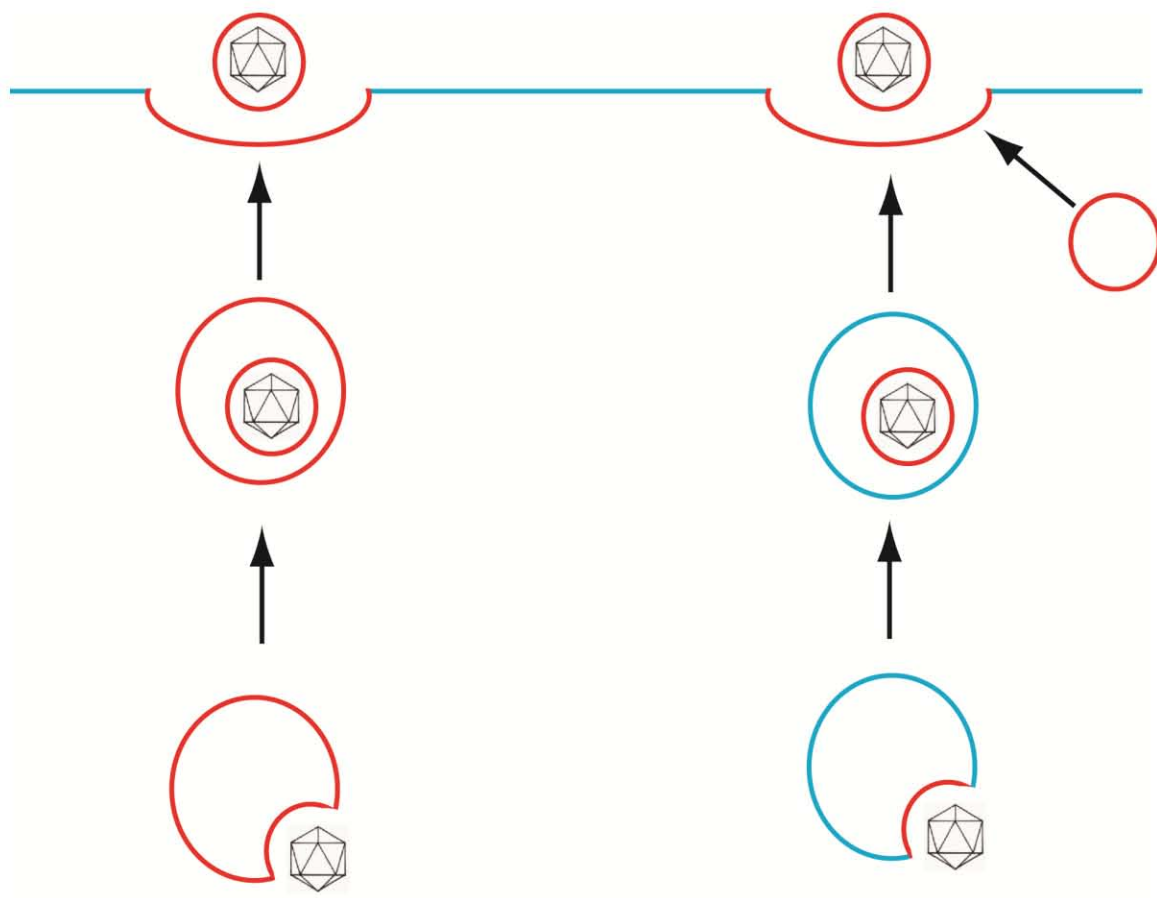
Figure 27: Differential Trafficking Between Glycoproteins and Virions as Represented by

Changes in the Density of Virions in Glycoprotein Patches under Different Conditions.

(A) VP26-GFP infected Vero cells were treated with DMSO, cytochalasin, or nococazole

as described for Figure 18. (B) VP26-GFP infected Vero cells were treated with myosin

II-inhibitor blebbistatin as described for Figure 20. (C) Cells were infected with WT

HSV-1 or gE deletion mutants as described in Figure 23. The number of virions within

each patch was calculated by dividing the virion grayscale value for each patch by the

total patch area. Note that the decreased virion densities shown in A and B indicate that

the treatments had a greater inhibitory effect on virion trafficking compared to

glycoprotein trafficking. In C, the opposite was true; the increased density of virions

within patches suggests that glycoprotein trafficking was inhibited compared to virion

secretion. This further supports the theory that glycoproteins traffic on vesicles that are

compositionally distinct from those that carry the virions.

Effect of Microtubule and Actin Depolymerization
on Virus / Patch Area
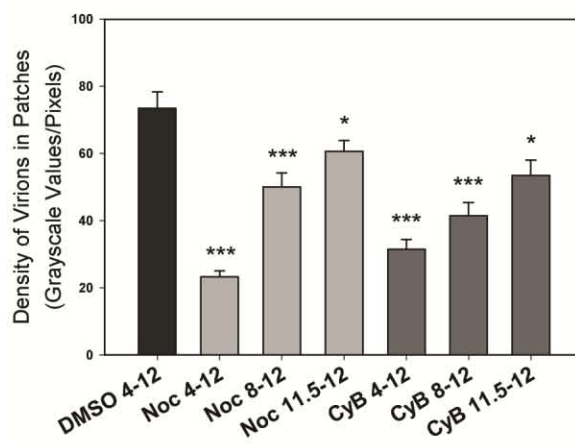
Effect of Myosin II Inhibition on Virus / Patch Area
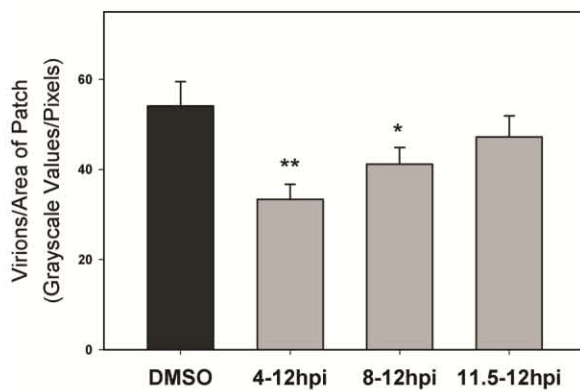
Effect of gE Deletions on Virions / Patch Area
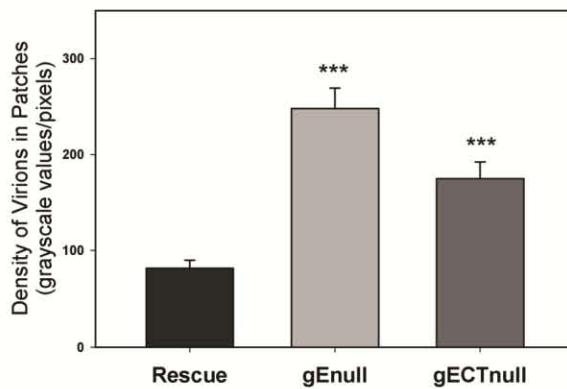
In the experiments quantitating the effect of treatments/conditions on egress patch formation, it was found that there were different effects between virion and glycoprotein trafficking. This effect was reflected in changes in the density of virions within a patch (Figure 27). An increase in virion density indicates an increase in virion trafficking compared to glycoprotein trafficking or a decrease in glycoprotein trafficking relative to virion trafficking. A decrease in virion density within the egress patches suggests a decrease in virus trafficking or increase in glycoprotein release. Virion density dropped in samples in which the microtubules, actin cytoskeleton, or myosin II filaments were disrupted (Figure 27). These findings were interpreted to indicate that treatment was having a greater inhibitory effect on the trafficking of virion-containing vesicles than on glycoprotein containing vesicles. Though this difference suggests differential trafficking between virus and glycoproteins, vesicles without virions may need less cytoskeletal assistance than those containing virus. However, in cells infected with the gE deletion mutants, virion release was not decreased while glycoprotein localization to the patches dropped. This could also be interpreted as evidence for differential sorting, though other possibilities could also explain this observation. A small decrease in patch size would be expected when a glycoprotein is deleted, although the size of the drop observed would suggest that there is more gE in patches than all other cellular and viral glycoproteins combined. I have also considered the prospect that the observed results are due to the contribution of gE to the stability of glycoprotein aggregations after fusion, i.e. glycoproteins form less stable associations that are easily disrupted when the gE protein is absent leading to patch disruption. I consider this unlikely for the reasons discussed in

the previous chapter. I think it highly probable that viral gE is directing the trafficking of glycoprotein-containing vesicles, but not virion-containing vesicles in this cell type. If so, then this would support the possibility that glycoproteins traffic by a different route than virions. It remains to be seen whether glycoprotein vesicles originate from the envelopment compartment or another vesicular pathway altogether.

Supporting evidence for the differential trafficking possibility is found in previous reports that indicate that glycoproteins can traffic independently to egress locations (177,178,193,214). In HSV-1-infected neurons, evidence suggests that glycoproteins are transported on separate vesicles, and it is assumed that envelopment occurs near the axon synapse (119,178,215). When gE is absent, trafficking of viral proteins into axons is greatly reduced (112,177,204). The lack of gE inhibited their movement into and down the axon length. A decrease in glycoprotein movement to cell junctions was also observed in polarized epithelial cells when gE was absent (114). Therefore, gE can direct movement of glycoprotein containing vesicles by direct or indirect means.

Proposed Role for gE and Glycoprotein Patches

In previous reports neurons were grown in a Campenot chamber system such that their axons alone stretched into the adjacent compartment. The authors then plated a variety of epithelial cell types (including Veros) on top of these axons and infected them. It was found that transfer of virus from infected epithelial cells to neurons was blocked in the gE null infection. However, gE null virus that was added to the axons directly had no trouble entering the neurons and traveling to the cell body to initiate infection (113,205).

As it only takes a small number of virions to create a productive infection in a cell, it seems unlikely that dispersed virus on the surface of an adjacent cell rather than concentrated virus at the egress site would be sufficient to create such a block. However, if in addition to the presence of a virus particle it is necessary to have a site that is conducive to its transfer, then these results would be logical. Since free virus is able to infect both epithelial cells and neurons, it is not necessary for an infected cell to induce the creation of a specialized entry site on an adjacent uninfected cell. However, since the majority of virus particles remain cell associated until late in infection, it is possible that such a site is necessary for viral release.

Previously published work has shown that changing the composition of the glycoproteins at egress sites can inhibit cell-cell transfer of virus. In polarized epithelial cells, exogenously expressed gE lacking its cytoplasmic tail is found on the lateral cell surface (rather than TGN) due to the removal of its trafficking motif (213). Exogenously expressed gD is found on all cell surfaces. Expression of either gEΔCT/gI or gD followed by infection with wild type virus induces virions to build up in the intracellular space rather than transfer to adjacent cells (Figure 28) (24). The authors of this finding suggest that both gEΔCT/gI and gD are acting through a similar mechanism, i.e. sequestering receptors necessary for entry. Indeed, evidence indicates that gD sequesters entry receptors. There have been multiple reports of this in the literature (60,183,184), and the authors observe a 10-fold reduction in the number of plaques that form on gD overexpressing cells in addition to the buildup of virions in the intercellular space. However, gEΔCT/gI overexpressing cells have no reduction in the number of plaques

Figure 28: These images from Collins 2003 depict HaCaT epithelial cells that are expressing gD, a gE construct lacking the cytoplasmic tail complexed to gI (gEΔCT/gI), or nothing (No Ad). These cells have been infected with WT HSV-1. Top images show the decrease in plaque size that occurs when either gD or gEΔCT/gI are expressed in cells prior to/during infection. Electron microsocpy images on the bottom show virions released at cell junctions in these construct expressing cells. Note that both gD and gEΔCT/gI overexpression induces the buildup of virions at the junctions in greater amounts than in non-expressing cells (No Ad).

No Ad **AdgD** **AdgEΔCT/gI**
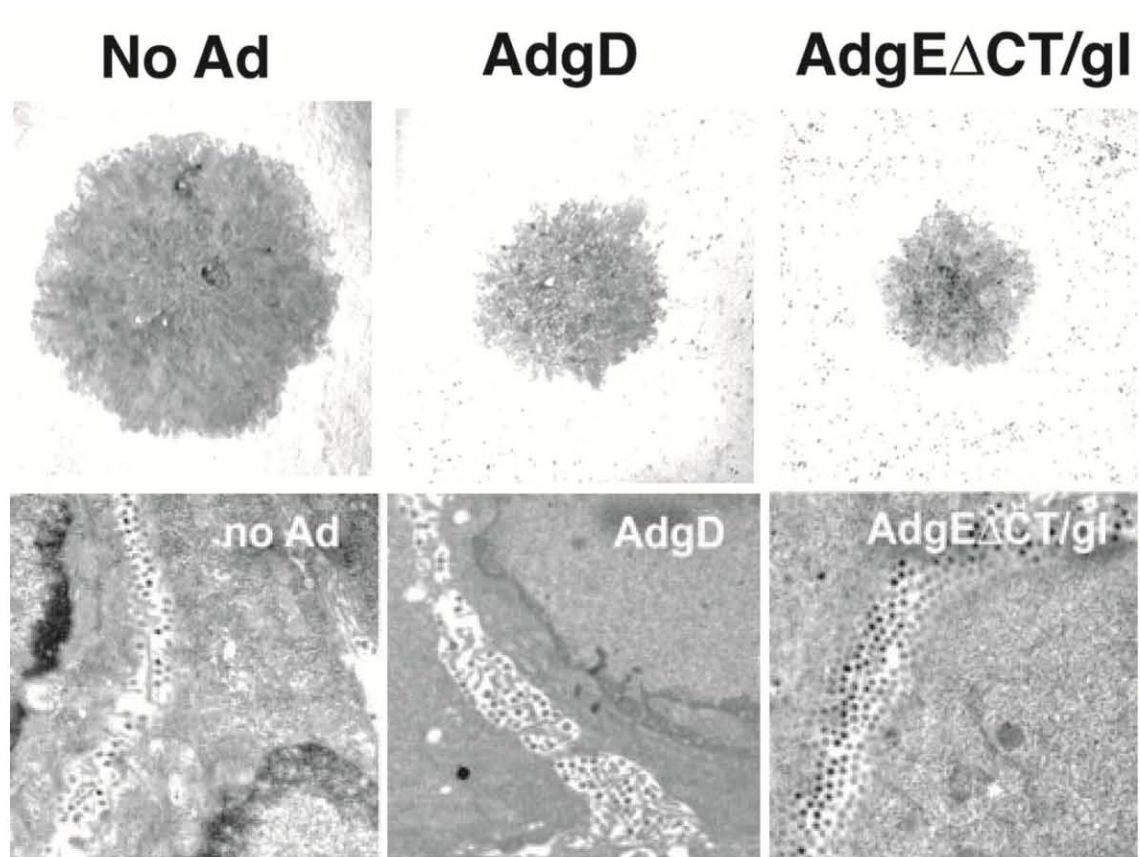
that form. In this situation, cells are being inoculated from the apical surface, so the authors propose that virus enters differently at junctions than it does on the cell surface, and this entry process needs the assistance of gE bound to a cellular receptor. Although there have been no reports of gE functioning in entry, this hypothesis would suggest that the proposed gE receptor is more important than the gD receptor since gEΔCT/gI expressing cell plaques are 35% of control plaques while gD expressing cells form plaques that are 50% of the size of the control plaques. Expressing both gD and gEΔCT/gI does not decrease plaque size past 30% and the authors interpret this to mean both gD and gE are acting on the same receptor that is experiencing fully saturated binding. Interestingly, overexpression of WT gE/gI had no effect even though it too builds up at the cell junctions. The authors propose a model to explain their findings. In their model, gE on the cell membrane binds to a putative cellular receptor on an adjacent cell, and its cytoplasmic tail somehow orchestrates the transfer of this ligand onto gE located on an extracellular virus. Once gE on the virus is bound to its receptor, entry can ensue. In addition, since ΔgE virus and gEΔCT virus are equally inhibited in cell-cell spread, this indicates that the cytoplasmic tail of gE is necessary for entry- a tail that is packed in dense tegument proteins in the virion. Though this model seems unlikely, subsequent studies have found that mutating portions of the gE extracellular domain can also block cell-cell spread while not affecting infectivity or trafficking, further supporting the existence of a gE cellular ligand (151).

The egress sites located along glass coverslips share several similarities with cell-cell adherent sites. The lack of gE affects the formation of these glass-adherent surface

sites, and previous reports have found that Vero cells infected with ΔgE mutants are inhibited in cell-cell spread and cell-neuron spread (7,113). We also have observed a decrease in plaque size when the Vero cells passaged for this study were infected with our two gE mutants, supporting evidence for gE's role in inhibiting cell-cell spread in this cell type (data not shown). Assuming the viral egress sites that form along the coverslip function similarly to those that form between cells, then the presence of infectious virus at a release site may not be enough to induce infection on an adjacent cell. These sites may need a buildup of cellular and/or viral glycoproteins whose sorting/trafficking is independent of virions.

In light of current reports on the function of gE and our data indicating a specific interaction between cell-associated virions and a protein expressed on egress site membranes, we would like to propose the following hypothetical model: gE directs the trafficking of virion-containing vesicles, glycoprotein-containing vesicles, or both to egress sites, depending on cell type. Virus is released in an area of dense glycoproteins that includes its tether/attachment protein, gE, and multiple other glycoproteins. gE binds a cell-cell contact site-specific cellular ligand in cis or in trans through its extracellular domain and signals for the downregulation of the putative viral attachment protein through its cytoplasmic domain (Figure 29), which is known to be rich in sorting motifs and phosphorylation sites (1,120,136,213). The virus is then released from its tether in a localized area that is advantageous for cell-cell spread. If no ligand is available for gE to bind, the virus remains cell associated until late in infection near the time when the cell is losing its capability to adhere to a surface. Virions are then released. There are various

Figure 29: Tether Model. Virion is tethered to the cell surface by a putative protein depicted in red. The viral protein that associates with this tether is shown in blue projecting from the virion surface. The gE/gI complex in green interacts with a putative cellular ligand in orange. This association is dependent on specific sequences in the extracellular domain of gE. The gE population on the surface of the virion is likely capable of binding to this cellular ligand as well. Upon binding to the ligand, the cytoplasmic tail of gE signals the release of the virion from the viral tether through cellular or tegument signaling (both possibilities are shown). In the scenario of ligand-induced cellular signaling, the engagement of gE induces the phosphorylation (yellow) of gE's cytoplasmic tail. This tail can then either bind to the tether directly or bind an adaptor protein (purple) that can induce the tether to release the virion. In the tegument signaling scenario, gE on the virion surface binds to its putative ligand and induces the protein on the virion surface to disassociate from the tether protein. This signal would occur within the dense network of proteins that compose the tegument, making this scenario less likely than the former possibility. In either scenario, the tether dissociates from the virion allowing it to bind entry receptors on the adjacent cell.

A.

Target Cell

gE Ligand

gE/gI Complex

Infected Cell

Tether

B.

Target Cell

Infected Cell

Tether
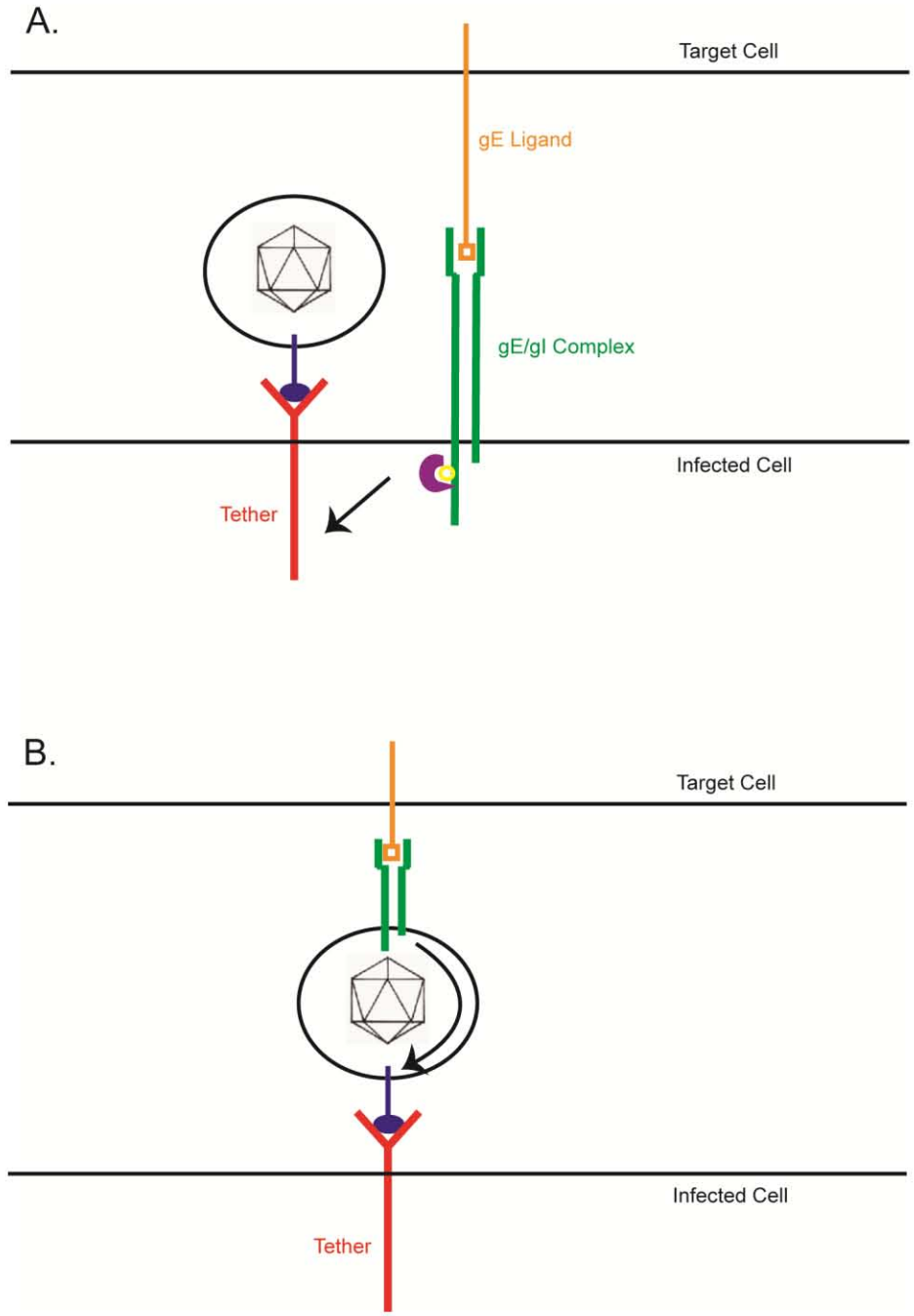
ways that this action could occur. Though conjecture at this point, this model does fit

with the current evidence for gE's role in cell-to-cell spread.

This project could be further explored in many possible directions. One area that

I spent a fair amount of time researching (with little success) is the determination of

possible cellular proteins recruited to egress patches during infection. I tested a wide

range of cellular proteins, including tetraspanins, integrins, and endosomal proteins, for

colocalization with glycoprotein patches using indirect immunofluorescence as well as

the expression of fluorescent constructs (see appendix). Several viruses have been

reported to recruit cellular proteins to their virological synapses (58,109,140,140). It is

likely that HSV-1 does so as well. The structure of these egress sites makes them

particularly suited for visualizing the cellular proteins needed for fusion of vesicles

containing virus with the plasma membrane.

The vesicular trafficking pathway used by the glycoprotein- containing vesicles is

also an area of further study. The vesicular source of the patch glycoproteins needs to be

further explored. In addition, the function of these structures remains to be elucidated. It

is possible that glycoprotein concentrations play a role in fusion of the vesicle during

egress, immunoprotection from α-HSV antibodies or cell attack, tethering of virus

particles in strategic areas, and/or transfer of virions to an uninfected cell. It will be

crucial to see if the inhibition of glycoprotein secretion by means other than those

discussed in this thesis directly translates to inhibited viral release or transfer.

The identity of the putative cell-surface protein with which progeny extracellular virions associate also remains to be determined. The bond between these proposed proteins may be weak and easily disrupted upon virus-receptor binding or may be strong and dependent on specific signals/modifications for the induction of viral release. The first step in assessing our hypothetical model will be to determine the existence and identity of the tether protein with which progeny virus associates. Once the identity of this protein is known, it will be possible to disrupt the protein-virion interaction by siRNA or other means and observe what effect this has on infection.

Lastly, the identity of the cellular ligand with which gE has been purported to interact awaits identification. Previous reports have shown that a truncated form of gE can concentrate at cell contact sites when expressed in both infected and uninfected cells. The ability of gE to accumulate at these locations indicates that the protein is interacting with a cellular protein in these areas. Once this cellular protein is identified, the role it plays in infection can be more easily determined. We believe this system for studying egress sites in Vero cells using TIRF microscopy will be useful for investigating the trafficking of virions to release sites and the mechanism of their maintenance there. As these sites are easier to visualize than those that form at cell junctions in polarized epithelial cells and synapses in neurons, we hope this infection model will contribute to the elucidation of viral egress in all cell types.

VI. ASM Image Licenses

Figure 3:

AMERICAN SOCIETY FOR MICROBIOLOGY LICENSE

This is a License Agreement between Rebecca Mingo ("You") and American Society for Microbiology ("American Society for Microbiology") provided by Copyright Clearance Center ("CCC"). The license consists of your order details, the terms and conditions provided by American Society for Microbiology, and the payment terms and conditions.

License Number   2832220088023

License date   Jan 18, 2012

Licensed content publisher   American Society for Microbiology

Licensed content publication   Molecular and Cellular Biology

Licensed content title   Herpes Simplex Virus Type 1 Entry into Host Cells: Reconstitution of Capsid Binding and Uncoating at the Nuclear Pore Complex In Vitro

Licensed content author   Päivi M. Ojala, Beate Sodeik, Melanie W. Ebersold, Ulrike Kutay, Ari Helenius

Licensed content date   Jul 1, 2000

Volume 20, **Start page** 4922, **End page** 4931

Type of Use   Dissertation/Thesis

Format   Print and electronic

Portion   Figures/tables/images

Number of figures/tables   1

Title of your thesis / dissertation   Characterization of HSV-1 Release Sites (Now "Formation of Specialized HSV-1 Egress Sites")

Expected completion date   Jan 2012

Estimated size(pages) 150

Billing Type   Invoice

Billing address

1300 Jefferson park Ave

 Jordan Hall Room 7063

 Charlottesville, VA 22908

 United States

Customer reference info

Total   0.00 USD

AMERICAN SOCIETY FOR MICROBIOLOGY LICENSE

This is a License Agreement between Rebecca Mingo ("You") and American Society for Microbiology ("American Society for Microbiology") provided by Copyright Clearance Center ("CCC"). The license consists of your order details, the terms and conditions provided by American Society for Microbiology, and the payment terms and conditions.

License Number   2832220676652

License date   Jan 18, 2012

Licensed content publisher   American Society for Microbiology

Licensed content publication   Journal of Virology

Licensed content title   Herpesvirus Assembly and Egress

Licensed content author   Thomas C. Mettenleiter

Licensed content date   Feb 1, 2002

Volume 76, **Start page** 1537, **End page** 1547

Type of Use   Dissertation/Thesis

Format   Print and electronic

Portion   Figures/tables/images

Number of figures/tables   1

Title of your thesis / dissertation   Characterization of HSV-1 Release Sites (Now "Formation of Specialized HSV-1 Egress Sites")

Expected completion date   Jan 2012

Estimated size(pages) 150

Billing Type   Invoice

Billing address

1300 Jefferson park Ave

 Jordan Hall Room 7063

 Charlottesville, VA 22908

 United States

Customer reference info

Total   0.00 USD

AMERICAN SOCIETY FOR MICROBIOLOGY LICENSE

This is a License Agreement between Rebecca Mingo ("You") and American Society for Microbiology ("American Society for Microbiology") provided by Copyright Clearance Center ("CCC"). The license consists of your order details, the terms and conditions provided by American Society for Microbiology, and the payment terms and conditions.

License Number   2832221273261

License date   Jan 18, 2012

Licensed content publisher   American Society for Microbiology

Licensed content publication   Journal of Virology

Licensed content title   Egress of Alphaherpesviruses: Comparative Ultrastructural Study

Licensed content author   Harald Granzow, Barbara G. Klupp, Walter Fuchs, Jutta Veits, Nikolaus Osterrieder, Thomas C. Mettenleiter

Licensed content date   Apr 1, 2001

Volume 75, **Start page** 3675, **End page** 3684

Type of Use   Dissertation/Thesis

Format   Print and electronic

Portion   Figures/tables/images

Number of figures/tables   2

Title of your thesis / dissertation   Characterization of HSV-1 Release Sites (Now "Formation of Specialized HSV-1 Egress Sites")

Expected completion date   Jan 2012

Estimated size(pages)   150

Billing Type   Invoice

Billing address

1300 Jefferson park Ave

 Jordan Hall Room 7063

 Charlottesville, VA 22908

 United States

Customer reference info

Total   0.00 USD

Figure 5 and 9:

AMERICAN SOCIETY FOR MICROBIOLOGY LICENSE

This is a License Agreement between Rebecca Mingo ("You") and American Society for Microbiology ("American Society for Microbiology") provided by Copyright Clearance Center ("CCC"). The license consists of your order details, the terms and conditions provided by American Society for Microbiology, and the payment terms and conditions.

License Number   2835440171848

License date   Jan 24, 2012

Licensed content publisher   American Society for Microbiology

Licensed content publication   Journal of Virology

Licensed content title   Herpes Simplex Virus gE/gI Sorts Nascent Virions to Epithelial Cell Junctions, Promoting Virus Spread

Licensed content author   David C. Johnson, Mike Webb, Todd W. Wisner, Craig Brunetti

Licensed content date   Jan 1, 2001

Volume 75, **Start page** 821, **End page** 833

Type of Use   Dissertation/Thesis

Format   Print and electronic

Portion   Figures/tables/images

Number of figures/tables   3

Title of your thesis / dissertation   Characterization of HSV-1 Release Sites (Now "Formation of Specialized HSV-1 Release Sites")

Expected completion date   Jan 2012

Estimated size(pages)   150

Billing Type   Invoice

Billing address

1300 Jefferson park Ave

Jordan Hall Room 7063

Charlottesville, VA 22908

United States

Customer reference info

Total   0.00 USD

Figure 6:

AMERICAN SOCIETY FOR MICROBIOLOGY LICENSE

This is a License Agreement between Rebecca Mingo ("You") and American Society for Microbiology ("American Society for Microbiology") provided by Copyright Clearance Center ("CCC"). The license consists of your order details, the terms and conditions provided by American Society for Microbiology, and the payment terms and conditions.

License Number   2835441005249

License date   Jan 24, 2012

Licensed content publisher   American Society for Microbiology

Licensed content publication   Journal of Virology

Licensed content title   Ultrastructural Analysis of Virion Formation and Intraaxonal Transport of Herpes Simplex Virus Type 1 in Primary Rat Neurons

Licensed content author   Alexandra Negatsch, Harald Granzow, Christina Maresch, Barbara G. Klupp, Walter Fuchs, Jens P. Teifke, Thomas C. Mettenleiter

Licensed content date   Dec 15, 2010

Volume 84, **Start page** 13031, **End page** 13035

Type of Use Dissertation/Thesis

Format Print and electronic

Portion Figures/tables/images

Number of figures/tables 2

Title of your thesis / dissertation Characterization of HSV-1 Release Sites (Now "Formation of Specialized HSV-1 Egress Sites")

Expected completion date Jan 2012

Estimated size(pages) 150

Billing Type Invoice

Billing address

1300 Jefferson park Ave

Jordan Hall Room 7063

Charlottesville, VA 22908

United States

Customer reference info

Total 0.00 USD

Figure 7:

AMERICAN SOCIETY FOR MICROBIOLOGY LICENSE

This is a License Agreement between Rebecca Mingo ("You") and American Society for Microbiology ("American Society for Microbiology") provided by Copyright Clearance Center ("CCC"). The license consists of your order details, the terms and conditions provided by American Society for Microbiology, and the payment terms and conditions.

License Number 2835450006970

License date   Jan 24, 2012

Licensed content publisher   American Society for Microbiology

Licensed content publication   Journal of Virology

Licensed content title   Cytoplasmic Domain of Herpes Simplex Virus gE Causes Accumulation in the trans-Golgi Network, a Site of Virus Envelopment and Sorting of Virions to Cell Junctions

Licensed content author   Tom N. McMillan, David C. Johnson

Licensed content date   Feb 1, 2001

Volume 75, **Start page** 1928, **End page** 1940

Type of Use   Dissertation/Thesis

Format   Print and electronic

Portion   Figures/tables/images

Number of figures/tables   1

Title of your thesis / dissertation   Characterization of HSV-1 Release Sites (Now "Formation of Specialized HSV-1 Egress Sites")

Expected completion date   Jan 2012

Estimated size(pages)   150

Billing Type   Invoice

Billing address

1300 Jefferson park Ave

Jordan Hall Room 7063

Charlottesville, VA 22908

United States

Customer reference info

Total   0.00 USD

Figure 10:

AMERICAN SOCIETY FOR MICROBIOLOGY LICENSE

This is a License Agreement between Rebecca Mingo ("You") and American Society for Microbiology ("American Society for Microbiology") provided by Copyright Clearance Center ("CCC"). The license consists of your order details, the terms and conditions provided by American Society for Microbiology, and the payment terms and conditions.

License Number   2792240443398

License date   Nov 18, 2011

Licensed content publisher   American Society for Microbiology

Licensed content publication   Journal of Virology

Licensed content title   Herpes Simplex Virus Type 1 Glycoprotein E Is Required for Axonal Localization of Capsid, Tegument, and Membrane Glycoproteins

Licensed content author   Fushan Wang, Waixing Tang, Helen M. McGraw, et al.

Licensed content date   Nov 1, 2005

Volume 79, **Issue** 21, **Start page** 13362, **End page** 13372

Type of Use   Dissertation/Thesis

Format   Electronic

Portion   Figures/tables/images

Number of figures/tables   1

Title of your thesis / dissertation   Characterization of HSV-1 Release Sites (Now "Formation of Specialized HSV-1 Egress Sites")

Expected completion date   Jan 2012

Estimated size(pages)   150

Billing Type   Invoice

Billing address

1300 Jefferson Park Ave

Jordan Hall Room 7063

Charlottesville, VA 22908

United States

Customer reference info

Total   0.00 USD

Figure 24:

AMERICAN SOCIETY FOR MICROBIOLOGY LICENSE

This is a License Agreement between Rebecca Mingo ("You") and American Society for Microbiology ("American Society for Microbiology") provided by Copyright Clearance Center ("CCC"). The license consists of your order details, the terms and conditions provided by American Society for Microbiology, and the payment terms and conditions.

License Number   2835450458099

License date   Jan 24, 2012

Licensed content publisher   American Society for Microbiology

Licensed content publication   Journal of Virology

Licensed content title   The Spread of Herpes Simplex Virus Type 1 from Trigeminal Neurons to the Murine Cornea: an Immunoelectron Microscopy Study

Licensed content author   Peter T. Ohara, Marian S. Chin, Jennifer H. LaVail

Licensed content date   May 1, 2001

Volume 74, **Start page** 4776, **End page** 4786

Type of Use   Dissertation/Thesis

Format   Print and electronic

Portion   Figures/tables/images

Number of figures/tables   1

Title of your thesis / dissertation   Characterization of HSV-1 Release Sites (Now "Formation of Specialized HSV-1 Egress Sites")

Expected completion date   Jan 2012

Estimated size(pages)   150

Billing Type   Invoice

Billing address

1300 Jefferson park Ave

Jordan Hall Room 7063

Charlottesville, VA 22908

United States

Customer reference info

Total   0.00 USD

Figure 26:

AMERICAN SOCIETY FOR MICROBIOLOGY LICENSE

This is a License Agreement between Rebecca Mingo ("You") and American Society for Microbiology ("American Society for Microbiology") provided by Copyright Clearance Center ("CCC"). The license consists of your order details, the terms and conditions provided by American Society for Microbiology, and the payment terms and conditions.

License Number   2835450876870

License date   Jan 24, 2012

Licensed content publisher   American Society for Microbiology

Licensed content publication   Journal of Virology

Licensed content title   Herpes Simplex Virus gE/gI Expressed in Epithelial Cells Interferes with Cell-to-Cell Spread

Licensed content author   Wendy J. Collins, David C. Johnson

Licensed content date   Feb 1, 2003

Volume 77, **Start page** 2686, **End page** 2695

Type of Use   Dissertation/Thesis

Format   Print and electronic

Portion   Figures/tables/images

Number of figures/tables   2

Title of your thesis / dissertation   Characterization of HSV-1 Release Sites (Now "Formation of Specialized HSV-1 Egress Sites")

Expected completion date   Jan 2012

Estimated size(pages)   150

Billing Type   Invoice

Billing address

1300 Jefferson park Ave

Jordan Hall Room 7063

Charlottesville, VA 22908

United States

Customer reference info

Total   0.00 USD

TERMS AND CONDITIONS

Publisher Terms and Conditions

The publisher for this copyrighted material is the American Society for Microbiology (ASM). By clicking "accept" in connection with completing this licensing transaction, you agree that the following terms and conditions apply to this transaction (along with the Billing and Payment terms and conditions established by Copyright Clearance Center, Inc. ("CCC"), at the time that you opened your Rightslink account and that are available at any time at http://myaccount.copyright.com).

1. ASM hereby grants to you a non-exclusive license to use this material. Licenses are for one-time use only with a maximum distribution equal to the number that you identified in the licensing process; any form of republication must be completed within 1 year from the date hereof (although copies prepared before then may be distributed thereafter). The copyright of all material specified remains with ASM, and permission for reproduction is limited to the formats and products indicated in your license. The text may not be altered in any way without the express permission of the copyright owners.

2. The licenses may be exercised anywhere in the world.

3. You must include the copyright and permission notice in connection with any reproduction of the licensed material, i.e. Journal name, year, volume, page numbers, DOI and reproduced/amended with permission from American Society for Microbiology.

4. The following conditions apply to photocopies:
a. The copies must be of high quality and match the standard of the original article.
b. The copies must be a true reproduction word for word.
c. No proprietary/trade names may be substituted.
d. No additional text, tables or figures may be added to the original text.
e. The integrity of the article should be preserved, i.e., no advertisements will be printed on the article.
f. The above permission does NOT include rights for any online or other electronic reproduction.

5. The following conditions apply to translations:
a. The translation must be of high quality and match the standard of the original article.
b. The translation must be a true reproduction word for word.
c. All drug names must be generic; no proprietary/trade names may be substituted.
d. No additional text, tables or figures may be added to the translated text.

e. The integrity of the article should be preserved, i.e., no advertisements will be printed on the article.

f. The translated version of ASM material must also carry a disclaimer in English and in the language of the translation. The two versions (English and other language) of the disclaimer MUST appear on the inside front cover or at the beginning of the translated material as follows:

The American Society for Microbiology takes no responsibility for the accuracy of the translation from the published English original and is not liable for any errors which may occur. No responsibility is assumed, and responsibility is hereby disclaimed, by the American Society for Microbiology for any injury and/or damage to persons or property as a matter of product liability, negligence or otherwise, or from any use or operation of methods, products, instructions or ideas presented in the Journal. Independent verification of diagnosis and drug dosages should be made. Discussions, views, and recommendations as to medical procedures, choice of drugs and drug dosages are the responsibility of the authors.

g. This license does NOT apply to translations made of manuscripts published ahead of print as "[ASM Journal] Accepts" papers. Translation permission is granted only for the final published version of the ASM article. Furthermore, articles translated in their entirety must honor the ASM embargo period, and thus may not appear in print or online until 6 months after the official publication date in the original ASM journal.

6. While you may exercise the rights licensed immediately upon issuance of the license at the end of the licensing process for the transaction, provided that you have disclosed complete and accurate details of your proposed use, no license is finally effective unless and until full payment is received from you (either by ASM or by CCC) as provided in CCC's Billing and Payment terms and conditions. If full payment is not received on a timely basis, then any license preliminarily granted shall be deemed automatically revoked and shall be void as if never granted. In addition, permission granted is contingent upon author permission, which you MUST obtain, and appropriate credit (see item number 3 for details). If you fail to comply with any material provision of this license, ASM shall be entitled to revoke this license immediately and retain fees paid for the grant of the license. Further, in the event that you breach any of these terms and conditions or any of CCC's Billing and Payment terms and conditions, the license is automatically revoked and shall be void as if never granted. Use of materials as described in a revoked license, as well as any use of the materials beyond the scope of an unrevoked license, may constitute copyright infringement and ASM reserves the right to take any and all action to protect its copyright in the materials.

7. ASM reserves all rights not specifically granted in the combination of (i) the license details provided by you and accepted in the course of this licensing transaction, (ii) these terms and conditions and (iii) CCC's Billing and Payment terms and conditions.

8. ASM makes no representations or warranties with respect to the licensed material and adopts on its own behalf the limitations and disclaimers established by CCC on its behalf in its Billing and Payment terms and conditions for this licensing transaction.

9. You hereby indemnify and agree to hold harmless ASM and CCC, and their respective officers, directors, employees and agents, from and against any and all claims arising out of your use of the licensed material other than as specifically authorized pursuant to this license.

10. This license is personal to you, but may be assigned or transferred by you to a business associate (or to your employer) if you give prompt written notice of the assignment or transfer to the publisher. No such assignment or transfer shall relieve you of the obligation to pay the designated license fee on a timely basis (although payment by the identified assignee can fulfill your obligation).

11. This license may not be amended except in a writing signed by both parties (or, in the case of ASM, by CCC on ASM 's behalf).

12. Objection to Contrary terms: ASM hereby objects to any terms contained in any purchase order, acknowledgment, check endorsement or other writing prepared by you, which terms are inconsistent with these terms and conditions or CCC's Billing and Payment terms and conditions. These terms and conditions, together with CCC's Billing and Payment terms and conditions (which are incorporated herein), comprise the entire agreement between you and ASM (and CCC) concerning this licensing transaction. In the event of any conflict between your obligations established by these terms and conditions and those established by CCC's Billing and Payment terms and conditions, these terms and conditions shall control.

13. The following terms and conditions apply to Commercial Photocopy and Commercial Reprint requests and should be considered by requestors to be additional terms. All other ASM terms and conditions indicating how the content may and may not be used also apply.

Limitations of Use:

The Materials you have requested permission to reuse in a commercial reprint or commercial photocopy are only for the use that you have indicated in your request, and they MAY NOT be used for either resale to others or republication to the public. Further, you may not decompile, reverse engineer, disassemble, rent, lease, loan, sell, sublicense, or create derivative works from the Materials without ASM's prior written permission.

14. Revocation: This license transaction shall be governed by and construed in accordance with the laws of Washington, DC. You hereby agree to submit to the jurisdiction of the federal and state courts located in Washington, DC for purposes of

resolving any disputes that may arise in connection with this licensing transaction. ASM or Copyright Clearance Center may, within 30 days of issuance of this License, deny the permissions described in this License at their sole discretion, for any reason or no reason, with a full refund payable to you. Notice of such denial will be made using the contact information provided by you. Failure to receive such notice will not alter or invalidate the denial. In no event will ASM or Copyright Clearance Center be responsible or liable for any costs, expenses or damage incurred by you as a result of a denial of your permission request, other than a refund of the amount(s) paid by you to ASM and/or Copyright Clearance Center for denied permissions.

v1.5

VII. Reference List

1. **Alconada, A., U. Bauer, B. Sodeik, and B. Hoflack**. 1999. Intracellular traffic of herpes simplex virus glycoprotein gE: characterization of the sorting signals required for its trans-Golgi network localization. J.Virol. **73**:377-387.

2. **Ammer, A. G. and S. A. Weed**. 2008. Cortactin branches out: roles in regulating protrusive actin dynamics. Cell Motil.Cytoskeleton **65**:687-707.

3. **Anderson, J. R. and H. J. Field**. 1984. An animal model of ocular herpes. Keratitis, retinitis and cataract in the mouse. Br.J.Exp.Pathol. **65**:283-297.

4. **Andzelm, M. M., X. Chen, K. Krzewski, J. S. Orange, and J. L. Strominger**. 2007. Myosin IIA is required for cytolytic granule exocytosis in human NK cells. J.Exp.Med. **204**:2285-2291.

5. **Arii, J., H. Goto, T. Suenaga, M. Oyama, H. Kozuka-Hata, T. Imai, A. Minowa, H. Akashi, H. Arase, Y. Kawaoka, and Y. Kawaguchi**. 2010. Non-muscle myosin IIA is a functional entry receptor for herpes simplex virus-1. Nature **467**:859-862.

6. **Baird, N. L., J. L. Starkey, D. J. Hughes, and J. W. Wills**. 2010. Myristylation and palmitylation of HSV-1 UL11 are not essential for its function. Virology **397**:80-88.

7. **Balan, P., N. Davis-Poynter, S. Bell, H. Atkinson, H. Browne, and T. Minson**. 1994. An analysis of the in vitro and in vivo phenotypes of mutants of herpes simplex virus type 1 lacking glycoproteins gG, gE, gI or the putative gJ. J.Gen.Virol. **75 (Pt 6)**:1245-1258.

8. **Batterson, W., D. Furlong, and B. Roizman**. 1983. Molecular genetics of herpes simplex virus. VIII. further characterization of a temperature-sensitive

mutant defective in release of viral DNA and in other stages of the viral reproductive cycle. J.Virol. **45**:397-407.

9. **Beitia Ortiz, d. Z., I, K. Kaelin, and F. Rozenberg**. 2004. Effects of mutations in the cytoplasmic domain of herpes simplex virus type 1 glycoprotein B on intracellular transport and infectivity. J.Virol. **78**:1540-1551.

10. **Bianchi, N. O. and J. Ayres**. 1971. Heterochromatin location on chromosomes of normal and transformed cells from African green monkey (Cercopithecus aethiops). DNA denaturation-renaturation method. Exp.Cell Res. **68**:253-258.

11. **Blank, H., C. F. Burgoon, G. D. Baldridge, P. L. McCarthy, and F. Urbach**. 1951. Cytologic smears in diagnosis of herpes simplex, herpes zoster, and varicella. J.Am.Med.Assoc. **146**:1410-1412.

12. **Brignati, M. J., J. S. Loomis, J. W. Wills, and R. J. Courtney**. 2003. Membrane association of VP22, a herpes simplex virus type 1 tegument protein. J.Virol. **77**:4888-4898.

13. **Brugha, R., K. Keersmaekers, A. Renton, and A. Meheus**. 1997. Genital herpes infection: a review. Int.J.Epidemiol. **26**:698-709.

14. **Brunetti, C. R., R. L. Burke, B. Hoflack, T. Ludwig, K. S. Dingwell, and D. C. Johnson**. 1995. Role of mannose-6-phosphate receptors in herpes simplex virus entry into cells and cell-to-cell transmission. J.Virol. **69**:3517-3528.

15. **Cai, W. H., B. Gu, and S. Person**. 1988. Role of glycoprotein B of herpes simplex virus type 1 in viral entry and cell fusion. J.Virol. **62**:2596-2604.

16. **Calistri, A., P. Sette, C. Salata, E. Cancellotti, C. Forghieri, A. Comin, H. Gottlinger, G. Campadelli-Fiume, G. Palu, and C. Parolin**. 2007. Intracellular trafficking and maturation of herpes simplex virus type 1 gB and virus egress require functional biogenesis of multivesicular bodies. J.Virol. **81**:11468-11478.

17. **Campadelli, G., R. Brandimarti, L. C. Di, P. L. Ward, B. Roizman, and M. R. Torrisi**. 1993. Fragmentation and dispersal of Golgi proteins and redistribution of glycoproteins and glycolipids processed through the Golgi apparatus after infection with herpes simplex virus 1. Proc.Natl.Acad.Sci.U.S.A **90**:2798-2802.

18. **Ch'ng, T. H. and L. W. Enquist**. 2005. Efficient axonal localization of alphaherpesvirus structural proteins in cultured sympathetic neurons requires viral glycoprotein E. J.Virol. **79**:8835-8846.

19. **Ch'ng, T. H. and L. W. Enquist**. 2005. Neuron-to-cell spread of pseudorabies virus in a compartmented neuronal culture system. J.Virol. **79**:10875-10889.

20. **Chapman, T. L., I. You, I. M. Joseph, P. J. Bjorkman, S. L. Morrison, and M. Raghavan**. 1999. Characterization of the interaction between the herpes simplex virus type I Fc receptor and immunoglobulin G. J.Biol.Chem. **274**:6911-6919.

21. **Chasserot-Golaz, S., N. Vitale, I. Sagot, B. Delouche, S. Dirrig, L. A. Pradel, J. P. Henry, D. Aunis, and M. F. Bader**. 1996. Annexin II in exocytosis: catecholamine secretion requires the translocation of p36 to the subplasmalemmal region in chromaffin cells. J.Cell Biol. **133**:1217-1236.

22. **Chatterjee, S., J. Koga, and R. J. Whitley**. 1989. A role for herpes simplex virus type 1 glycoprotein E in induction of cell fusion. J.Gen.Virol. **70 (Pt 8)**:2157-2162.

23. **Chowdary, T. K. and E. E. Heldwein**. 2010. Syncytial phenotype of C-terminally truncated herpes simplex virus type 1 gB is associated with diminished membrane interactions. J.Virol. **84**:4923-4935.

24. **Collins, W. J. and D. C. Johnson**. 2003. Herpes simplex virus gE/gI expressed in epithelial cells interferes with cell-to-cell spread. J.Virol. **77**:2686-2695.

25. **Copeland, A. M., W. W. Newcomb, and J. C. Brown**. 2009. Herpes simplex virus replication: roles of viral proteins and nucleoporins in capsid-nucleus attachment. J.Virol. **83**:1660-1668.

26. **Crump, C. M., B. Bruun, S. Bell, L. E. Pomeranz, T. Minson, and H. M. Browne**. 2004. Alphaherpesvirus glycoprotein M causes the relocalization of plasma membrane proteins. J.Gen.Virol. **85**:3517-3527.

27. **Crump, C. M., C. Yates, and T. Minson**. 2007. Herpes simplex virus type 1 cytoplasmic envelopment requires functional Vps4. J.Virol. **81**:7380-7387.

28. **David, G. and M. Bernfield**. 1998. The emerging roles of cell surface heparan sulfate proteoglycans. Matrix Biol. **17**:461-463.

29. **Davis-Poynter, N., S. Bell, T. Minson, and H. Browne**. 1994. Analysis of the contributions of herpes simplex virus type 1 membrane proteins to the induction of cell-cell fusion. J.Virol. **68**:7586-7590.

30. **Dawson, C. R. and B. Togni**. 1976. Herpes simplex eye infections: clinical manifestations, pathogenesis and management. Surv.Ophthalmol. **21**:121-135.

31. **De, R. N., H. J. Nauwynck, K. Geenen, C. Krummenacher, G. H. Cohen, R. J. Eisenberg, T. C. Mettenleiter, and H. W. Favoreel**. 2006. Alpha-herpesvirus glycoprotein D interaction with sensory neurons triggers formation of varicosities that serve as virus exit sites. J.Cell Biol. **174**:267-275.

32. **Desai, P. and S. Person**. 1998. Incorporation of the green fluorescent protein into the herpes simplex virus type 1 capsid. J.Virol. **72**:7563-7568.

33. **Desai, P., G. L. Sexton, E. Huang, and S. Person**. 2008. Localization of herpes simplex virus type 1 UL37 in the Golgi complex requires UL36 but not capsid structures. J.Virol. **82**:11354-11361.

34. **Desmyter, J., J. L. Melnick, and W. E. Rawls**. 1968. Defectiveness of interferon production and of rubella virus interference in a line of African green monkey kidney cells (Vero). J.Virol. **2**:955-961.

35. **Desnos, C., S. Huet, and F. Darchen**. 2007. 'Should I stay or should I go?': myosin V function in organelle trafficking. Biol.Cell **99**:411-423.

36. **Desplanques, A. S., H. J. Nauwynck, K. Tilleman, D. Deforce, and H. W. Favoreel**. 2007. Tyrosine phosphorylation and lipid raft association of pseudorabies virus glycoprotein E during antibody-mediated capping. Virology **362**:60-66.

37. **Diefenbach, R. J., M. Miranda-Saksena, M. W. Douglas, and A. L. Cunningham**. 2008. Transport and egress of herpes simplex virus in neurons. Rev.Med.Virol. **18**:35-51.

38. **Dillon, C. and Y. Goda**. 2005. The actin cytoskeleton: integrating form and function at the synapse. Annu.Rev.Neurosci. **28**:25-55.

39. **Dingwell, K. S., C. R. Brunetti, R. L. Hendricks, Q. Tang, M. Tang, A. J. Rainbow, and D. C. Johnson**. 1994. Herpes simplex virus glycoproteins E and I facilitate cell-to-cell spread in vivo and across junctions of cultured cells. J.Virol. **68**:834-845.

40. **Dingwell, K. S., L. C. Doering, and D. C. Johnson**. 1995. Glycoproteins E and I facilitate neuron-to-neuron spread of herpes simplex virus. J.Virol. **69**:7087-7098.

41. **Dingwell, K. S. and D. C. Johnson**. 1998. The herpes simplex virus gE-gI complex facilitates cell-to-cell spread and binds to components of cell junctions. J.Virol. **72**:8933-8942.

42. **Dixit, R., V. Tiwari, and D. Shukla**. 2008. Herpes simplex virus type 1 induces filopodia in differentiated P19 neural cells to facilitate viral spread. Neurosci.Lett. **440**:113-118.

43. **Doane, F., A. J. Rhodes, and H. L. Ormsby**. 1955. Tissue culture techniques in the study of herpetic infections of the eye. Am.J.Ophthalmol. **40**:189-193.

44. **Doherty, G. J. and H. T. McMahon**. 2009. Mechanisms of endocytosis. Annu.Rev.Biochem. **78**:857-902.

45. **Dohner, K., A. Wolfstein, U. Prank, C. Echeverri, D. Dujardin, R. Vallee, and B. Sodeik**. 2002. Function of dynein and dynactin in herpes simplex virus capsid transport. Mol.Biol.Cell **13**:2795-2809.

46. **Dubin, G., I. Frank, and H. M. Friedman**. 1990. Herpes simplex virus type 1 encodes two Fc receptors which have different binding characteristics for monomeric immunoglobulin G (IgG) and IgG complexes. J.Virol. **64**:2725-2731.

47. **Evans, D. T., R. Serra-Moreno, R. K. Singh, and J. C. Guatelli**. 2010. BST-2/tetherin: a new component of the innate immune response to enveloped viruses. Trends Microbiol. **18**:388-396.

48. **Even, D. L., A. M. Henley, and R. J. Geraghty**. 2006. The requirements for herpes simplex virus type 1 cell-cell spread via nectin-1 parallel those for virus entry. Virus Res. **119**:195-207.

49. **Even-Ram, S., A. D. Doyle, M. A. Conti, K. Matsumoto, R. S. Adelstein, and K. M. Yamada**. 2007. Myosin IIA regulates cell motility and actomyosin-microtubule crosstalk. Nat.Cell Biol. **9**:299-309.

50. **Fais, S., M. R. Capobianchi, I. Abbate, C. Castilletti, M. Gentile, F. P. Cordiali, F. Ameglio, and F. Dianzani**. 1995. Unidirectional budding of HIV-1

at the site of cell-to-cell contact is associated with co-polarization of intercellular adhesion molecules and HIV-1 viral matrix protein. AIDS **9**:329-335.

51. **Fan, Z., M. L. Grantham, M. S. Smith, E. S. Anderson, J. A. Cardelli, and M. I. Muggeridge**. 2002. Truncation of herpes simplex virus type 2 glycoprotein B increases its cell surface expression and activity in cell-cell fusion, but these properties are unrelated. J.Virol. **76**:9271-9283.

52. **Farnsworth, A., K. Goldsmith, and D. C. Johnson**. 2003. Herpes simplex virus glycoproteins gD and gE/gI serve essential but redundant functions during acquisition of the virion envelope in the cytoplasm. J.Virol. **77**:8481-8494.

53. **Farnsworth, A. and D. C. Johnson**. 2006. Herpes simplex virus gE/gI must accumulate in the trans-Golgi network at early times and then redistribute to cell junctions to promote cell-cell spread. J.Virol. **80**:3167-3179.

54. **Farnsworth, A., T. W. Wisner, and D. C. Johnson**. 2007. Cytoplasmic residues of herpes simplex virus glycoprotein gE required for secondary envelopment and binding of tegument proteins VP22 and UL11 to gE and gD. J.Virol. **81**:319-331.

55. **Favoreel, H. W., H. J. Nauwynck, O. P. Van, T. C. Mettenleiter, and M. B. Pensaert**. 1997. Antibody-induced and cytoskeleton-mediated redistribution and shedding of viral glycoproteins, expressed on pseudorabies virus-infected cells. J.Virol. **71**:8254-8261.

56. **Felts, R. L., K. Narayan, J. D. Estes, D. Shi, C. M. Trubey, J. Fu, L. M. Hartnell, G. T. Ruthel, D. K. Schneider, K. Nagashima, J. W. Bess, Jr., S. Bavari, B. C. Lowekamp, D. Bliss, J. D. Lifson, and S. Subramaniam**. 2010. 3D visualization of HIV transfer at the virological synapse between dendritic cells and T cells. Proc.Natl.Acad.Sci.U.S.A **107**:13336-13341.

57. **Fodor, S., Z. Jakus, and A. Mocsai**. 2006. ITAM-based signaling beyond the adaptive immune response. Immunol.Lett. **104**:29-37.

58. **Franke, E. K., H. E. Yuan, and J. Luban**. 1994. Specific incorporation of cyclophilin A into HIV-1 virions. Nature **372**:359-362.

59. **Garner, J. A.** 2003. Herpes simplex virion entry into and intracellular transport within mammalian cells. Adv.Drug Deliv.Rev. **55**:1497-1513.

60. **Geraghty, R. J., C. R. Jogger, and P. G. Spear**. 2000. Cellular expression of alphaherpesvirus gD interferes with entry of homologous and heterologous alphaherpesviruses by blocking access to a shared gD receptor. Virology **268**:147-158.

61. **Geraghty, R. J., C. Krummenacher, G. H. Cohen, R. J. Eisenberg, and P. G. Spear**. 1998. Entry of alphaherpesviruses mediated by poliovirus receptor-related protein 1 and poliovirus receptor. Science **280**:1618-1620.

62. **Gianni, T., A. Cerretani, R. Dubois, S. Salvioli, S. S. Blystone, F. Rey, and G. Campadelli-Fiume**. 2010. Herpes simplex virus glycoproteins H/L bind to cells independently of {alpha}V{beta}3 integrin and inhibit virus entry, and their constitutive expression restricts infection. J.Virol. **84**:4013-4025.

63. **Giner, D., P. Neco, M. M. Frances, I. Lopez, S. Viniegra, and L. M. Gutierrez**. 2005. Real-time dynamics of the F-actin cytoskeleton during secretion from chromaffin cells. J.Cell Sci. **118**:2871-2880.

64. **Glorieux, S., C. Bachert, H. W. Favoreel, A. P. Vandekerckhove, L. Steukers, A. Rekecki, W. Van den Broeck, J. Goossens, S. Croubels, R. F. Clayton, and H. J. Nauwynck**. 2011. Herpes simplex virus type 1 penetrates the basement membrane in human nasal respiratory mucosa. PLoS.One. **6**:e22160.

65. **Gompels, U. and A. Minson**. 1986. The properties and sequence of glycoprotein H of herpes simplex virus type 1. Virology **153**:230-247.

66. **Gousset, K., S. D. Ablan, L. V. Coren, A. Ono, F. Soheilian, K. Nagashima, D. E. Ott, and E. O. Freed**. 2008. Real-time visualization of HIV-1 GAG trafficking in infected macrophages. PLoS.Pathog. **4**:e1000015.

67. **Granzow, H., B. G. Klupp, W. Fuchs, J. Veits, N. Osterrieder, and T. C. Mettenleiter**. 2001. Egress of alphaherpesviruses: comparative ultrastructural study. J.Virol. **75**:3675-3684.

68. **Granzow, H., B. G. Klupp, and T. C. Mettenleiter**. 2005. Entry of pseudorabies virus: an immunogold-labeling study. J.Virol. **79**:3200-3205.

69. **Grunewald, K., P. Desai, D. C. Winkler, J. B. Heymann, D. M. Belnap, W. Baumeister, and A. C. Steven**. 2003. Three-dimensional structure of herpes simplex virus from cryo-electron tomography. Science **302**:1396-1398.

70. **Haake, A., G. A. Scott, and K. A. Holbrook**. 2001. Structure and function of the skin: overview of the epidermis and dermis, p. 19-45. *In*: R. K. Freinkel and D. T. Woodley (eds.), The Biology of the Skin. Parthenon Publishing, New York, NY.

71. **Hanke, T., F. L. Graham, V. Lulitanond, and D. C. Johnson**. 1990. Herpes simplex virus IgG Fc receptors induced using recombinant adenovirus vectors expressing glycoproteins E and I. Virology **177**:437-444.

72. **Heeg, U., H. P. Dienes, S. Muller, and D. Falke**. 1986. Involvement of actin-containing microfilaments in HSV-induced cytopathology and the influence of inhibitors of glycosylation. Arch.Virol. **91**:257-270.

73. **Heldwein, E. E. and C. Krummenacher**. 2008. Entry of herpesviruses into mammalian cells. Cell Mol.Life Sci. **65**:1653-1668.

74. **HOGGAN, M. D. and B. Roizman**. 1959. The isolation and properties of a variant of Herpes simplex producing multinucleated giant cells in monolayer cultures in the presence of antibody. Am.J.Hyg. **70**:208-219.

75. **Johnson, D. C. and J. D. Baines**. 2011. Herpesviruses remodel host membranes for virus egress. Nat.Rev.Microbiol. **9**:382-394.

76. **Johnson, D. C. and V. Feenstra**. 1987. Identification of a novel herpes simplex virus type 1-induced glycoprotein which complexes with gE and binds immunoglobulin. J.Virol. **61**:2208-2216.

77. **Johnson, D. C., M. C. Frame, M. W. Ligas, A. M. Cross, and N. D. Stow**. 1988. Herpes simplex virus immunoglobulin G Fc receptor activity depends on a complex of two viral glycoproteins, gE and gI. J.Virol. **62**:1347-1354.

78. **Johnson, D. C. and M. T. Huber**. 2002. Directed egress of animal viruses promotes cell-to-cell spread. J.Virol. **76**:1-8.

79. **Johnson, D. C., M. Webb, T. W. Wisner, and C. Brunetti**. 2001. Herpes simplex virus gE/gI sorts nascent virions to epithelial cell junctions, promoting virus spread. J.Virol. **75**:821-833.

80. **Jolly, C. and Q. J. Sattentau**. 2004. Retroviral spread by induction of virological synapses. Traffic. **5**:643-650.

81. **Jouvenet, N., S. J. Neil, M. Zhadina, T. Zang, Z. Kratovac, Y. Lee, M. McNatt, T. Hatziioannou, and P. D. Bieniasz**. 2009. Broad-spectrum inhibition of retroviral and filoviral particle release by tetherin. J.Virol. **83**:1837-1844.

82. **Kalamvoki, M., J. Qu, and B. Roizman**. 2008. Translocation and colocalization of ICP4 and ICP0 in cells infected with herpes simplex virus 1 mutants lacking glycoprotein E, glycoprotein I, or the virion host shutoff product of the UL41 gene. J.Virol. **82**:1701-1713.

83. **Kalamvoki, M. and B. Roizman**. 2007. Bcl-2 blocks accretion or depletion of stored calcium but has no effect on the redistribution of IP3 receptor I mediated by glycoprotein E of herpes simplex virus 1. J.Virol. **81**:6316-6325.

84. **Kaletsky, R. L., J. R. Francica, C. Agrawal-Gamse, and P. Bates**. 2009. Tetherin-mediated restriction of filovirus budding is antagonized by the Ebola glycoprotein. Proc.Natl.Acad.Sci.U.S.A **106**:2886-2891.

85. **Kanaani, J., A. el-Husseini, A. Aguilera-Moreno, J. M. Diacovo, D. S. Bredt, and S. Baekkeskov**. 2002. A combination of three distinct trafficking signals mediates axonal targeting and presynaptic clustering of GAD65. J.Cell Biol. **158**:1229-1238.

86. **Keyser, J., M. Lorger, J. Pavlovic, G. Radziwill, and K. Moelling**. 2007. Role of AF6 protein in cell-to-cell spread of Herpes simplex virus 1. FEBS Lett. **581**:5349-5354.

87. **Kimura, T., H. Kihara, S. Bhattacharyya, H. Sakamoto, E. Appella, and R. P. Siraganian**. 1996. Downstream signaling molecules bind to different phosphorylated immunoreceptor tyrosine-based activation motif (ITAM) peptides of the high affinity IgE receptor. J.Biol.Chem. **271**:27962-27968.

88. **Kohler, K. and A. Zahraoui**. 2005. Tight junction: a co-ordinator of cell signalling and membrane trafficking. Biol.Cell **97**:659-665.

89. **Kotsakis, A., L. E. Pomeranz, A. Blouin, and J. A. Blaho**. 2001. Microtubule reorganization during herpes simplex virus type 1 infection facilitates the nuclear localization of VP22, a major virion tegument protein. J.Virol. **75**:8697-8711.

90. **Krummenacher, C., I. Baribaud, R. J. Eisenberg, and G. H. Cohen**. 2003. Cellular localization of nectin-1 and glycoprotein D during herpes simplex virus infection. J.Virol. **77**:8985-8999.

91. **Kusumi, A., C. Nakada, K. Ritchie, K. Murase, K. Suzuki, H. Murakoshi, R. S. Kasai, J. Kondo, and T. Fujiwara**. 2005. Paradigm shift of the plasma membrane concept from the two-dimensional continuum fluid to the partitioned

fluid: high-speed single-molecule tracking of membrane molecules. Annu.Rev.Biophys.Biomol.Struct. **34**:351-378.

92. **Lansbergen, G., I. Grigoriev, Y. Mimori-Kiyosue, T. Ohtsuka, S. Higa, I. Kitajima, J. Demmers, N. Galjart, A. B. Houtsmuller, F. Grosveld, and A. Akhmanova**. 2006. CLASPs attach microtubule plus ends to the cell cortex through a complex with LL5beta. Dev.Cell **11**:21-32.

93. **Laquerre, S., R. Argnani, D. B. Anderson, S. Zucchini, R. Manservigi, and J. C. Glorioso**. 1998. Heparan sulfate proteoglycan binding by herpes simplex virus type 1 glycoproteins B and C, which differ in their contributions to virus attachment, penetration, and cell-to-cell spread. J.Virol. **72**:6119-6130.

94. **LaVail, J. H., A. N. Tauscher, A. Sucher, O. Harrabi, and R. Brandimarti**. 2007. Viral regulation of the long distance axonal transport of herpes simplex virus nucleocapsid. Neuroscience **146**:974-985.

95. **Law, D. A., F. R. DeGuzman, P. Heiser, K. Ministri-Madrid, N. Killeen, and D. R. Phillips**. 1999. Integrin cytoplasmic tyrosine motif is required for outside-in alphaIIbbeta3 signalling and platelet function. Nature **401**:808-811.

96. **Lee, G. E., J. W. Murray, A. W. Wolkoff, and D. W. Wilson**. 2006. Reconstitution of herpes simplex virus microtubule-dependent trafficking in vitro. J.Virol. **80**:4264-4275

97. **Li, G., E. Rungger-Brandle, I. Just, J. C. Jonas, K. Aktories, and C. B. Wollheim**. 1994. Effect of disruption of actin filaments by Clostridium botulinum C2 toxin on insulin secretion in HIT-T15 cells and pancreatic islets. Mol.Biol.Cell **5**:1199-1213.

98. **Linnartz, B., Y. Wang, and H. Neumann**. 2010. Microglial immunoreceptor tyrosine-based activation and inhibition motif signaling in neuroinflammation. Int.J.Alzheimers.Dis. **2010**.

99. **Liu, M., E. E. Schmidt, and W. P. Halford**. 2010. ICP0 dismantles microtubule networks in herpes simplex virus-infected cells. PLoS.One. **5**:e10975.

100. **Llewellyn, G. N., I. B. Hogue, J. R. Grover, and A. Ono**. 2010. Nucleocapsid promotes localization of HIV-1 gag to uropods that participate in virological synapses between T cells. PLoS.Pathog. **6**:e1001167.

101. **Loomis, J. S., J. B. Bowzard, R. J. Courtney, and J. W. Wills**. 2001. Intracellular trafficking of the UL11 tegument protein of herpes simplex virus type 1. J.Virol. **75**:12209-12219.

102. **Luxton, G. W., S. Haverlock, K. E. Coller, S. E. Antinone, A. Pincetic, and G. A. Smith**. 2005. Targeting of herpesvirus capsid transport in axons is coupled to association with specific sets of tegument proteins. Proc.Natl.Acad.Sci.U.S.A **102**:5832-5837.

103. **Lyman, M. G. and L. W. Enquist**. 2009. Herpesvirus interactions with the host cytoskeleton. J.Virol. **83**:2058-2066

104. **Malacombe, M., M. F. Bader, and S. Gasman**. 2006. Exocytosis in neuroendocrine cells: new tasks for actin. Biochim.Biophys.Acta **1763**:1175-1183.

105. **Maldonado-Baez, L. and B. Wendland**. 2006. Endocytic adaptors: recruiters, coordinators and regulators. Trends Cell Biol. **16**:505-513.

106. **Mansouri, M., K. Viswanathan, J. L. Douglas, J. Hines, J. Gustin, A. V. Moses, and K. Fruh**. 2009. Molecular mechanism of BST2/tetherin downregulation by K5/MIR2 of Kaposi's sarcoma-associated herpesvirus. J.Virol. **83**:9672-9681.

107. **Margadant, C., H. N. Monsuur, J. C. Norman, and A. Sonnenberg**. 2011. Mechanisms of integrin activation and trafficking. Curr.Opin.Cell Biol. **23**:607-614.

108. **Marsh, M., K. Theusner, and A. Pelchen-Matthews**. 2009. HIV assembly and budding in macrophages. Biochem.Soc.Trans. **37**:185-189.

109. **Martin-Serrano, J., T. Zang, and P. D. Bieniasz**. 2001. HIV-1 and Ebola virus encode small peptide motifs that recruit Tsg101 to sites of particle assembly to facilitate egress. Nat.Med. **7**:1313-1319.

110. **Masedunskas, A., M. Sramkova, L. Parente, K. U. Sales, P. Amornphimoltham, T. H. Bugge, and R. Weigert**. 2011. Role for the actomyosin complex in regulated exocytosis revealed by intravital microscopy. Proc.Natl.Acad.Sci.U.S.A **108**:13552-13557.

111. **Maurer, U. E., B. Sodeik, and K. Grunewald**. 2008. Native 3D intermediates of membrane fusion in herpes simplex virus 1 entry. Proc.Natl.Acad.Sci.U.S.A **105**:10559-10564.

112. **McGraw, H. M., S. Awasthi, J. A. Wojcechowskyj, and H. M. Friedman**. 2009. Anterograde spread of herpes simplex virus type 1 requires glycoprotein E and glycoprotein I but not Us9. J.Virol. **83**:8315-8326.

113. **McGraw, H. M. and H. M. Friedman**. 2009. Herpes simplex virus type 1 glycoprotein E mediates retrograde spread from epithelial cells to neurites. J.Virol. **83**:4791-4799.

114. **McMillan, T. N. and D. C. Johnson**. 2001. Cytoplasmic domain of herpes simplex virus gE causes accumulation in the trans-Golgi network, a site of virus envelopment and sorting of virions to cell junctions. J.Virol. **75**:1928-1940.

115. **McNab, A. R., P. Desai, S. Person, L. L. Roof, D. R. Thomsen, W. W. Newcomb, J. C. Brown, and F. L. Homa**. 1998. The product of the herpes simplex virus type 1 UL25 gene is required for encapsidation but not for cleavage of replicated viral DNA. J.Virol. **72**:1060-1070.

116. **Mettenleiter, T. C.** 2002. Herpesvirus assembly and egress. J.Virol. **76**:1537-1547.

117. **Mettenleiter, T. C.** 2004. Budding events in herpesvirus morphogenesis. Virus Res. **106**:167-180.

118. **Mettenleiter, T. C., B. G. Klupp, and H. Granzow**. 2006. Herpesvirus assembly: a tale of two membranes. Curr.Opin.Microbiol. **9**:423-429.

119. **Miranda-Saksena, M., R. A. Boadle, A. Aggarwal, B. Tijono, F. J. Rixon, R. J. Diefenbach, and A. L. Cunningham**. 2009. Herpes simplex virus utilizes the large secretory vesicle pathway for anterograde transport of tegument and envelope proteins and for viral exocytosis from growth cones of human fetal axons. J.Virol. **83**:3187-3199.

120. **Miriagou, V., L. Stevanato, R. Manservigi, and P. Mavromara**. 2000. The C-terminal cytoplasmic tail of herpes simplex virus type 1 gE protein is phosphorylated in vivo and in vitro by cellular enzymes in the absence of other viral proteins. J.Gen.Virol. **81**:1027-1031.

121. **Miyakawa, K., A. Ryo, T. Murakami, K. Ohba, S. Yamaoka, M. Fukuda, J. Guatelli, and N. Yamamoto**. 2009. BCA2/Rabring7 promotes tetherin-dependent HIV-1 restriction. PLoS.Pathog. **5**:e1000700.

122. **Moffat, J. F., L. Zerboni, P. R. Kinchington, C. Grose, H. Kaneshima, and A. M. Arvin**. 1998. Attenuation of the vaccine Oka strain of varicella-zoster virus and role of glycoprotein C in alphaherpesvirus virulence demonstrated in the SCID-hu mouse. J.Virol. **72**:965-974.

123. **Morita, K., M. Itoh, M. Saitou, Y. Ando-Akatsuka, M. Furuse, K. Yoneda, S. Imamura, K. Fujimoto, and S. Tsukita**. 1998. Subcellular distribution of tight junction-associated proteins (occludin, ZO-1, ZO-2) in rodent skin. J.Invest Dermatol. **110**:862-866.

124. **Moriyama, K., S. Imayama, S. Mohri, T. Kurata, and R. Mori**. 1992. Localization of herpes simplex virus type 1 in sebaceous glands of mice. Arch.Virol. **123**:13-27.

125. **Morone, N., T. Fujiwara, K. Murase, R. S. Kasai, H. Ike, S. Yuasa, J. Usukura, and A. Kusumi**. 2006. Three-dimensional reconstruction of the membrane skeleton at the plasma membrane interface by electron tomography. J.Cell Biol. **174**:851-862.

126. **Mothes, W., N. M. Sherer, J. Jin, and P. Zhong**. 2010. Virus cell-to-cell transmission. J.Virol. **84**:8360-8368

127. **Murata, T., F. Goshima, T. Daikoku, H. Takakuwa, and Y. Nishiyama**. 2000. Expression of herpes simplex virus type 2 US3 affects the Cdc42/Rac pathway and attenuates c-Jun N-terminal kinase activation. Genes Cells **5**:1017-1027.

128. **Nagafuchi, A.** 2001. Molecular architecture of adherens junctions. Curr.Opin.Cell Biol. **13**:600-603.

129. **Nagashunmugam, T., J. Lubinski, L. Wang, L. T. Goldstein, B. S. Weeks, P. Sundaresan, E. H. Kang, G. Dubin, and H. M. Friedman**. 1998. In vivo immune evasion mediated by the herpes simplex virus type 1 immunoglobulin G Fc receptor. J.Virol. **72**:5351-5359.

130. **Neco, P., C. Fernandez-Peruchena, S. Navas, L. M. Gutierrez, G. A. de Toledo, and E. Ales**. 2008. Myosin II contributes to fusion pore expansion during exocytosis. J.Biol.Chem. **283**:10949-10957.

131. **Negatsch, A., H. Granzow, C. Maresch, B. G. Klupp, W. Fuchs, J. P. Teifke, and T. C. Mettenleiter**. 2010. Ultrastructural analysis of virion formation and intraaxonal transport of herpes simplex virus type 1 in primary rat neurons. J.Virol. **84**:13031-13035.

132. **Neil, S. J., V. Sandrin, W. I. Sundquist, and P. D. Bieniasz**. 2007. An interferon-alpha-induced tethering mechanism inhibits HIV-1 and Ebola virus particle release but is counteracted by the HIV-1 Vpu protein. Cell Host.Microbe **2**:193-203.

133. **Nejmeddine, M. and C. R. Bangham**. 2010. The HTLV-1 Virological Synapse. Viruses. **2**:1427-1447.

134. **Newcomb, W. W. and J. C. Brown**. 2009. Time-dependent transformation of the herpesvirus tegument. J.Virol. **83**:8082-8089.

135. **Newcomb, W. W. and J. C. Brown**. 2010. Structure and capsid association of the herpesvirus large tegument protein UL36. J.Virol. **84**:9408-9414.

136. **Ng, T. I., W. O. Ogle, and B. Roizman**. 1998. UL13 protein kinase of herpes simplex virus 1 complexes with glycoprotein E and mediates the phosphorylation of the viral Fc receptor: glycoproteins E and I. Virology **241**:37-48.

137. **Nicola, A. V., A. M. McEvoy, and S. E. Straus**. 2003. Roles for endocytosis and low pH in herpes simplex virus entry into HeLa and Chinese hamster ovary cells. J.Virol. **77**:5324-5332.

138. **Noble, A. G., G. T. Lee, R. Sprague, M. L. Parish, and P. G. Spear**. 1983. Anti-gD monoclonal antibodies inhibit cell fusion induced by herpes simplex virus type 1. Virology **129**:218-224.

139. **Norrild, B., V. P. Lehto, and I. Virtanen**. 1986. Organization of cytoskeleton elements during herpes simplex virus type 1 infection of human fibroblasts: an immunofluorescence study. J.Gen.Virol. **67 (Pt 1)**:97-105.

140. **Nydegger, S., S. Khurana, D. N. Krementsov, M. Foti, and M. Thali**. 2006. Mapping of tetraspanin-enriched microdomains that can function as gateways for HIV-1. J.Cell Biol. **173**:795-807.

141. **Oh, M. J., J. Akhtar, P. Desai, and D. Shukla**. 2010. A role for heparan sulfate in viral surfing. Biochem.Biophys.Res.Commun. **391**:176-181.

142. **Ohara, P. T., M. S. Chin, and J. H. LaVail**. 2000. The spread of herpes simplex virus type 1 from trigeminal neurons to the murine cornea: an immunoelectron microscopy study. J.Virol. **74**:4776-4786.

143. **Ojala, P. M., B. Sodeik, M. W. Ebersold, U. Kutay, and A. Helenius**. 2000. Herpes simplex virus type 1 entry into host cells: reconstitution of capsid binding and uncoating at the nuclear pore complex in vitro. Mol.Cell Biol. **20**:4922-4931.

144. **Owens, R. J., J. W. Dubay, E. Hunter, and R. W. Compans**. 1991. Human immunodeficiency virus envelope protein determines the site of virus release in polarized epithelial cells. Proc.Natl.Acad.Sci.U.S.A **88**:3987-3991.

145. **Pais-Correia, A. M., M. Sachse, S. Guadagnini, V. Robbiati, R. Lasserre, A. Gessain, O. Gout, A. Alcover, and M. I. Thoulouze**. 2010. Biofilm-like extracellular viral assemblies mediate HTLV-1 cell-to-cell transmission at virological synapses. Nat.Med. **16**:83-89.

146. **Pardieu, C., R. Vigan, S. J. Wilson, A. Calvi, T. Zang, P. Bieniasz, P. Kellam, G. J. Towers, and S. J. Neil**. 2010. The RING-CH ligase K5 antagonizes restriction of KSHV and HIV-1 particle release by mediating ubiquitin-dependent endosomal degradation of tetherin. PLoS.Pathog. **6**:e1000843.

147. **Pawliczek, T. and C. M. Crump**. 2009. Herpes simplex virus type 1 production requires a functional ESCRT-III complex but is independent of TSG101 and ALIX expression. J.Virol. **83**:11254-11264.

148. **Penfold, M. E., P. Armati, and A. L. Cunningham**. 1994. Axonal transport of herpes simplex virions to epidermal cells: evidence for a specialized mode of virus transport and assembly. Proc.Natl.Acad.Sci.U.S.A **91**:6529-6533.

149. **Perez-Caballero, D., T. Zang, A. Ebrahimi, M. W. McNatt, D. A. Gregory, M. C. Johnson, and P. D. Bieniasz**. 2009. Tetherin inhibits HIV-1 release by directly tethering virions to cells. Cell **139**:499-511.

150. **Peters, B. P., S. Ebisu, I. J. Goldstein, and M. Flashner**. 1979. Interaction of wheat germ agglutinin with sialic acid. Biochemistry **18**:5505-5511.

151. **Polcicova, K., K. Goldsmith, B. L. Rainish, T. W. Wisner, and D. C. Johnson**. 2005. The extracellular domain of herpes simplex virus gE is indispensable for efficient cell-to-cell spread: evidence for gE/gI receptors. J.Virol. **79**:11990-12001.

152. **Potten, C. S. and R. J. Morris**. 1988. Epithelial stem cells in vivo. J.Cell Sci.Suppl **10**:45-62.

153. **Pummi, K., M. Malminen, H. Aho, S. L. Karvonen, J. Peltonen, and S. Peltonen**. 2001. Epidermal tight junctions: ZO-1 and occludin are expressed in mature, developing, and affected skin and in vitro differentiating keratinocytes. J.Invest Dermatol. **117**:1050-1058.

154. **Radtke, K., K. Dohner, and B. Sodeik**. 2006. Viral interactions with the cytoskeleton: a hitchhiker's guide to the cell. Cell Microbiol. **8**:387-400.

155. **Radtke, K., D. Kieneke, A. Wolfstein, K. Michael, W. Steffen, T. Scholz, A. Karger, and B. Sodeik**. 2010. Plus- and minus-end directed microtubule motors

bind simultaneously to herpes simplex virus capsids using different inner tegument structures. PLoS.Pathog. **6**:e1000991.

156. **Raiborg, C., T. E. Rusten, and H. Stenmark**. 2003. Protein sorting into multivesicular endosomes. Curr.Opin.Cell Biol. **15**:446-455.

157. **Rak, G. D., E. M. Mace, P. P. Banerjee, T. Svitkina, and J. S. Orange**. 2011. Natural killer cell lytic granule secretion occurs through a pervasive actin network at the immune synapse. PLoS.Biol. **9**:e1001151.

158. **Remillard-Labrosse, G., C. Mihai, J. Duron, G. Guay, and R. Lippe**. 2009. Protein kinase D-dependent trafficking of the large Herpes simplex virus type 1 capsids from the TGN to plasma membrane. Traffic. **10**:1074-1083.

159. **Rixon, F. J., C. Addison, A. McGregor, S. J. Macnab, P. Nicholson, V. G. Preston, and J. D. Tatman**. 1996. Multiple interactions control the intracellular localization of the herpes simplex virus type 1 capsid proteins. J.Gen.Virol. **77 (Pt 9)**:2251-2260.

160. **Rizvi, S. M. and M. Raghavan**. 2003. Responses of herpes simplex virus type 1-infected cells to the presence of extracellular antibodies: gE-dependent glycoprotein capping and enhancement in cell-to-cell spread. J.Virol. **77**:701-708.

161. **Roberts, K. L. and J. D. Baines**. 2010. Myosin Va enhances secretion of herpes simplex virus 1 virions and cell surface expression of viral glycoproteins. J.Virol. **84**:9889-9896.

162. **Rohrer, J. and R. Kornfeld**. 2001. Lysosomal hydrolase mannose 6-phosphate uncovering enzyme resides in the trans-Golgi network. Mol.Biol.Cell **12**:1623-1631.

163. **Rudnicka, D., J. Feldmann, F. Porrot, S. Wietgrefe, S. Guadagnini, M. C. Prevost, J. Estaquier, A. T. Haase, N. Sol-Foulon, and O. Schwartz**. 2009.

Simultaneous cell-to-cell transmission of human immunodeficiency virus to multiple targets through polysynapses. J.Virol. **83**:6234-6246.

164. **Sakisaka, T., T. Taniguchi, H. Nakanishi, K. Takahashi, M. Miyahara, W. Ikeda, S. Yokoyama, Y. F. Peng, K. Yamanishi, and Y. Takai**. 2001. Requirement of interaction of nectin-1alpha/HveC with afadin for efficient cell-cell spread of herpes simplex virus type 1. J.Virol. **75**:4734-4743.

165. **Saksena, M. M., H. Wakisaka, B. Tijono, R. A. Boadle, F. Rixon, H. Takahashi, and A. L. Cunningham**. 2006. Herpes simplex virus type 1 accumulation, envelopment, and exit in growth cones and varicosities in mid-distal regions of axons. J.Virol. **80**:3592-3606.

166. **Sakuma, T., T. Noda, S. Urata, Y. Kawaoka, and J. Yasuda**. 2009. Inhibition of Lassa and Marburg virus production by tetherin. J.Virol. **83**:2382-2385.

167. **Saldanha, C. E., J. Lubinski, C. Martin, T. Nagashunmugam, L. Wang, K. H. van Der, R. Tal-Singer, and H. M. Friedman**. 2000. Herpes simplex virus type 1 glycoprotein E domains involved in virus spread and disease. J.Virol. **74**:6712-6719.

168. **Sarkar, A., R. B. Robertson, and J. M. Fernandez**. 2004. Simultaneous atomic force microscope and fluorescence measurements of protein unfolding using a calibrated evanescent wave. Proc.Natl.Acad.Sci.U.S.A **101**:12882-12886.

169. **Schmidt, M. R. and V. Haucke**. 2007. Recycling endosomes in neuronal membrane traffic. Biol.Cell **99**:333-342.

170. **Schmitz, J., H. Dahmen, C. Grimm, C. Gendo, G. Muller-Newen, P. C. Heinrich, and F. Schaper**. 2000. The cytoplasmic tyrosine motifs in full-length glycoprotein 130 have different roles in IL-6 signal transduction. J.Immunol. **164**:848-854.

171. **Selvaraj, P., N. Fifadara, S. Nagarajan, A. Cimino, and G. Wang**. 2004. Functional regulation of human neutrophil Fc gamma receptors. Immunol.Res. **29**:219-230.

172. **Shanda, S. K. and D. W. Wilson**. 2008. UL36p is required for efficient transport of membrane-associated herpes simplex virus type 1 along microtubules. J.Virol. **82**:7388-7394.

173. **Shimeld, C., T. J. Hill, W. A. Blyth, and D. L. Easty**. 1990. Reactivation of latent infection and induction of recurrent herpetic eye disease in mice. J.Gen.Virol. **71 (Pt 2)**:397-404.

174. **Simpson, C. L., D. M. Patel, and K. J. Green**. 2011. Deconstructing the skin: cytoarchitectural determinants of epidermal morphogenesis. Nat.Rev.Mol.Cell Biol. **12**:565-580.

175. **Skepper, J. N., A. Whiteley, H. Browne, and A. Minson**. 2001. Herpes simplex virus nucleocapsids mature to progeny virions by an envelopment --> deenvelopment --> reenvelopment pathway. J.Virol. **75**:5697-5702.

176. **Smith, G. L., A. Vanderplasschen, and M. Law**. 2002. The formation and function of extracellular enveloped vaccinia virus. J.Gen.Virol. **83**:2915-2931.

177. **Snyder, A., K. Polcicova, and D. C. Johnson**. 2008. Herpes simplex virus gE/gI and US9 proteins promote transport of both capsids and virion glycoproteins in neuronal axons. J.Virol. **82**:10613-10624.

178. **Snyder, A., T. W. Wisner, and D. C. Johnson**. 2006. Herpes simplex virus capsids are transported in neuronal axons without an envelope containing the viral glycoproteins. J.Virol. **80**:11165-11177.

179. **Sodeik, B.** 2000. Mechanisms of viral transport in the cytoplasm. Trends Microbiol. **8**:465-472.

180. **Sodeik, B., M. W. Ebersold, and A. Helenius**. 1997. Microtubule-mediated transport of incoming herpes simplex virus 1 capsids to the nucleus. J.Cell Biol. **136**:1007-1021.

181. **Sowinski, S., C. Jolly, O. Berninghausen, M. A. Purbhoo, A. Chauveau, K. Kohler, S. Oddos, P. Eissmann, F. M. Brodsky, C. Hopkins, B. Onfelt, Q. Sattentau, and D. M. Davis**. 2008. Membrane nanotubes physically connect T cells over long distances presenting a novel route for HIV-1 transmission. Nat.Cell Biol. **10**:211-219.

182. **Sternberg, S.** Biomedical Image Processing. IEEE Computer 16(1), 22-34. 1983.

183. **Stiles, K. M. and C. Krummenacher**. 2010. Glycoprotein D actively induces rapid internalization of two nectin-1 isoforms during herpes simplex virus entry. Virology **399**:109-119.

184. **Stiles, K. M., R. S. Milne, G. H. Cohen, R. J. Eisenberg, and C. Krummenacher**. 2008. The herpes simplex virus receptor nectin-1 is down-regulated after trans-interaction with glycoprotein D. Virology **373**:98-111.

185. **Stylianou, J., K. Maringer, R. Cook, E. Bernard, and G. Elliott**. 2009. Virion incorporation of the herpes simplex virus type 1 tegument protein VP22 occurs via glycoprotein E-specific recruitment to the late secretory pathway. J.Virol. **83**:5204-5218.

186. **Sugimoto, H., M. Sugahara, H. Folsch, Y. Koide, F. Nakatsu, N. Tanaka, T. Nishimura, M. Furukawa, C. Mullins, N. Nakamura, I. Mellman, and H. Ohno**. 2002. Differential recognition of tyrosine-based basolateral signals by AP-1B subunit mu1B in polarized epithelial cells. Mol.Biol.Cell **13**:2374-2382.

187. **Sugimoto, K., M. Uema, H. Sagara, M. Tanaka, T. Sata, Y. Hashimoto, and Y. Kawaguchi**. 2008. Simultaneous tracking of capsid, tegument, and envelope

protein localization in living cells infected with triply fluorescent herpes simplex virus 1. J.Virol. **82**:5198-5211.

188. **Sun, P. D.** 2003. Structure and function of natural-killer-cell receptors. Immunol.Res. **27**:539-548.

189. **Swanson, J. A. and A. D. Hoppe**. 2004. The coordination of signaling during Fc receptor-mediated phagocytosis. J.Leukoc.Biol. **76**:1093-1103.

190. **Takai, Y. and H. Nakanishi**. 2003. Nectin and afadin: novel organizers of intercellular junctions. J.Cell Sci. **116**:17-27.

191. **Thali, M.** 2009. The roles of tetraspanins in HIV-1 replication. Curr.Top.Microbiol.Immunol. **339**:85-102

192. **Tognon, M., D. Furlong, A. J. Conley, and B. Roizman**. 1981. Molecular genetics of herpes simplex virus. V. Characterization of a mutant defective in ability to form plaques at low temperatures and in a viral fraction which prevents accumulation of coreless capsids at nuclear pores late in infection. J.Virol. **40**:870-880.

193. **Tomishima, M. J. and L. W. Enquist**. 2001. A conserved alpha-herpesvirus protein necessary for axonal localization of viral membrane proteins. J.Cell Biol. **154**:741-752.

194. **Tomishima, M. J. and L. W. Enquist**. 2002. In vivo egress of an alphaherpesvirus from axons. J.Virol. **76**:8310-8317.

195. **Tomishima, M. J., G. A. Smith, and L. W. Enquist**. 2001. Sorting and transport of alpha herpesviruses in axons. Traffic. **2**:429-436.

196. **Traub, L. M.** 2010. The reverse logic of multivesicular endosomes. EMBO Rep. **11**:79-81.

197. **Trus, B. L., W. W. Newcomb, F. P. Booy, J. C. Brown, and A. C. Steven**. 1992. Distinct monoclonal antibodies separately label the hexons or the pentons of herpes simplex virus capsid. Proc.Natl.Acad.Sci.U.S.A **89**:11508-11512.

198. **Tucker, S. P. and R. W. Compans**. 1993. Virus infection of polarized epithelial cells. Adv.Virus Res. **42**:187-247.

199. **Turcotte, S., J. Letellier, and R. Lippe**. 2005. Herpes simplex virus type 1 capsids transit by the trans-Golgi network, where viral glycoproteins accumulate independently of capsid egress. J.Virol. **79**:8847-8860.

200. **Van Vliet, K. E., L. A. De Graaf-Miltenburg, J. Verhoef, and J. A. Van Strijp**. 1992. Direct evidence for antibody bipolar bridging on herpes simplex virus-infected cells. Immunology **77**:109-115.

201. **van, L. H., G. Elliott, and P. O'Hare**. 2002. Evidence of a role for nonmuscle myosin II in herpes simplex virus type 1 egress. J.Virol. **76**:3471-3481.

202. **Van, M. G., H. W. Favoreel, L. Jacobs, and H. J. Nauwynck**. 2003. Pseudorabies virus US3 protein kinase mediates actin stress fiber breakdown. J.Virol. **77**:9074-9080.

203. **Vicente-Manzanares, M., X. Ma, R. S. Adelstein, and A. R. Horwitz**. 2009. Non-muscle myosin II takes centre stage in cell adhesion and migration. Nat.Rev.Mol.Cell Biol. **10**:778-790.

204. **Wang, F., W. Tang, H. M. McGraw, J. Bennett, L. W. Enquist, and H. M. Friedman**. 2005. Herpes simplex virus type 1 glycoprotein e is required for axonal localization of capsid, tegument, and membrane glycoproteins. J.Virol. **79**:13362-13372.

205. **Wang, F., E. E. Zumbrun, J. Huang, H. Si, L. Makaroun, and H. M. Friedman**. 2010. Herpes simplex virus type 2 glycoprotein E is required for

efficient virus spread from epithelial cells to neurons and for targeting viral proteins from the neuron cell body into axons. Virology **405**:269-279.

206. **Ward, P. L., E. Avitabile, G. Campadelli-Fiume, and B. Roizman**. 1998. Conservation of the architecture of the Golgi apparatus related to a differential organization of microtubules in polykaryocytes induced by syn- mutants of herpes simplex virus 1. Virology **241**:189-199.

207. **Warner, M. S., R. J. Geraghty, W. M. Martinez, R. I. Montgomery, J. C. Whitbeck, R. Xu, R. J. Eisenberg, G. H. Cohen, and P. G. Spear**. 1998. A cell surface protein with herpesvirus entry activity (HveB) confers susceptibility to infection by mutants of herpes simplex virus type 1, herpes simplex virus type 2, and pseudorabies virus. Virology **246**:179-189.

208. **Weeks, B. S., P. Sundaresan, T. Nagashunmugam, E. Kang, and H. M. Friedman**. 1997. The herpes simplex virus-1 glycoprotein E (gE) mediates IgG binding and cell-to-cell spread through distinct gE domains. Biochem.Biophys.Res.Commun. **235**:31-35.

209. **Wessells, N. K.** 1964. Substrate and Nutrient Effects Upon Epidermal Basal Cell Orientation and Proliferation. Proc.Natl.Acad.Sci.U.S.A **52**:252-259.

210. **Wheeler, C. E., Jr.** 1964. Biologic Comparison of a Syncytial and a Small Giant Cell-Forming Strain of Herpes Simplex. J.Immunol. **93**:749-756.

211. **Winckler, B., P. Forscher, and I. Mellman**. 1999. A diffusion barrier maintains distribution of membrane proteins in polarized neurons. Nature **397**:698-701.

212. **Winkler, M., G. J. Dawson, T. S. Elizan, and S. Berl**. 1982. Distribution of actin and myosin in a rat neuronal cell line infected with herpes simplex virus. Arch.Virol. **72**:95-103.

213. **Wisner, T., C. Brunetti, K. Dingwell, and D. C. Johnson**. 2000. The extracellular domain of herpes simplex virus gE is sufficient for accumulation at cell junctions but not for cell-to-cell spread. J.Virol. **74**:2278-2287.

214. **Wisner, T. W. and D. C. Johnson**. 2004. Redistribution of cellular and herpes simplex virus proteins from the trans-golgi network to cell junctions without enveloped capsids. J.Virol. **78**:11519-11535.

215. **Wisner, T. W., K. Sugimoto, P. W. Howard, Y. Kawaguchi, and D. C. Johnson**. 2011. Anterograde transport of herpes simplex virus capsids in neurons by both separate and married mechanisms. J.Virol. **85**:5919-5928.

216. **Wollenberg, A., C. Zoch, S. Wetzel, G. Plewig, and B. Przybilla**. 2003. Predisposing factors and clinical features of eczema herpeticum: a retrospective analysis of 100 cases. J.Am.Acad.Dermatol. **49**:198-205.

217. **Yang, K., F. Homa, and J. D. Baines**. 2007. Putative terminase subunits of herpes simplex virus 1 form a complex in the cytoplasm and interact with portal protein in the nucleus. J.Virol. **81**:6419-6433.

218. **Yap, C. C., R. L. Nokes, D. Wisco, E. Anderson, H. Folsch, and B. Winckler**. 2008. Pathway selection to the axon depends on multiple targeting signals in NgCAM. J.Cell Sci. **121**:1514-1525.

219. **Yasumura, Y. and Kawakita, Y.** Study of SV40 in tissue culture. Nippon Rinsho 21, 1201-1205. 1963.

220. **Zieske, J. D. and I. A. Bernstein**. 1982. Modification of cell surface glycoprotein: addition of fucosyl residues during epidermal differentiation. J.Cell Biol. **95**:626-631.

221. **Zurzolo, C., C. Polistina, M. Saini, R. Gentile, L. Aloj, G. Migliaccio, S. Bonatti, and L. Nitsch**. 1992. Opposite polarity of virus budding and of viral envelope glycoprotein distribution in epithelial cells derived from different tissues. J.Cell Biol. **117**:551-564.

VIII. Appendix

Timecourse of Infection

The following four figures (Figures A-D) depict the progression of a VP26-GFP HSV infection in Vero cells. Vero cells were plated at 300,000 cells/well of a 6 well plate. 24 hours later cells were infected at an MOI of 5. The production of infectious virus proceeded as shown in Figure A. Small amounts of infectious virus were first detected in cell samples at 6 hpi. Low levels of virus were first detectable in the media at 10 hpi. By 12 hpi a large amount of infectious virions had been made, but very few had been released into the media. Rhodamine-WGA staining indicates the change in glycoprotein localization throughout infection (Figure B). TIRF microscopy images indicate that glycoprotein patches first began to form along the glass coverslip around 6 hpi. Wide-field microscopy shows the movement of WGA stain from perinuclear vesicles to the egress sites as infection proceeded. At 6hpi some stain was visible at cell-cell contact sites, and by 8hpi this staining was more intense. At 12hpi most glycoproteins were at cell-cell contacts or egress patches along the coverslip-adherent surface.

The cytoskeletal structure also reorganized as infection proceeded. Figure C shows the changes that occur to the microtubule skeletal structure. The TIRF images show how the majority of microtubules disappear from view. The only microtubules that remain visible by TIRF are those few located along the cell periphery. Wide-field

microscopy gives a more comprehensive view. The MTOC is disrupted and becomes dispersed early in infection between 2 and 4hpi. This dispersal is complete by 8hpi. The reorganization of the actin cytoskeleton follows a similar timeline (Figure D). Actin stress fibers begin to depolymerize between 2 and 4 hpi, with extensive disruption by 8-10hpi.

Non-specific Staining of Virions

In the process of exploring the possible cellular proteins recruited to viral egress sites we found that most polyclonal antibodies bind to virions non-specifically. Most monoclonals do not do this. Though HSV has an FcR protein (gE), this non-specific binding occurred even in ΔgE infections. It appears that antibodies bind to the tegument of the virions. Other reports have also suggested that tegument proteins can be "sticky" in IP experiments. Figure E depicts non-specific binding of anti-caveolin antibody. In future experiments, colocalization between antibodies and virus should always be checked with multiple controls.

Cellular Proteins and the Patch Membrane

Since non-specific binding of polyclonal antibodies was an issue, we decided to look for the presence of vesicular and endosomal cellular protein markers in egress patches by either using monoclonal antibodies or expressing exogenous GFP-tagged constructs. Constructs were transfected into cells using Amaxa (Lonza) technology.

Figure A: HSV-1 titre at spaced time points during infection. Supernatant and cell scrapings were collected from 2-12hpi. Titre is represented as PFUs/ml. Note that infectious virus is first detectable around 6 hpi, and little virus is released into the media during this 12 hour time period.

Hours Post Infection	Cell Associated Virus	Virus in Supernatant
2	2.5×10^2	0
4	1.5×10^2	0
6	1.5×10^3	0
8	1.5×10^5	0
10	9.5×10^5	2.5×10^2
12	1.6×10^7	3×10^3

Figure B: Timecourse of patch formation in VP26-GFP HSV infected Vero cells from 2-12hpi. Cells have been stained with rhodamine-WGA to label glycoproteins. Top sequence images were obtained with a TIRF microscope. Bottom sequence samples were viewed with standard wide-field microscopy.

TIRF Microscopy

Mock | 2hpi | 4hpi | 6hpi

WGA/Virus

8hpi | 10hpi | 12hpi

Wide-Field Microscopy

Mock | 2hpi | 4hpi | 6hpi

WGA/Virus

8hpi | 10hpi | 12hpi
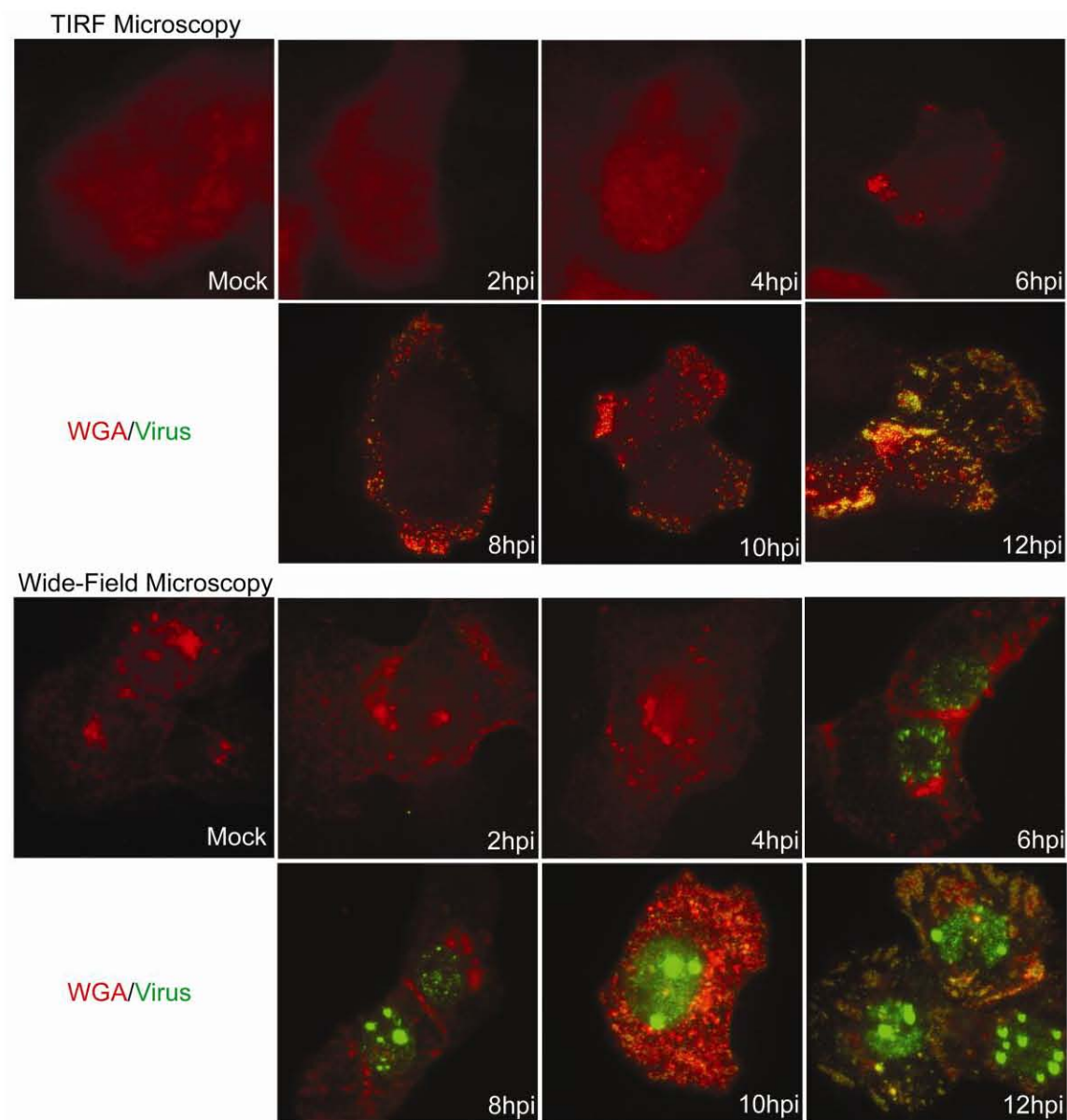
Figure C: Timecourse of microtubule disruption in VP26-GFP HSV infected Vero cells from 2-12hpi. Cells have been stained with anti-α-tubulin monoclonal antibody and Alexa 594-conjugated goat anti-mouse secondary antibody. Top sequence images were taken with a TIRF microscope. Bottom sequence images were viewed with standard wide-field microscopy.

TIRF Microscopy

Tubulin/Virus

Wide-Field Microscopy

Tubulin/Virus
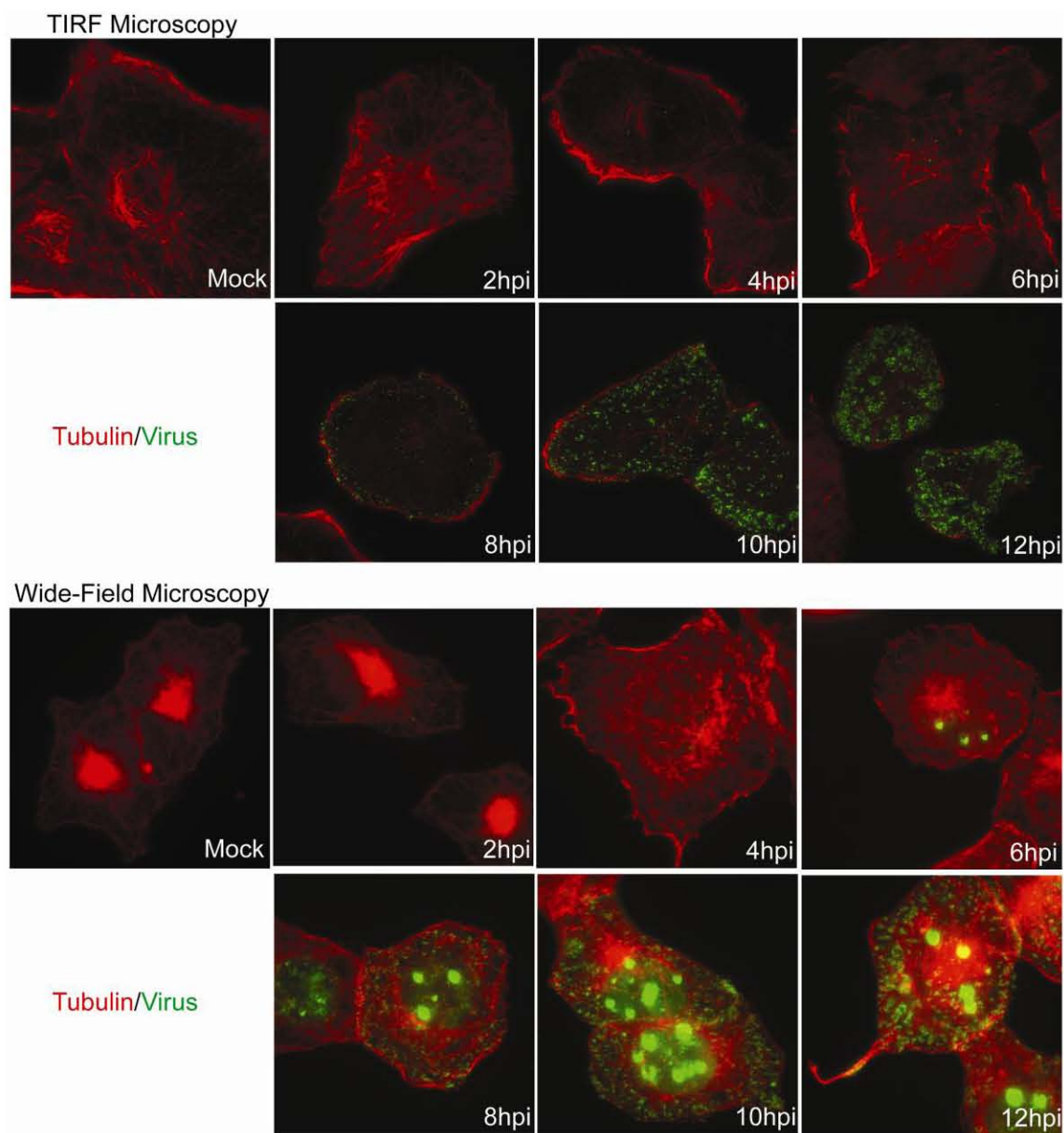
Figure D: Timecourse of actin stress fiber depletion and cortex changes in VP26-GFP

HSV infected Vero cells from 2-12hpi. Cells have been stained with Texas red-

phalloidin. Top sequence images were obtained with a TIRF microscope. Bottom

sequence samples were viewed with wide-field microscopy.

TIRF Microscopy

Actin/Virus

Wide-Field Microscopy

Actin/Virus
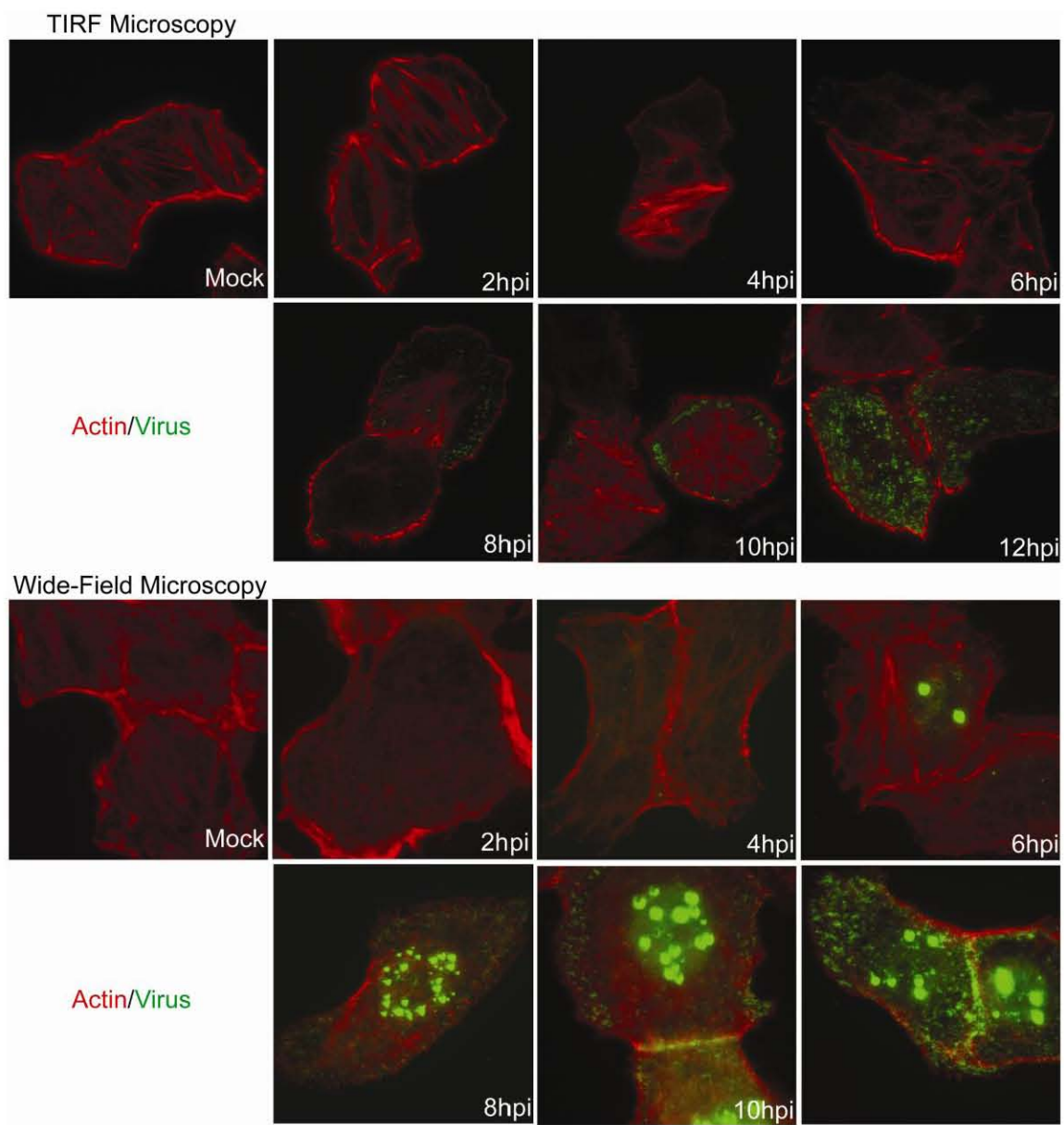
Figure E: Non-specific binding of polyclonal antibodies to HSV virus as demonstrated by caveolin-1 staining. WT HSV-1 infected Vero cells were fixed at 12hpi and stained with anti-VP5 (8F5) monoclonal antibody to label capsids and anti-caveolin-1 polyclonal antibody. Tight colocalization was seen between virus and cav-1 staining, though this staining was non-specific.

VP5 Cav-1 Merge 5μm
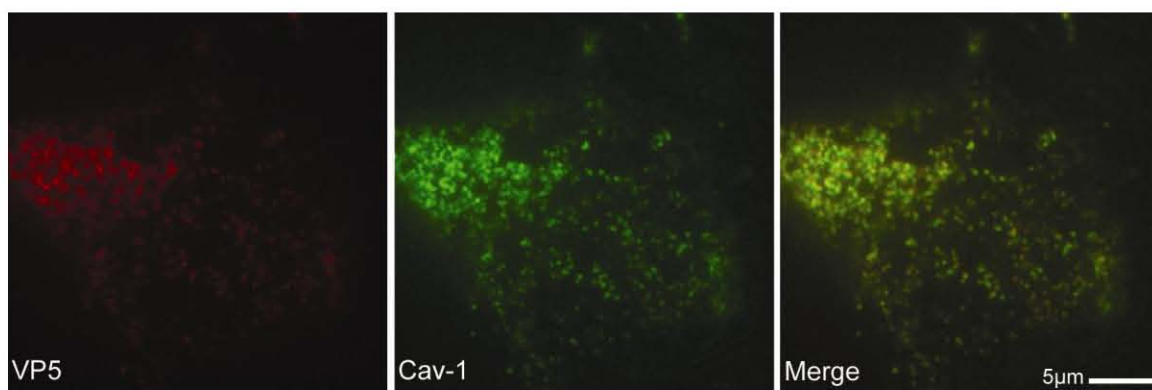
Amaxa (Lonza) technology. 12 hours post transfection cells were infected, and samples were fixed at 12hpi. Figure F shows vesicular/endosomal markers expressed in infected cells and viewed with TIRF microscopy. UCE (uncoating enzyme) was the only marker that colocalized with RFP-labeled virus. UCE is generally found in the trans-Golgi network, though low levels have been reported to cycle to the cell surface, similar to TGN46 (162). Rab5 (an early endosomal marker), Rab7 (a late endosomal marker), Lamp-1 (a late endosome/ lysosomal marker), and TfnR (transferrin receptor- a recycling endosome marker) did not colocalize with viral patches. Very little Rab5, Rab7, and Lamp-1 were on the cell surface; the brightly stained dots are most likely endosomes located near the cell surface. This data supports the theory that the virus is enveloped in the TGN.

The presence of defined patches suggests that cholesterol-rich membrane platforms may assist in the stabilization of these domains. I, therefore, tested for tetraspanin-enriched microdomains, caveolin-enriched rafts, and lipid rafts (Figure G). We found that the tetraspanins did not colocalize with viral patches. However, these proteins did localize to the small cellular extensions that project from the plasma membrane during infection. Some of these small microvilli-like extensions formed at or near the patch sites. Tetraspanins occasionally colocalized with patches located near cell edges, but this occurred in a small minority of cells. Caveolin-1 also did not colocalize with virus, indicating that caveolin-enriched microdomains are not present at these sites. Surprisingly, the lipid raft marker CTxB (cholera toxin B subunit) was found in no greater amounts at the viral patches than the rest of the cell membrane. It is possible that

the HSV-1 virus does not hijack existing cellular membrane microdomains but creates

new domains that do not label with cellular membrane protein markers.

A variety of other cellular membrane proteins were tested for their presence in

viral patches (Figure H). Cortactin is involved in the remodeling of the actin cortex (2).

In light of our observations of actin depletion at viral patches, it seemed likely that this

protein could be active at these domains. However, cortactin did not colocalize with

virus. ELKS is involved in linking microtubules to the cell surface (92). Though ELKS

staining was occasionally seen near viral patches, there was no common pattern of

staining and no direct colocalization. Integrins link the cell membrane with the

substratum (107). HSV gH has been reported to bind to α5β3 integrin (62). I, therefore,

looked for the presence of exogenous α5 integrin at viral patches. No colocalization

occurred, though as with the tetraspanins, α5 was found on the infection-induced cell

extensions, some of which formed near patches. Nectin-1 is an HSV-1 entry receptor and

is found at cell-cell contact sites in Vero cells (61,207). It is also present at the preferred

viral egress sites of polarized epithelial cells and neurons (128,190). Nectin-1 was not

seen at the substrate-adherent surface of infected Vero cells. This is not surprising since

nectin depends on dimerization with nectin on an adjacent cell surface for its localization.

The few bright nectin-1 dots seen in this figure are most likely due to vesicular nectin-1

near the cell surface. Lastly, annexin II is involved in secretion of secretory vesicles (21).

It too did not colocalize with viral patches and was in fact depleted in these areas

compared to the surrounding membrane.

Figure F: Vesicular/endosomal markers and viral patches. Vero cells underwent Amaxa (Lonza) nucleofection of the noted GFP-tagged constructs. 12 hours post transfection cells were infected with VP26-RFP HSV-1. At 12hpi cells were fixed and viewed with TIRF microscopy. Note that the TGN marker UCE colocalizes with patches while the endosomal markers do not.

UCE (TGN) | VP26-RFP Virus | Merge

Rab5 (EE) | VP26-RFP Virus | Merge

Rab7 (LE) | VP26-RFP Virus | Merge

Lamp-1 (LE/Lys) | VP26-RFP Virus | Merge

TfnR (RE) | VP26-RFP Virus | 10µm | Merge
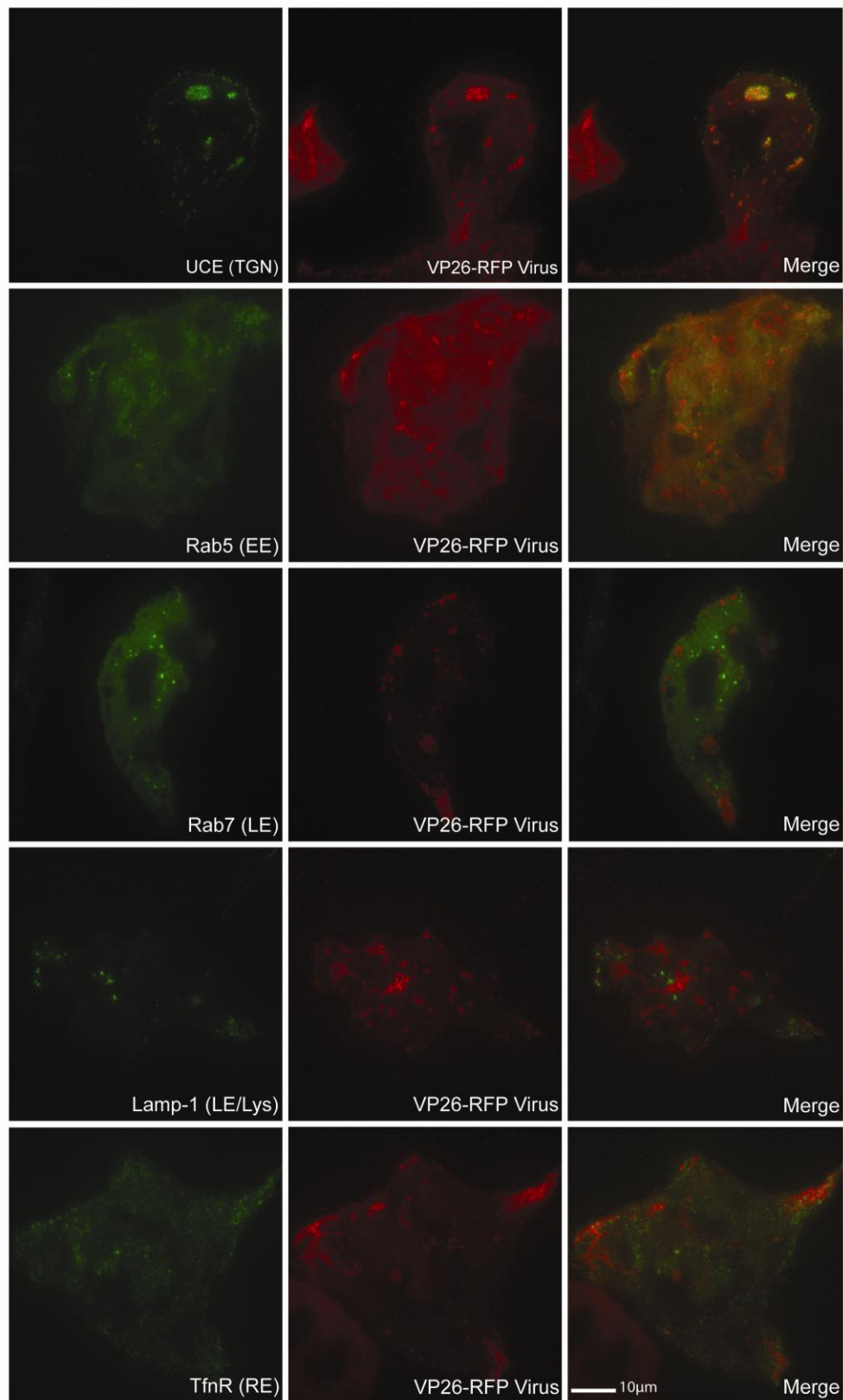
Figure G: Membrane microdomains and viral patches. Vero cells underwent Amaxa (Lonza) nucleofection of the noted GFP-tagged constructs in the top 4 rows. 12 hours post transfection cells were infected with VP26-RFP HSV-1. At 12hpi cells were fixed and viewed with TIRF microscopy. Cells shown in the last row were infected with VP26-GFP HSV-1 and stained with Texas Red-labeled CTxB. Note that neither tetraspanin-enriched microdomain markers, a caveolin-enriched microdomain marker, nor a lipid raft maker were found in viral egress patches.
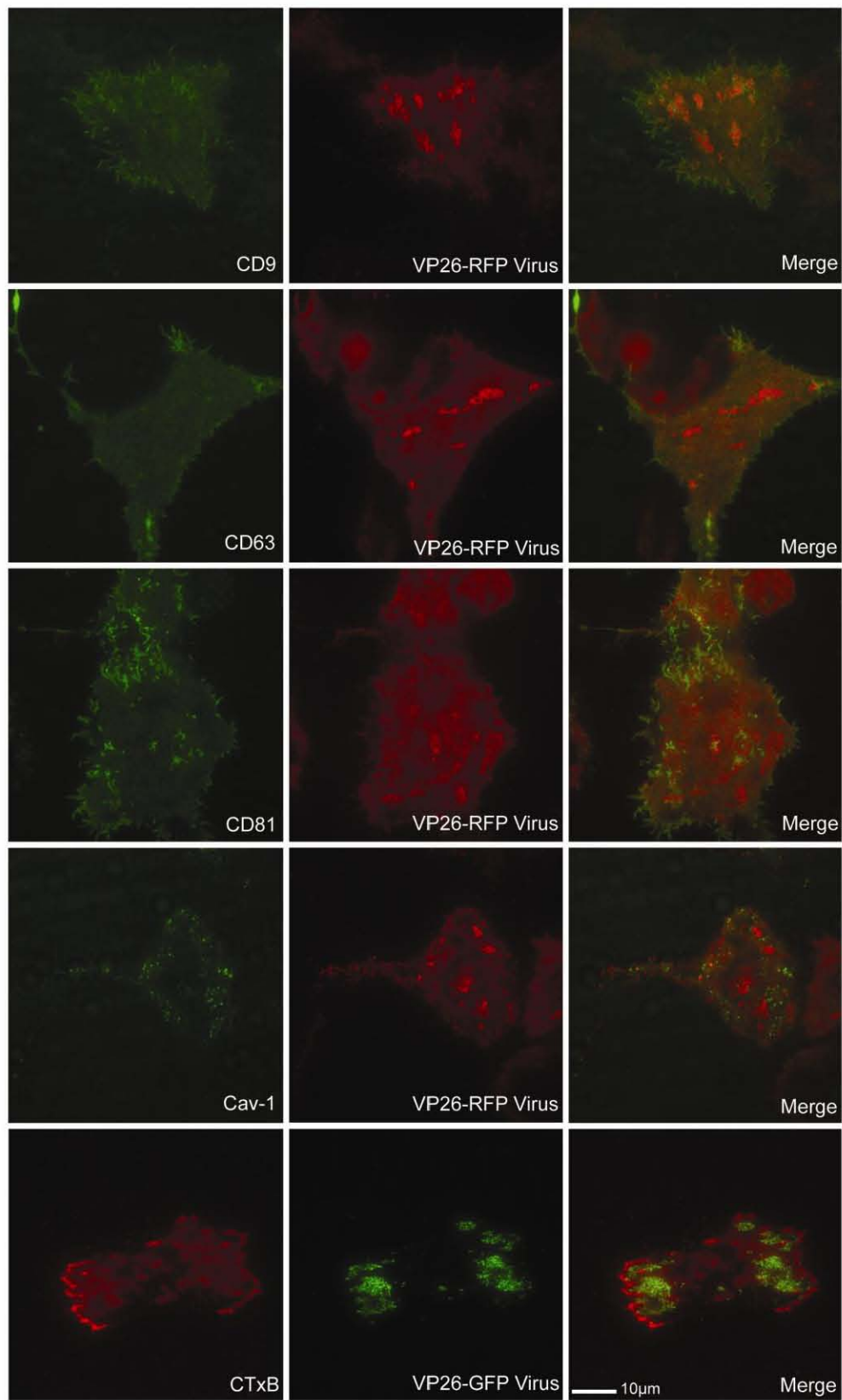
Figure H: Cell membrane proteins and viral patches. In the top 2 image rows cells were infected with VP26-GFP virus and stained with anti-cortactin monoclonal antibody or anti-ELKS monoclonal antibody. In the bottom 3 rows, Vero cells underwent Amaxa (Lonza) nucleofection of the noted GFP-tagged constructs. 12 hours post transfection cells were infected with VP26-RFP HSV-1. At 12hpi cells were fixed and viewed with TIRF microscopy. Though the reported functions of each of the labeled cellular proteins indicated a possible action at egress sites, these cellular proteins did not colocalize with virus.

Cortactin | VP26-GFP Virus | Merge

ELKS | VP26-GFP Virus | Merge

10µm

α5 integrin | VP26-RFP Virus | Merge

nectin-1 | VP26-RFP Virus | Merge

Annexin II | VP26-RFP Virus | Merge

10µm